Title

Differential sensitivity to SHH signaling and neural crest-mediated Gas1 expression regulate jaw size during development and evolution

Journal

Developmental Dynamics

ISSN

1058-8388

Authors

Vavrušová, Zuzana
Chu, Daniel B
Nguyen, An
et al.

Publication Date

2026-07-22

DOI

10.1002/dvdy.70177

Received: 5 June 2026 | Revised: 5 June 2026 | Accepted: 29 June 2026

DOI: 10.1002/dvdy.70177

RESEARCH ARTICLE

Developmental Dynamics | AMERICAN ASSOCIATION FOR ANATOMY | WILEY

Differential sensitivity to SHH signaling and neural crest-mediated *Gas1* expression regulate jaw size during development and evolution

Zuzana Vavrušová[1] | **Daniel B. Chu**[1] | **An Nguyen**[1] | **Yeniko Ta**[1] | **Jennifer L. Fish**[2] | **Richard A. Schneider**[1]

[1]Department of Orthopaedic Surgery, University of California San Francisco, San Francisco, California, USA

[2]Department of Biological Sciences, University of Massachusetts Lowell, Lowell, Massachusetts, USA

Correspondence
Richard A. Schneider, Department of Orthopaedic Surgery, University of California at San Francisco, 513 Parnassus Avenue, S-1164, San Francisco, CA 94143-0514, USA.
Email: rich.schneider@ucsf.edu

Funding information
National Institute of Dental and Craniofacial Research, Grant/Award Numbers: R01 DE016402, R01 DE025668, F30 DE027616; NIH Office of the Director, Grant/Award Numbers: S10 OD021664, S10 OD021822; National Institute of Diabetes and Digestive and Kidney Diseases, Grant/Award Number: P30 DK063720; National Institute of Arthritis and Musculoskeletal and Skin Diseases, Grant/Award Number: P30 AR075055

Abstract

Background: Developmental control of jaw size is crucial to prevent birth defects and facilitate evolutionary adaptation. We have shown that jaw size is established by neural crest mesenchyme (NCM), which are progenitor cells that migrate into the mandibular primordia and produce the jaws. NCM relies on multiple signaling pathways including Sonic Hedgehog (SHH) to mediate interactions with mandibular epithelium and promote jaw outgrowth. We investigated if NCM-mediated regulation of the SHH pathway underlies species-specific evolution of jaw size.

Results: We analyze expression of SHH pathway members over time and find that Growth Arrest-Specific 1 (GAS1), which is a SHH co-receptor, is expressed 20–75-fold higher in mandibular primordia of duck relative to those of quail. We generate quail-duck chimeras and demonstrate *Gas1* expression is NCM-regulated. Gain- and loss-of-function experiments reveal species-specific sensitivity to SHH signaling, especially for *Gas1*. *Gas1* overexpression and knockdown in NCM alters cell number and jaw size, and differentially affects genes involved in the SHH and WNT pathways, the cell cycle, and others. We also uncover intriguing differences in the *Gas1* promoter and coding sequence between duck and quail.

Conclusions: Our work suggests changes to *Gas1* expression and function may modulate jaw size during development, disease, and evolution.

KEYWORDS

avian embryos, evolutionary developmental biology, Gas1, jaw size, neural crest, quail-duck chimeras, SHH signaling, species-specific pattern

Zuzana Vavrušová and Daniel B. Chu have contributed equally to this study.

1 | INTRODUCTION

Animals belonging to a given group typically share a conserved body plan that contains homologous structures. Such structures often appear to be iterative versions of a common template that can vary in relative size and/or proportions along a normal distribution, which is a phenomenon known as allometry or biological scaling.[1–9] For purposes of functional morphology, proper scaling of structures is robustly maintained during development of individuals even though the size of these same structures can vary enormously both within a species and among members of related taxa.[10–12] Additionally, tissue regeneration and transplantation experiments demonstrate structures retain intrinsic mechanisms enabling them to know their proper size and to regulate growth.[13–18] But how these intrinsic mechanisms function and how they potentiate normal to abnormal phenotypic variation in size is poorly understood. Moreover, molecular and cellular processes that enable early embryos to establish growth trajectories in support of requisite adult form and function remain to be identified particularly as a means to understand etiologies of birth defects and modes of evolution.[19,20]

On the molecular level, biological scaling likely involves species-specific modulations to levels and patterns of gene expression that affect proliferation dynamics of cells and the corresponding growth of tissues and organs. Such ideas emerged in the first half of the 20th century with concepts about genes that alter the timing and rates of development,[2,21–23] and they led to theories and quantitative methods during the rebirth of evolutionary developmental biology in the 1970s predicting how even small changes affecting developmental time and rates could generate significant phenotypic variation and transformations in size.[24–30] In this context, molecules that act as morphogens seem to play a key role, primarily when genetic changes alter their expression levels, source (i.e., cells that produce the morphogen), distribution (i.e., release of the morphogen), transportation (i.e., diffusion of the morphogen), and detection (i.e., cellular sensitivity to the morphogen) within the local environment.[31–38] One well studied example is the classic morphogen, Sonic Hedgehog (SHH).

SHH binds to the canonical receptor Patched (PTCH1) and co-receptors Cell Adhesion Molecule-related/downregulated by Oncogenes (CDON) and Brother of CDON (BOC), as well as Growth Arrest-Specific 1 (GAS1).[39–42] Binding of SHH by PTCH1 results in derepression and accumulation of Smoothened (SMO), and signal transduction through Glioma-associated oncogene (GLI) transcription factors.[43–48] GLI2 and GLI3 are bifunctional transcription factors that can either activate or inhibit transcription of target genes whereas GLI1 lacks a transcriptional repressor domain and functions as a transcriptional activator.[49–56] CDON, BOC, and GAS1 sit at the plasma membrane of SHH-responding cells and cooperate with PTCH1 to form a receptor complex that facilitates high-affinity binding of SHH and modulates signal specificity and range.[41,57,58] By capturing and concentrating SHH at the cell surface near PTCH1, these co-receptors affect the dynamics of the SHH morphogen gradient by influencing effective ligand concentration and sharpening gradient readouts, which in turn can modulate cell survival, proliferation, and differentiation, and ultimately affect the size and shape of organs.[59–67]

In the mandibular primordia, SHH is secreted by epithelium derived from pharyngeal endoderm and oral ectoderm[15,68–72] and is required for patterned outgrowth of neural crest mesenchyme (NCM), which are jaw precursor cells.[73–75] In this context, SHH is critical for establishing anteroposterior polarity of the NCM-derived jaw skeleton.[70,76–81] Similarly, SHH secreted by the surface ectoderm and ventral forebrain regulates species-specific shape and outgrowth of the mid- and upper face[82–86] and its spatiotemporal expression in overlying epithelium is dependent upon NCM.[87,88] Disruptions to SHH signaling via its co-receptors as well as other pathway members can result in micrognathia and other craniofacial defects associated with a spectrum of holoprosencephaly disorders.[49,54,57,59,89–103] Yet the extent to which the SHH pathway is differentially regulated by NCM and whether changes to its regulation relate to species-specific jaw size have not been tested.

In the current study, we investigate if differential regulation of the SHH pathway relates to species-specific scaling of the developing jaw primordia. We employ duck and quail, which are two species of birds with distinctly different jaw sizes (i.e., relatively larger in duck vs. relatively smaller in quail) and rates of maturation (28 days from fertilization to hatching in duck and 17 days in quail).[87,104] Previously, we have shown that NCM controls species-specific jaw size through multiple molecular and cellular mechanisms.[17,19,87,105] These include the allocation of approximately 15% more jaw progenitors to the mandibular primordia of duck versus quail during early stages of NCM migration and a longer cell cycle length (13.5 h in duck and 11.0 h in quail) over an extended period of absolute time.[9,15] We have also demonstrated that during later stages of cell proliferation and skeletal differentiation, NCM exerts species-specific control over several signaling pathways that directly affect jaw size.[14,81,106–108]

Here, we analyze embryonic stages when NCM arrives in the mandibular primordia and undergoes patterned outgrowth, which includes Hamburger Hamilton (HH) stages[109] HH15 to HH27. We quantify the amount

of mandibular mesenchyme and measure expression of *Shh*, *Ptch1*, *Cdon*, *Boc*, *Gas1*, *Smo*, *Gli1*, *Gli2*, and *Gli3*. We generate chimeras (i.e., "quck") in which we transplant presumptive NCM from quail to duck. Quck chimeras offer a way to assess the extent to which NCM differentially regulates gene expression, simply by asking if resulting spatiotemporal patterns and levels are more like the quail donor or duck host.[87,88,106–108,110–112] Our strategy uncovers stage- and species-specific expression levels for some SHH pathway members but not others and reveals which ones are NCM-mediated, including *Gas1*. We also test if duck and quail have intrinsic species-specific responses to SHH signaling by treating mandibular explants with a SHH pathway inhibitor or recombinant SHH (rSHH) protein. These inhibition and activation experiments reveal a species-specific response to SHH signaling, with duck *Gas1* being especially sensitive to manipulations. *In ovo* overexpression and knockdown of *Gas1* in NCM alters cell number and mandible size and differentially regulates downstream genes as determined by RNA-seq analyses. Comparison of the *Gas1* promoter in duck versus quail uncovers species-specific polymorphisms that indicates *Gas1* is differentially regulated by distinct compliments of upstream transcription factors. Similarly, analysis of GAS1 protein domains in duck and quail reveal amino acid composition and sequence length differences that may have implications for GAS1 structure and function. Overall, our work suggests that species-specific changes in the response of NCM to SHH signaling and differential regulation of *Gas1* may be a mechanism by which NCM controls jaw size during development, disease, and evolution.

2 | RESULTS

2.1 | Species-specific differences in size arise early and progress during development

Duck embryos develop more slowly than quail embryos but nonetheless both species can be aligned using the HH staging system, which operates independent of body size and incubation time and relies on external morphological criteria (Figure 1A and Table S1).[87,109,113–121] In terms of absolute size, duck mandibles are consistently larger than those of quail at equivalent HH stages (Figure 1B). To quantify the size of mandibular primordia in duck and quail, we counted the number of mandibular mesenchymal cells at HH18, HH21, HH24, and HH27 (Figure 1C). The majority of mandibular mesenchyme is derived from NCM but some cells are also mesodermal in origin.[122] We observe significant differences in mandibular mesenchyme population size for every embryonic stage examined (Table S2). Mandibular mesenchyme population size is on average 4.1 times larger in duck than in quail across HH18, HH21, HH24, and HH27.

To characterize cellular dynamics underlying species-specific differences in the size of the mandibular mesenchyme population in duck and quail, we generated a model using the initial number of migratory NCM and known cell cycle lengths that we calculated in an earlier study,[15] and absolute time that duck and quail take to reach each successive developmental stage (Figure 1A). When accounting for differences in cell cycle length of mandibular mesenchyme (i.e., proliferation rate), and developmental rate (i.e., absolute time), our model predicts an approximately 26% increase in the size of the pre-migratory NCM population in duck compared to quail,[15] which leads to an average 4.1-fold larger population of mandibular mesenchyme in duck (Figure 1D and Table S3). Comparing modeled data to the quantified population size in vivo (Figure 1E and Table S4) shows we were able to replicate closely the relative mandibular mesenchyme population size observed in vivo for duck and quail.

2.2 | SHH pathway activation is stage- and species-specific

Prior studies have shown that SHH regulates growth and proliferation of the mandibular primordia[65,72,80,91,123–125] and that *Shh* is expressed in similar domains (i.e., in the pharyngeal endoderm) in duck and quail.[15] To test the hypothesis that species-specific expression of SHH pathway members underlies differential rates of proliferation that ultimately affect mandibular mesenchyme population size, we analyzed expression of SHH pathway members. Using quantitative polymerase chain reaction (qPCR), we quantified relative mRNA levels of *Shh*, *Ptch1*, *Smo*, *Cdon*, *Boc*, *Gas1*, *Gli1*, *Gli2*, and *Gli3* (Figure 2A–I) in duck and quail mandibular primordia at HH15, HH18, HH21, HH24, and HH27. We find stage- and species-specific differences in all genes (Table S5). Each of the nine genes is higher in duck at HH15 and HH18, but then all except *Ptch1*, *Boc*, and *Gas1* become higher in quail at HH21, HH24, and HH27. The most striking difference between duck and quail across all stages is the relative expression of *Gas1*. *Gas1* levels are approximately 20 to 75 times higher in duck with relative differences trending upwards from HH15 to HH27 (Figure 2F).

Since *Gas1* stood out among all SHH pathway members, we performed whole mount in situ hybridization to understand the spatial expression patterns of *Gas1* in the

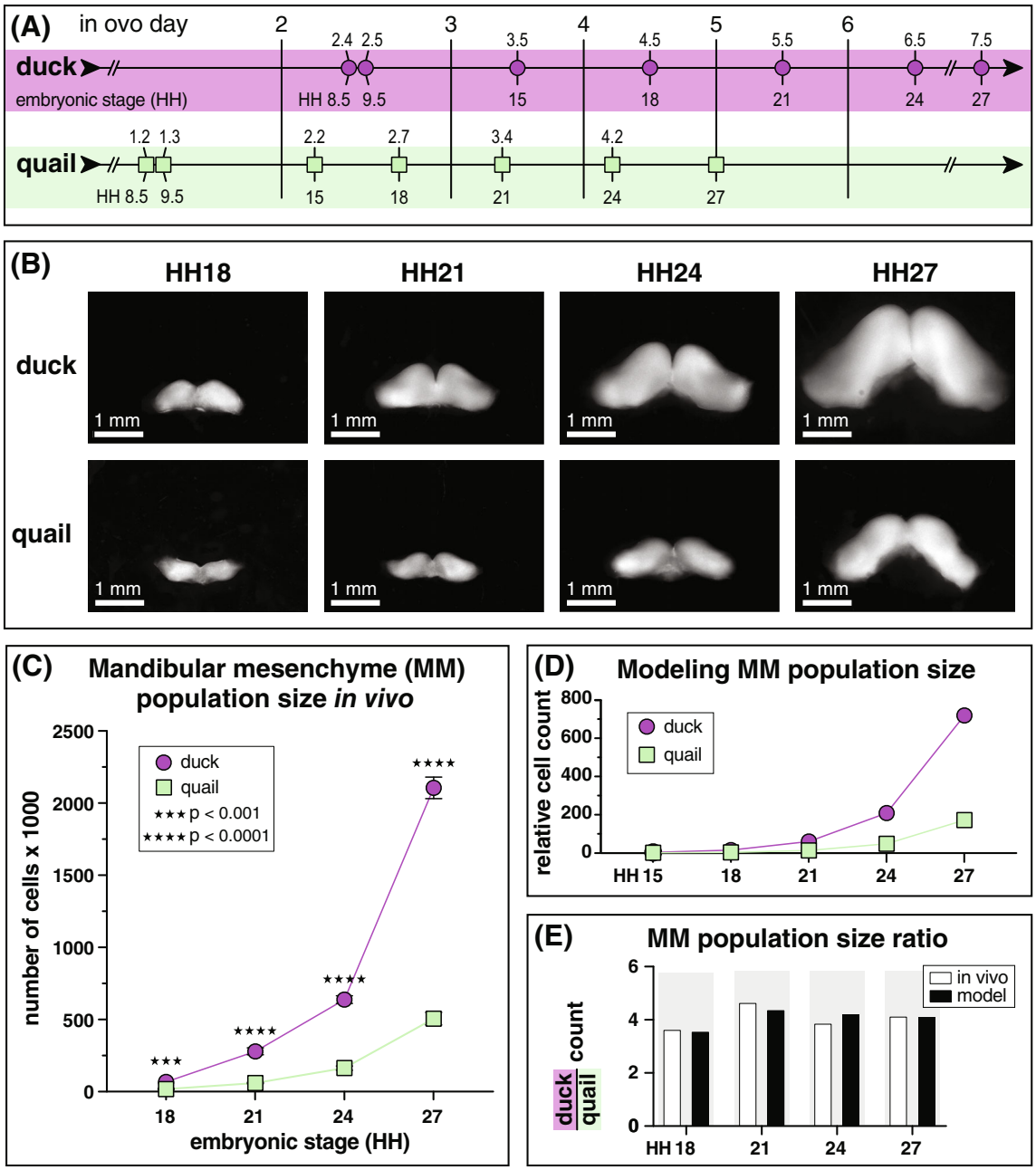

FIGURE 1 Species-specific growth of the mandibular primordia during early embryogenesis. (A) The Hamburger-Hamilton (HH) staging system functions independent of absolute time and instead relies on external morphological features.[109] Thus, embryos from duck (violet) and quail (green) can be matched at equivalent stages by incubating them for different lengths of time. *In ovo* day represents the number of incubation days needed to reach equivalent HH stages for each species. (B) Dissected mandibular primordia from duck and quail at HH18, HH21, HH24, and HH27 showing progressive differences in size. (C) Mandibular mesenchyme (MM) population size (i.e., number of cells counted) in duck (violet) and quail (green) at HH18, HH21, HH24, and HH27. Significance (stars) is shown for each group and data point ($n \geq 7$), and error bars represent SEM for comparisons between each species at the same embryonic stage. (D) Model showing the relative mandibular mesenchyme population size at HH15, HH18, HH21, HH24, and HH27 in duck (violet) and quail (green) derived from previously published data on numbers of migratory NCM cells, cell cycle length, and absolute time to reach each HH stage in duck and quail.[15] (E) Comparison (i.e., ratios) of in vivo data on mandibular mesenchyme population size (white) to estimates based on modeling (black) at HH18, HH21, HH24, and HH27.

mandibular primordia of duck and quail at HH21 and HH27. We find that *Gas1* expression is symmetrical for both species with one lateral domain within the mesenchymal core on each side of the mandibular primordia at HH21 (Figure 2J,K) and two distinct domains at HH27 comprising one lateral domain on each side and

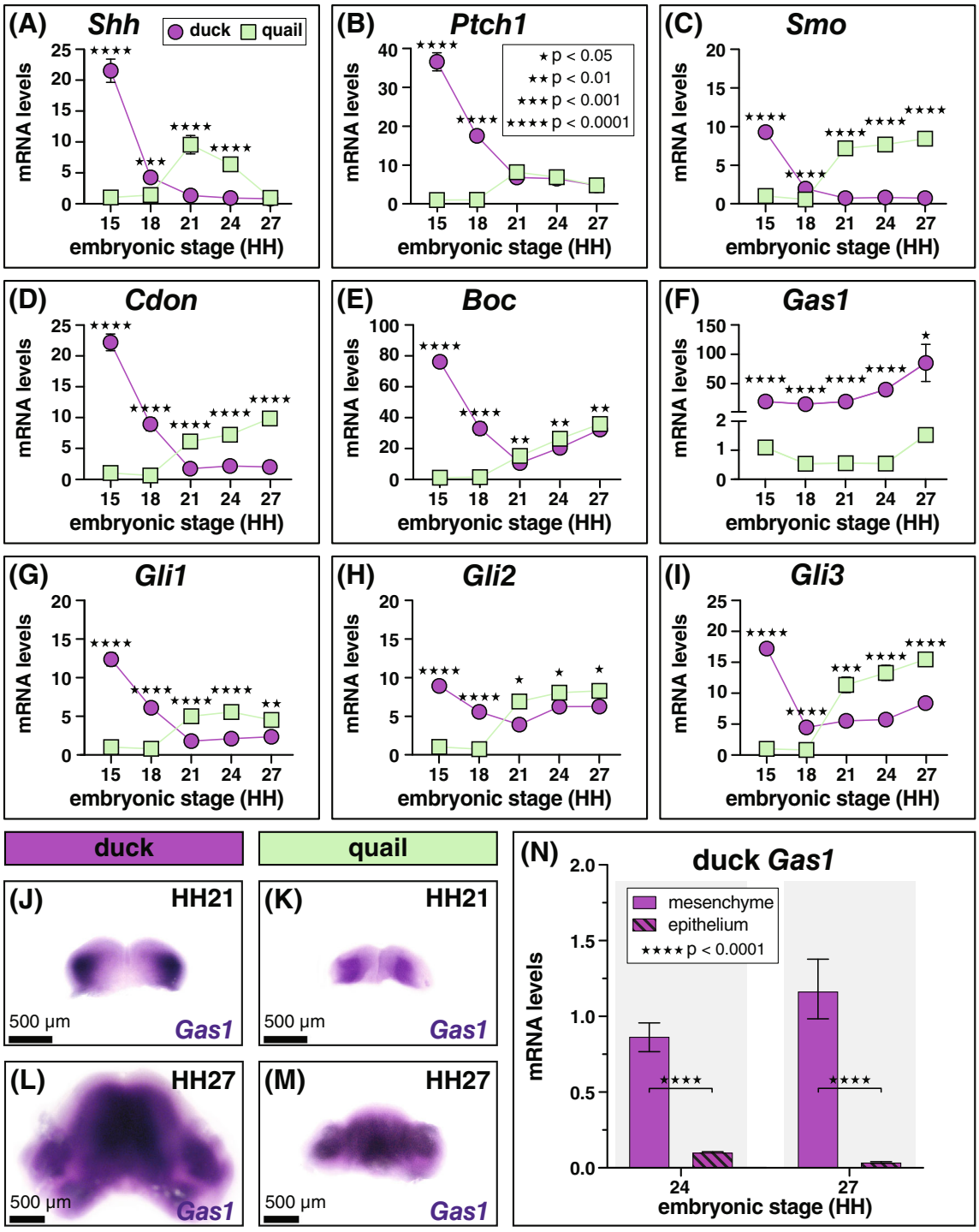

FIGURE 2 Expression of SHH pathway members and pathway activation in mandibular primordia of duck and quail. Relative mRNA levels of (A) *Shh*, (B) *Ptch1*, (C) *Smo*, (D) *Cdon*, (E) *Boc*, (F) *Gas1*, (G) *Gli1*, (H) *Gli2*, and (I) *Gli3* in mandibular primordia of duck (violet) and quail (green) at HH15, HH18, HH21, HH24, and HH27. Expression levels were assayed by RT-qPCR and normalized to *r18s*. Significance (stars) is shown for each group and data point ($n \geq 6$), and error bars represent SEM for comparisons between each species at the same embryonic stage. Whole mount in situ hybridization showing *Gas1* expression (purple stain) in mandibular primordia from (J) duck and (K) quail at HH21; and in (L) duck and (M) quail at HH27. (N) Relative levels of mRNA expression for *Gas1* in duck mandibular mesenchyme (violet) and epithelium (striped) at HH24 and HH27. Expression levels were assayed by RT-qPCR and normalized to *r18s*. Significance (stars) is shown for comparisons between mesenchyme and epithelium at the same embryonic stage as denoted by brackets. n ≥ 7 for each group and data point, and error bars represent SEM.

one medial domain (Figure 2L,M). Using qPCR, we also quantified *Gas1* expression in mandibular mesenchyme versus epithelium of duck at HH24 and HH27 (Figure 2N). We observe higher *Gas1* expression in mandibular mesenchyme compared to epithelium at both stages (Table S6). At HH24, *Gas1* levels are more than 8-fold greater, and at HH27 almost 23-fold greater in mesenchyme compared to epithelium.

2.3 | NCM differentially regulates members of the SHH pathway

To assess the extent to which NCM differentially regulates the SHH pathway, we compared gene expression levels in mandibular primordia of chimeric quck to that observed in duck and quail. Using qPCR, we quantified relative mRNA expression in mandibular primordia of duck, quail, and quck at stage HH21 and HH24 (for quck, duck host is at HH21 and HH24, but quail donor cells are at HH24 and HH27, respectively, given their faster maturation rate [see Figure 3A for relative stage of donor vs. host cells in chimeras]). We find that expression of *Shh* is duck-like in quck at HH21, but indeterminant at HH24 (i.e., similar to both duck and quail; Figure 3B and Table S7). Expression of *Ptch1*, *Gli2*, and *Gli3* is indeterminant at both stages (i.e., similar to both duck and quail or lower than both in quck; Figure 3C,I,J). Expression of *Gas1* and *Gli1* is more quail donor-like (i.e., regulated by NCM) whereas *Smo*, *Cdon*, and *Boc* are not, instead being more like the duck-host (Figure 3D–F). Specifically, we observe lower quail-like *Gas1* gene expression in quck relative to the duck host that is trending at HH21 and significant at HH27 (Figure 3G); we also see higher quail-like *Gli1* expression (Figure 3H) in quck compared to host levels at both stages.

2.4 | Duck and quail mandibular primordia are differentially sensitive to SHH signaling

To determine if there are intrinsic species-specific differences in sensitivity to SHH signaling (i.e., a dose–response to pathway inhibition and/or activation), we cultured explants of HH21 mandibular primordia from duck and quail and treated them with cyclopamine (i.e., SHH pathway inhibitor) or rSHH protein (i.e., pathway activator). After 24 h of treatment, we quantified relative expression of *Shh*, *Ptch1*, *Smo*, *Cdon*, *Boc*, *Gas1*, *Gli1*, *Gli2*, and *Gli3* (Figure 4). We find that pathway inhibition positively affects expression of *Shh*, *Cdon*, and *Gas1* in duck but not quail (Figure 4A, D, F); negatively affects expression of *Ptch1* and *Gli1* in duck and quail (Figure 4B,G); and negatively affects expression of *Gli2* and *Gli3* in quail but not duck (Figure 4H,I). For pathway activation, we find both duck and quail down-regulate *Shh* in response to rSHH (Figure 4A), with duck responding at lower concentrations. Quail but not duck down-regulate *Smo*, *Cdon*, *Boc*, *Gas1*, *Gli2*, and *Gli3* in response to rSHH (Figure 4C–F, H, I). Duck and quail both up-regulate *Ptch1* at the highest concentration of rSHH (Figure 4B) whereas only duck up-regulate *Gli1* (Figure 4G). While each of the SHH pathway members exhibit species-specific differences in their relative expression following treatments, we observe the greatest interspecies differences in sensitivity to SHH pathway manipulations with *Gas1* (Figure 4F). *Gas1* expression is increased in duck when treated with cyclopamine, while there is no significant difference in quail. In contrast, *Gas1* is downregulated in quail starting at 0.1 ng/mL of rSHH protein and every concentration thereafter, whereas there is no significant change at any concentration of rSHH for duck (Table S8).

2.5 | Changes in Gas1 expression affect mandibular primordia size in vivo

Our in vivo molecular data along with results from our SHH pathway manipulations in mandibular explant cultures indicate *Gas1* may be a key component of the SHH pathway mediating species-specific differences in cell number and jaw size. To test if changes in levels of *Gas1* expression can affect the size of the mandibular primordia, we altered *Gas1* expression in duck and quail. First, we bilaterally electroporated an integrating doxycycline (dox)-inducible plasmid containing *Gas1*, which we designed and characterized previously,[126] into presumptive NCM of duck and quail at HH8.5. We treated these embryos with dox at HH15. We collected duck and quail at HH18, HH21, and HH24 and quantified the number of mandibular mesenchymal cells. We observe a reduction in the amount of mandibular mesenchyme at HH21 and HH24 in duck overexpressing *Gas1* (Figure 5A). The extent of *Gas1*-positive NCM was validated in whole mount by mScarlet fluorescence (RFP) at each stage (Figure 5B–G). Although not statistically significant, we observe a similar trend towards reduction in the amount of mandibular mesenchyme in quail (Figure 5H and Table S9).

To assess the effects of overexpression on mandibular morphology, we electroporated *Gas1* overexpression plasmid unilaterally into the right side of presumptive NCM of quail at HH8.5 and then treated these embryos with dox at HH15. By HH27, quail show a clear reduction in

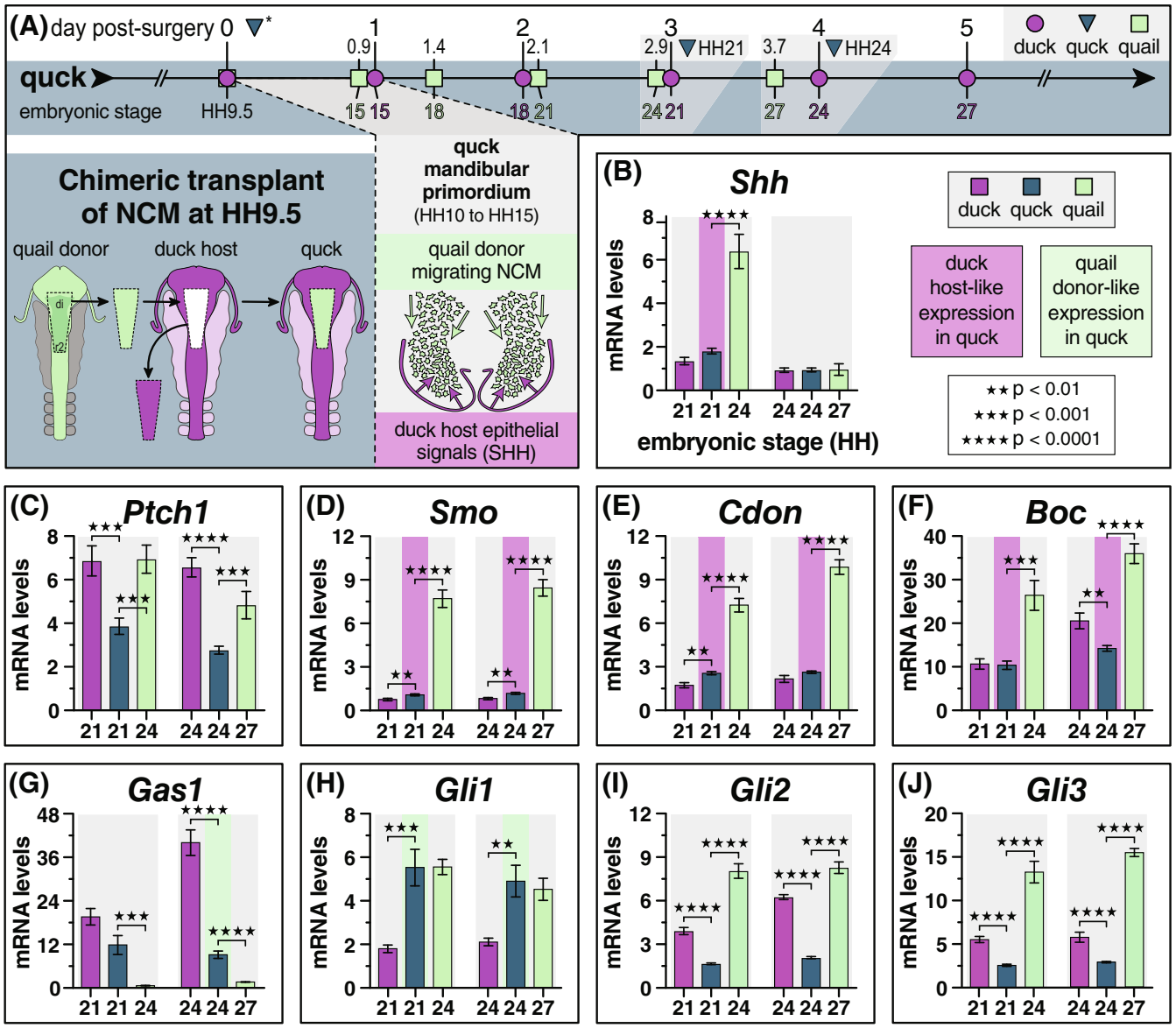

FIGURE 3 Neural-crest mediated gene expression of SHH pathway members in mandibular primordia. (A) To generate quail-duck chimeras ("quck"), quail and duck are stage-matched for surgery at HH9.5 (i.e., post-surgery day 0) by starting the incubation of their eggs at different times (see Figure 1A). Bilateral neural folds from the mid-diencephalon (di) to rhombomere 2 (r2) of the hindbrain (dark green), which generate neural crest mesenchyme (NCM), are transplanted from quail to duck. Quail donor NCM (green cells) migrates (green arrows) into mandibular primordia between HH10 and HH15. Due to its faster rate of maturation, quail NCM develops approximately three stages ahead of the slower-maturing duck host within 2 days post-surgery. Quail NCM receives cues from and interacts with duck-host derived epithelium (violet arrows). Relative mRNA levels of (B) *Shh*, (C) *Ptch1*, (D) *Smo*, (E) *Cdon*, (F) *Boc*, (G) *Gas1*, (H) *Gli1*, (I) *Gli2*, (J) *Gli3* in mandibular primordia of duck (violet), quck (blue), and quail (green) at quck embryonic stage HH21 (i.e., host-duck cells at HH21 and donor-quail cells at HH24) and HH24 (i.e., host-duck cells at HH24 and donor-quail cells at HH27). Expression levels were assayed by RT-qPCR and normalized to *r18s*. Significance (stars) is shown for comparisons between species at each stage as denoted by brackets and p-values are as indicated. $n \geq 6$ for each group and data point, and error bars represent SEM. Host-like expression is denoted where the relative mRNA expression and/or the expression pattern is not significantly different and/or similar to host (i.e., duck) values. Donor-like expression represents when the relative mRNA expression and/or the expression pattern is significantly different from the host (i.e., duck) and/or similar to donor (i.e., quail) values.

the size of the developing jaw on the electroporated side (Figure 5I,K) coincident with high levels of RFP expression (Figure 5J,L), which is indicative of *Gas1*-positive overexpression in NCM relative to the internal control side. We also knocked-down *Gas1* expression in quail by injecting control anti-*GFP* or anti-*Gas1* morpholinos into the right side of the mandibular primordia at HH18. Morpholino translation assays validate the specificity of anti-

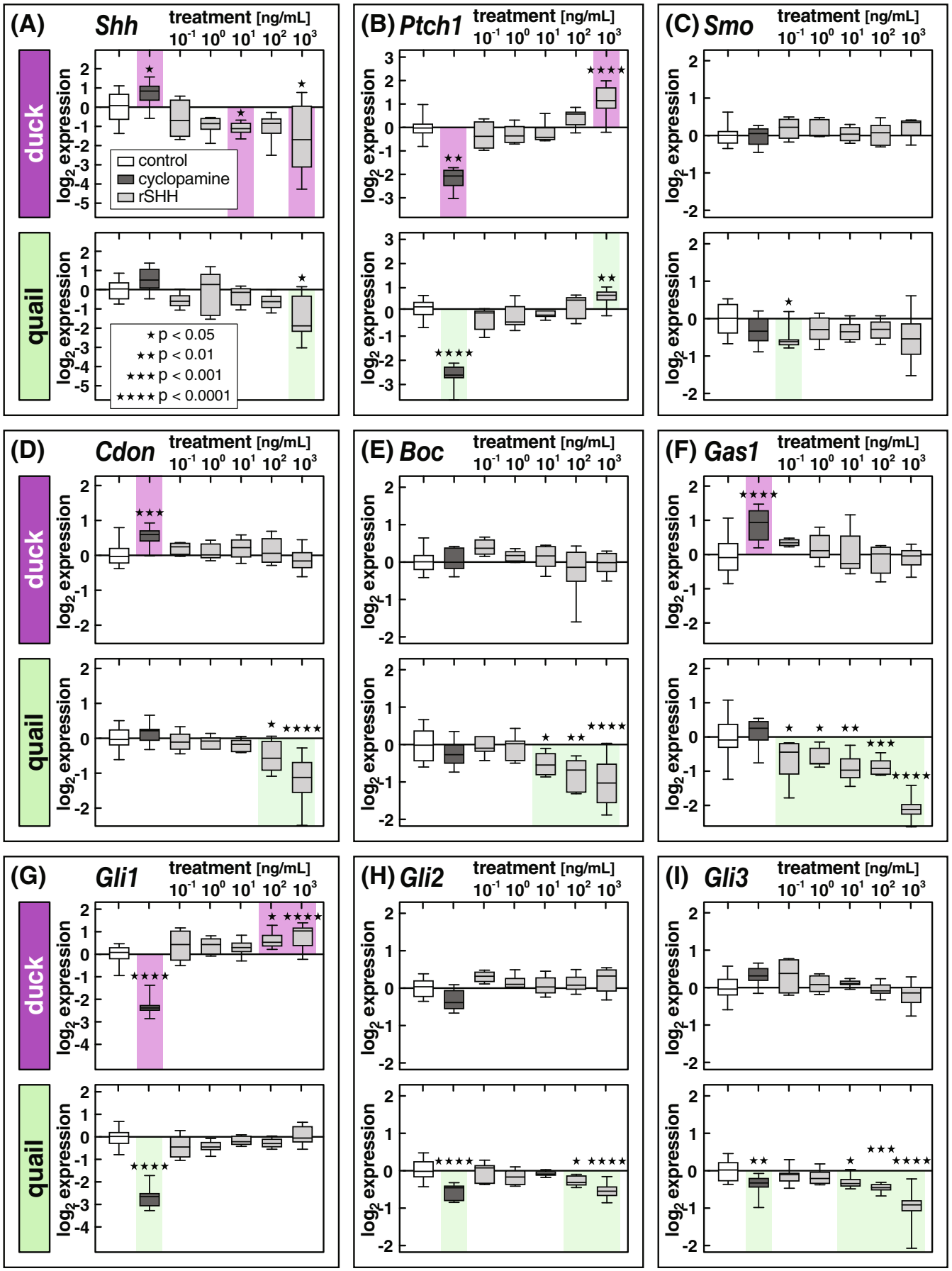

FIGURE 4 Legend on next page.

Gas1 morpholinos for duck- and quail-specific target sequences (Figure S1D, E). We find that anti-GFP control morpholinos have no observable effect on jaw morphology (Figure 5M) as the left and rights sides appear equivalent (Figure 5N,O). However, in anti-*Gas1* morpholino-injected embryos we observe left–right asymmetry in the developing jaw with the right side (i.e., morpholino-treated) qualitatively smaller (Figure 5P–R).

2.6 | Knockdown and overexpression of Gas1 causes differential gene expression

To assess effects of *Gas1* knockdown and overexpression on the transcriptome in duck and quail, we performed bilateral anti-*Gas1* morpholino injections at HH18. We also electroporated *Gas1* overexpression plasmid bilaterally into presumptive NCM at HH8.5 and then treated these embryos with dox at HH15. Mandibular primordia were harvested at HH24 for RNA-seq analysis. We identified 14,089 expressed genes in duck and 14,161 in quail, of which 2445 (17.4%) and 2083 (14.7%), respectively, were assigned LOC identifiers (LOC identifiers represent predicted or uncharacterized gene models lacking curated gene symbols[127]). Using a batch annotation pipeline, we were able to assign Ensembl gene identifiers to 255 duck LOC identifiers (10.4%) and 1136 quail LOC identifiers (54.5%). However, Ensembl Compara lacked curated chick, mouse, or human orthologs for these Ensembl gene identifiers. Thus, final gene names were assigned to corresponding LOC entries based on best-hit protein homology (agnostic to species) from the Swiss-Prot database.

Differentially expressed (DE) genes were identified for duck and quail *Gas1* morpholino and overexpression treatments relative to controls (Tables S10–S13). Multidimensional scaling plots show biological replicates clustering by treatment group for both species (Figure S1A,B). In duck, *Gas1* perturbations yield 752 DE genes: 322 morpholino-only (43%), 278 overexpression-only (37%), and 152 shared (20%) (Figure 6A). In quail, 590 DE genes are driven by morpholino treatments (561 morpholino-only, 95%), with only 16 overexpression-only (3%) and 13 shared (2%) (Figure 6B). While duck exhibits a broader transcriptional response, quail shows greater sensitivity specifically to *Gas1* knockdown (~1.7× more morpholino-only genes). Conversely, duck responds more to overexpression (430 vs. 29 genes) and maintains a higher fraction of overlapping targets (20% of the union) than quail (2%). Despite these differences, both species retain distinct sets of DE genes unique to each treatment.

We performed a gene ontology (GO) enrichment analysis using the Database for Annotation, Visualization and Integrated Discovery (DAVID).[128] When we examine specific pathways and/or processes affected by our *Gas1* perturbations (Table S14), we find 53 gene ontology (GO) biological process terms for duck control versus *Gas1* morpholino (354 genes), 52 terms for duck control versus *Gas1* overexpression (325 genes), 31 terms for quail control versus *Gas1* morpholino (433 genes), and nine terms for quail control versus *Gas1* overexpression (17 genes). Collectively, GO results show recurring enrichment for development/differentiation-related processes (e.g., *multicellular organism development* and *cell fate commitment*) across multiple comparisons, with a clear treatment-linked pattern in which overexpression in both duck and quail show shared enrichment for *cell adhesion/junction organization* and *canonical WNT signaling pathway*, while knockdown in both species shares enrichment for broader developmental, differentiation, junctional, and transcriptional-regulatory categories.

GO terms associated with cell cycle–related processes (e.g., proliferation, growth control, centrosome/cytoskeleton organization) are enriched in a treatment- and species-specific manner. For example, duck control versus *Gas1* morpholino includes GO terms and genes with well-established roles in growth control and checkpoint/apoptosis programs such as *apoptotic signaling pathway in response to DNA damage by p53 class mediator* (*Cdkn1a*, *Tp63*, *Tp73*, *Phlda3*), *keratinocyte proliferation* (*Cdkn1a*, *Irf6*, *Wnt16*), *keratinocyte differentiation* (*Cdkn1a*, *Mafb*, *Irf6*, *Wnt16*, *Tp63*), *negative regulation of cell growth* (*Minar1*, *Cdkn1a*, *Hnf4a*, *Myl2*), *positive regulation of B cell proliferation* (*Cdkn1a*, *Tfrc*, *Ada*), and *positive regulation of*

FIGURE 4 Effects of inhibition and activation of the SHH pathway in mandibular primordia of duck and quail. Mandibular primordia (MP) from duck (violet) and quail (green) were harvested at HH21, placed in culture, and treated with cyclopamine (cycl, dark gray) to inhibit the SHH pathway or with five concentrations of recombinant (r) SHH protein (light gray) to activate the SHH pathway. Box plots show relative levels of mRNA expression compared to controls (on the y-axis in $\log_2$ scale) for SHH pathway members including (A) *Shh*, (B) *Ptch1*, (C) *Smo*, (D) *Cdon*, (E) *Boc*, (F) *Gas1*, (G) *Gli1*, (H) *Gli2*, (I) *Gli3* 24 h after treatment. Control (ctrl, white) and treatment groups are shown on the x-axis. Expression levels were assayed by RT-qPCR and normalized to *r18s*. Significance (stars) is shown for comparisons between control and treatment groups (i.e., cyclopamine or rSHH) within each species as indicated by colored shading and *p*-values are as indicated. $n \geq 6$ for each group and data point, and error bars represent SEM.

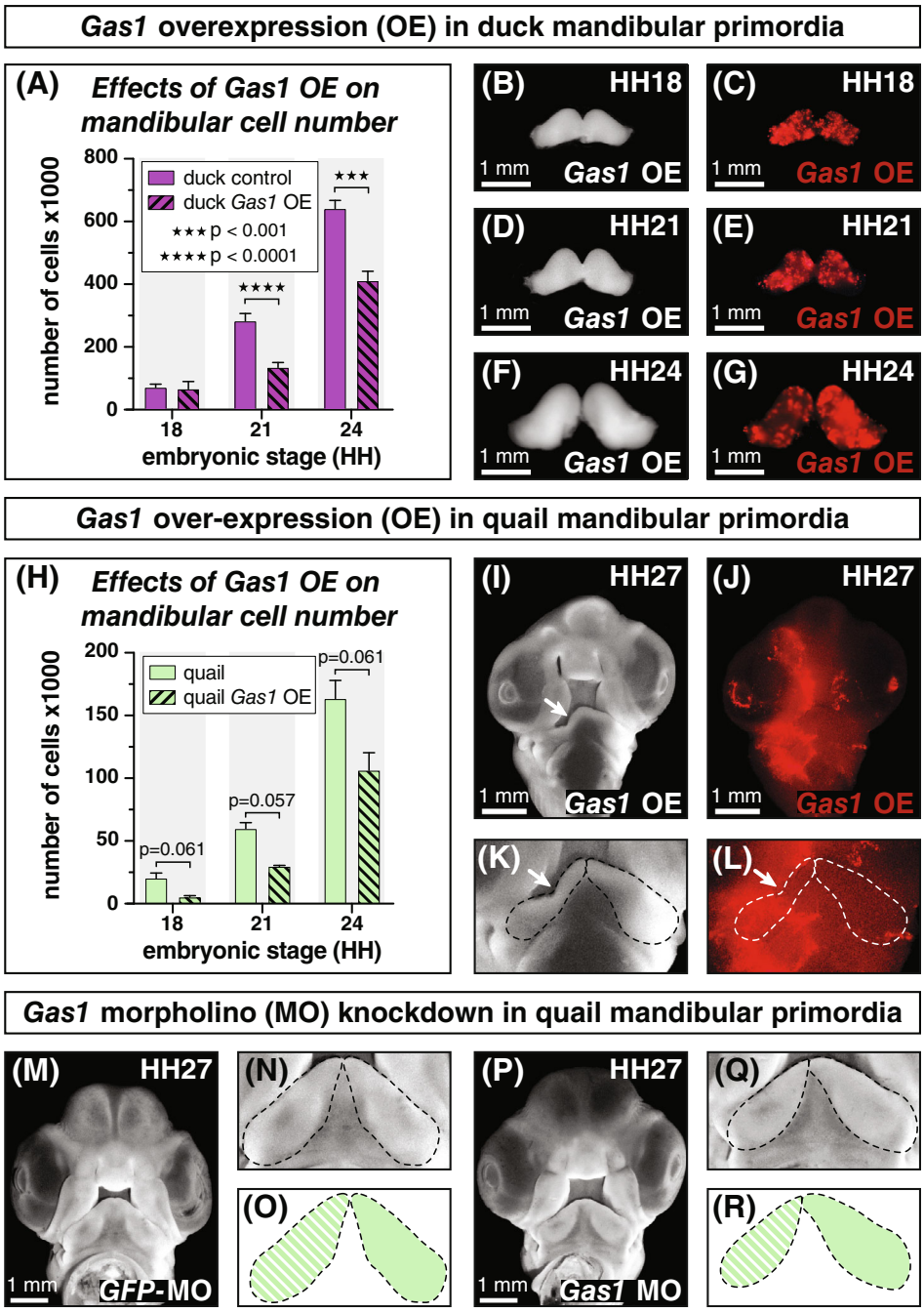

FIGURE 5 Effects of *Gas1* knockdown and overexpression in duck and quail. (A) Mesenchymal cell number in duck mandibular primordia following bilateral *in ovo* electroporation of a doxycycline (dox)-inducible *Gas1* overexpression (OE) vector into NCM at HH8.5. Overexpression was induced at HH15, and mandibular primordia were collected at HH18, HH21, and HH24. (B) Dissected duck mandibular primordia at HH18 following bilateral *Gas1* overexpression. (C) *Gas1*-positive NCM can be visualized by mScarlet fluorescence (RFP). *Gas1* overexpression (D) in whole mount and (E) by RFP at HH21, and (F) in whole mount and (G) by RFP at HH24. (H) Mesenchymal cell number in quail mandibular primordia following bilateral *in ovo* electroporation of *Gas1*. (I) Quail embryo in whole mount at HH27 following unilateral overexpression of *Gas1*. The treated size appears smaller (white arrow) than the contralateral control side. (J) Unilateral distribution of *Gas1*-positive NCM can be visualized by RFP. Higher magnification view of quail mandibular primordia (dashed lines) in (K) whole-mount and (L) with RFP showing a size reduction on the treated (arrow) versus control side. (M) Quail embryo in whole mount at HH27 following unilateral *in ovo* injection of a control anti-GFP morpholino (MO) at HH18. At higher magnification in (N) whole-mount and (O) in schematic view, the mandibular primordia (dashed lines) appear the same size on the treated (striped) and control (green) sides. (P) Quail embryo in whole mount at HH27 following unilateral *in ovo* injection of an anti-*Gas1* morpholino (MO) at HH18. In higher magnification (Q) whole-mount and (R) schematic view, the mandibular primordia (dashed lines) appear smaller on the treated *Gas1* (striped) versus control (green) sides. Significance (stars) is shown for comparisons between control and treatment groups as denoted by brackets and p-values. $n \geq 2$ for each group and data point. Error bars represent SEM.

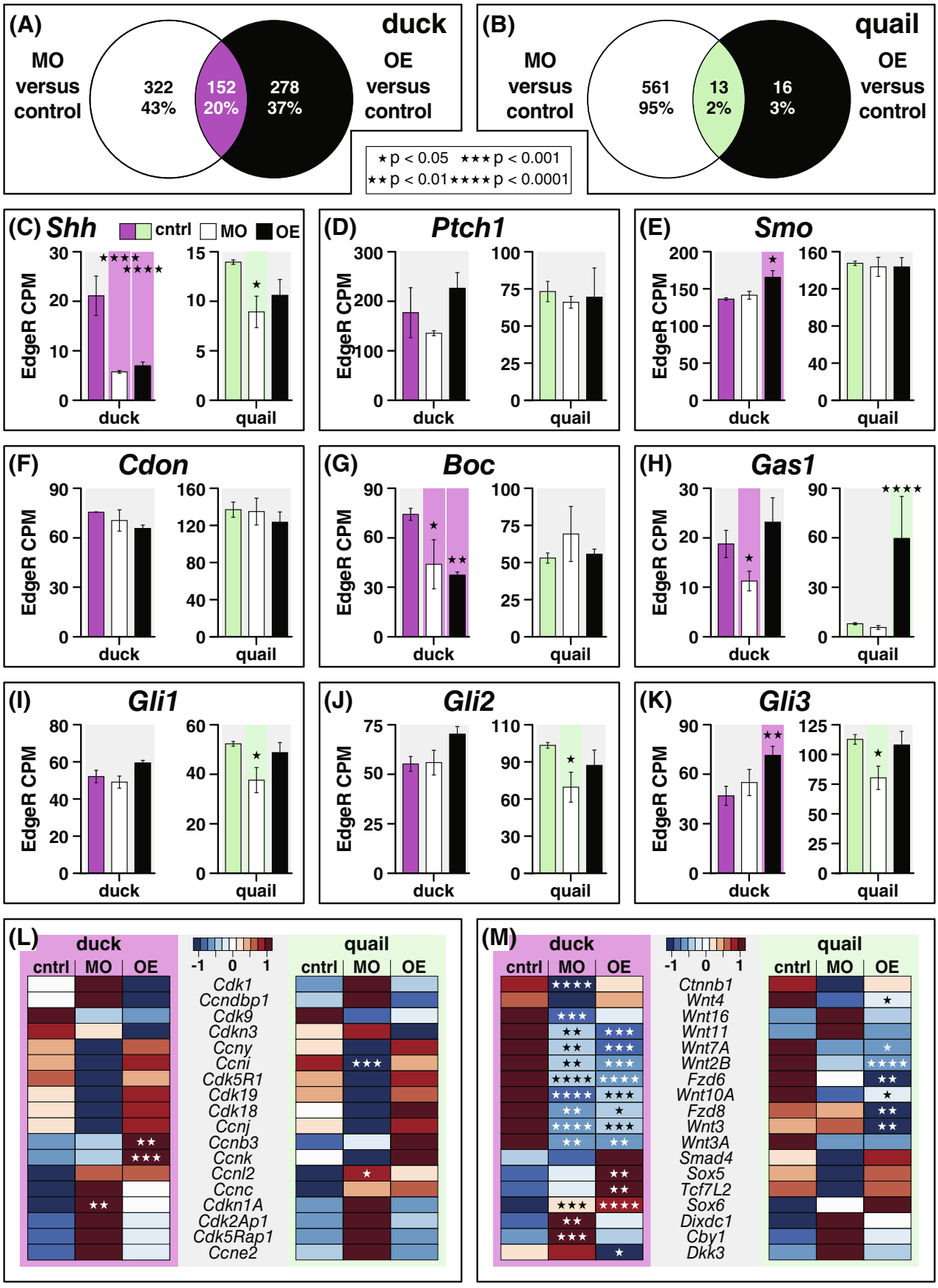

FIGURE 6 Legend on next page.

fibroblast apoptotic process (*Stk17a*, *Tp63*). *Canonical WNT signaling pathway* appears as an enriched term following *Gas1* morpholino treatment in duck (9 genes), is the top GO term following *Gas1* overexpression in quail, and WNT pathway genes (e.g., WNT ligands and/or FZD receptors) appear within enriched developmental/neural terms in multiple comparisons.

Given our goal of understanding potential effects of altered *Gas1* expression on SHH signaling and cell cycle regulators, and the fact that WNT pathway genes were consistently affected in both species and treatment groups, we used our RNA-seq datasets to assay more directly for changes in relative expression for relevant genes in duck and quail. For SHH pathway members (Table S15), we find that *Shh* (Figure 6C) is reduced in duck in both *Gas1* morpholino and overexpression conditions, whereas in quail *Shh* is reduced with morpholino and not significantly changed with *Gas1* overexpression. *Ptch1* (Figure 6D) does not change significantly in either species under either treatment. *Smo* (Figure 6E) is increased in duck with *Gas1* overexpression and not significantly changed with morpholino and shows no significant changes in quail. *Cdon* (Figure 6F) shows no significant changes in either species. *Boc* (Figure 6G) is reduced in duck under both morpholino and overexpression, with no significant changes in quail. *Gas1* (Figure 6H) is reduced in duck with *Gas1* morpholino treatment and not significantly changed with overexpression, whereas in quail *Gas1* is increased with overexpression and not significantly changed with morpholino. *Gli1* (Figure 6I) does not change significantly in duck under either treatment but is reduced in quail with morpholino and not significantly changed with overexpression. *Gli2* (Figure 6J) is not significantly changed in duck but is reduced in quail with morpholino and not significantly changed with overexpression. *Gli3* (Figure 6K) is increased in duck with overexpression and not significantly changed with morpholino, whereas in quail *Gli3* is reduced with morpholino and not significantly changed with overexpression. Overall, *Gas1* manipulation affects multiple SHH pathway members in both species, with duck showing changes in ligand, co-receptors, and transcriptional effectors under both conditions, while quail responses occur predominantly with morpholino knockdown affecting ligand and transcriptional effectors.

For cell cycle regulators, we analyzed expression of *Cdk1*, *Ccndbp1*, *Cdk9*, *Cdkn3*, *Ccny*, *Ccni*, *Cdk5R1*, *Cdk19*, *Cdk18*, *Ccnj*, *Ccnb3*, *Ccnk*, *Ccnl2*, *Ccnc*, *Cdkn1A*, *Cdk2Ap1*, *Cdk5Rap1*, and *Ccne2* (Figure 6L and Table S16). In duck, most genes are not significantly affected by either treatment, although *Gas1* overexpression increases *Ccnb3* and *Ccnk*, and *Gas1* morpholino treatment increases *Cdkn1A*. In quail, *Gas1* morpholino treatment reduces *Ccni* and increases *Ccnl2*, while no other genes show significant changes under either treatment. Overall, *Gas1* manipulation has limited effects on cell cycle regulators in both species, with duck showing increased cyclin expression with overexpression and increased cyclin-dependent kinase inhibitor expression with morpholino; while quail show mixed effects on cyclin expression with morpholino.

For the WNT pathway, we analyzed ligands (canonical and noncanonical) including *Wnt2B*, *Wnt3*, *Wnt3A*, *Wnt4*, *Wnt7A*, *Wnt10A*, *Wnt11*, and *Wnt16*; receptors including *Fzd6* and *Fzd8*; core intracellular mediators/effectors including *Ctnnb1* (*β-catenin*) and *Tcf7L2*; intracellular modulators/regulators of β-catenin signaling including *Dixdc1* and *Cby1*; extracellular modulators including *Dkk3*; and genes involved in crosstalk with other pathways and/or are WNT-responsive including *Smad4*, *Sox5*, and *Sox6* (Figure 6M and Table S17). Treatment-associated changes in duck include reductions in *Wnt16* following *Gas1* morpholino treatment; reduced *Wnt11*, *Wnt7A*, *Wnt2B*, *Wnt10A*, *Wnt3*, *Wnt3A*, and *Fzd6* following *Gas1* overexpression; increased *Sox6* with both treatments; increased *Sox5* and *Tcf7L2* following *Gas1* overexpression; increased *Dixdc1* and *Cby1* following *Gas1* morpholino treatment; reduced *Dkk3* with overexpression; and reduced *Ctnnb1* with morpholino. In quail, *Gas1* morpholino treatment reduces *Ctnnb1*, *Wnt4*, *Wnt7A*, *Wnt2B*, *Wnt10A*, *Wnt3A*, and *Tcf7L2*, while

FIGURE 6 Effects of *Gas1* knockdown and overexpression on downstream gene expression in duck and quail. Venn diagrams representing a summary of the overlap and distinctions between the differentially expressed genes in (A) duck and (B) quail mandibular primordia following *Gas1* morpholino knockdown (MO) and *Gas1* overexpression (OE) treatments. (C-K) Expression levels of key SHH pathway genes measured by EdgeR CPM (counts per million) in duck and quail under control (cntrl), morpholino (MO), and overexpression (OE) conditions for (C) *Shh*, (D) *Ptch1*, (E) *Smo*, (F) *Cdon*, (G) *Boc*, (H) *Gas1*, (I) *Gli1*, (J) *Gli2*, and (K) *Gli3*. (L) Heatmap showing expression changes of cell cycle-related genes following *Gas1* morpholino (MO) knockdown and overexpression (OE) in duck and quail. (M) Heatmap displaying expression changes of WNT signaling pathway genes following *Gas1* morpholino (MO) knockdown and overexpression (OE) in duck and quail. Expression values are shown as log2 fold changes relative to control conditions, with red indicating upregulation and blue indicating downregulation. Significance (stars) is shown for comparisons between control and treatment groups with p-values are as indicated. $n = 3$ for each group. Error bars represent SEM.

increasing *Wnt11* and *Dkk3*. *Gas1* overexpression reduces *Wnt4*, *Wnt7A*, *Wnt2B*, *Wnt10A*, *Wnt3*, *Wnt3A*, and *Fzd6*. Overall, *Gas1* manipulation broadly affects WNT pathway gene expression in both species, with duck showing predominantly reduced ligand and receptor expression with overexpression and increased core mediator expression with morpholino; while quail show reduced ligand, receptor, and core mediator expression under both conditions.

2.7 | Gas1 promoter differs between duck and quail

Given higher expression of *Gas1* in duck, we assayed for species-specific differences in *cis*-regulatory elements. We sequenced and annotated the *Gas1* promoter across 2 kb upstream of the translation start site (ATG) in duck and quail and compared predicted transcription factor–binding sites (TFBS). Across this interval, the two promoters share multiple recurring predicted motifs, including a conserved block of homeodomain sites (e.g., HOXA1–HOXD4 with POU6F1) in the ~0.80–0.88 kb region upstream of ATG, NFAT-family motifs, and extended tracts of ZNF384 motifs associated with poly A runs (Table S18). Shared predicted sites also include multiple FOXN1 motifs at several positions, RBPJ motifs, clusters of C2H2 zinc-finger motifs (e.g., SP5, VEZF1, and ZNF354C/ZNF263, as well as MAZ), nuclear receptor motifs (e.g., NR2C2, NR1H3, and NR2E3), and dense bHLH/E-box modules with predicted binding for ARNT/HIF1A-class motifs and associated factors such as MAX, MLXIP, and MNT.

Features that diverge between duck and quail (Figure 7A) include multiple predicted TFBS present in duck but not quail, including RFX7 sites in the first kilobase, a DMRT3/DMRTA2/CLOCK block near ~1.47–1.48 kb, and additional distal motifs in the 1.79–1.90 kb region (including ZSCAN21, LBX1, ZIC1::ZIC2, ZIC3, and an additional FOXN1 site). In the proximal promoter, duck also contain an ~84–90 bp insertion immediately upstream of ATG, within which predicted motifs include SP5/ZNF354C and IKZF2/ZNF263. In contrast, quail-specific predicted TFBS include TFAP2E near the proximal promoter, additional proximal sites such as TFAP2A and SMAD2, a homeobox module (including NKX2-3, NKX2-8, NKX3-1, and ISL2) around ~1.36–1.37 kb together with NKX2-5 near ~1.39 kb, and a block of sites spanning ~1.43–1.60 kb that includes GMEB1, BCL11A, ETV6/ETV7, TCF7, SATB1, and ARID3A/ARID3B. Additional quail-only motifs in the distal promoter include HES1 (~1.95–1.96 kb), TEAD3 (~1.99–2.00 kb), and a distal IKZF2 site near ~2.00 kb.

We also identify 12 loci where SNPs switch predicted TFBS identity between species. Examples include NR2C2 in duck versus TFAP2E in quail, VEZF1/KLF1/2/7/15 in duck versus SMAD2 in quail, HIC2 in duck versus ZNF354C in quail, ISL2 in duck versus BARHL2 in quail, ZNF93 in duck versus ZNF549 in quail, SP5 in duck versus IKZF2 in quail, NR1H3/HIC2 in duck versus STAT3 in quail, RBPJ in duck versus NFATC1 in quail, SP5 in duck versus FOXN1 in quail, LIN54 in duck versus SOX10 in quail, and SOX10/11 in duck versus RHOXF1 in quail. We further observe species-specific differences in predicted TFBS motifs linked to putative SHH-responsive programs. In duck, we identify three including prominent E-box/bHLH modules with predicted ARNT::HIF1A-class binding around ~1.47–1.48 kb and HIF1A/ARNT::HIF1A-class motifs around ~1.69–1.70 kb, multiple FOXN1 motifs distributed across the promoter (including distal FOXN1 near ~1.90 kb), and distal motifs including LBX1 and ZIC family factors. In quail we identified nine motifs linked to SHH-responsive programs including the NKX/ISL2 module near ~1.36–1.37 kb and NKX2-5 near ~1.39 kb, a STAT cluster (including STAT1/STAT3/STAT4/STAT5B) overlapping an RBPJ site near ~1.84 kb, multiple BARHL2 motifs across the promoter, and distal bHLH motifs including ATOH1, NEUROD1/NEUROD2, NEUROG2, HAND2 (~1.81 kb) and HES1 (~1.95–1.96 kb). Several predicted motifs on the *Gas1* promoter are for genes not annotated in birds (i.e., a mismatch in motif-labelling, gene orthology, and/or nomenclature, which is consistent with TFBS libraries being heavily mammal-derived). These include predicted motifs for ZNF93, ZNF549, RHOXF1, ZNF354C, MAZ, and KLF1.

2.8 | Gas1 protein differs between duck and quail

To assay for species-specific variation in GAS1 protein structure, we cloned full-length duck and quail *Gas1* coding sequences (CDS) and compared them with those published for chick.[126] Chick and quail *Gas1* CDSs are 942 bp (excluding the stop codon), whereas duck is 1011 bp, and the CDS in all three species is a single exon. Within the CDS GC content is high in all species and differs modestly among them (chick 75.48%, quail 74.63%, duck 77.15%). Translation of these sequences yields GAS1 proteins enriched for amino acids encoded by GC-rich codons; A + G + P + R comprise 43.63% of chick GAS1 (A = 48, G = 39, p = 27, R = 23), 42.68% of quail GAS1 (A = 46, G = 38, p = 27, R = 23), and 44.81% of duck GAS1 (A = 48, G = 49, p = 29, R = 25). Overall, chick and quail have the same CDS length and

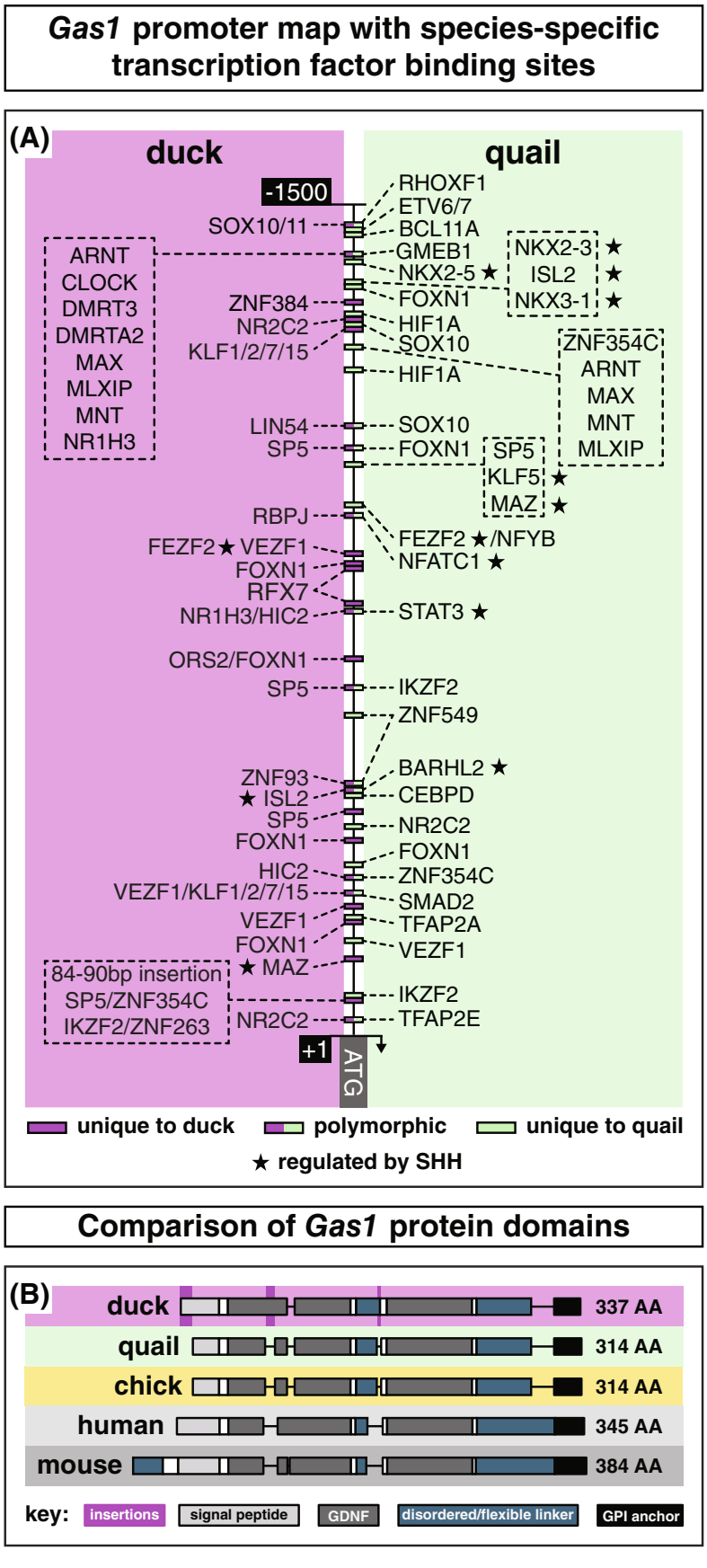

FIGURE 7 Legend on next page.

similar GC content, whereas duck have a longer *Gas1* CDS with higher GC content, and their translated protein contains more A + G + P + R residues.

Using a multi-species alignment, we compared the translated predicted amino acid sequences among duck, chick, quail, and representative mammals (i.e., human and mouse) (Figures 7B and S2). We annotated major structural components of GAS1 including an N-terminal signal peptide, two GDNF domain–containing regions, a disordered/flexible linker, and a C-terminal glycosylphosphatidylinositol (GPI)-anchor signal.[129–132] We find this architecture is conserved across all aligned GAS1 proteins. Quail and chick GAS1 share the same domain organization and are the same length (314 aa), whereas duck GAS1 is longer (337 aa) and contains multiple insertions relative to quail and chick. Based on amino acid alignment, these duck-specific differences localize primarily to low-complexity segments, including an N-terminal region in which duck GAS1 sequence contains additional residues (quail/chick share a short MPA sequence where duck contain an extended MLARHGGG segment), an internal insertion enriched in proline/glutamine residues (QP-rich) in the N-terminal half of the protein, and an expanded glycine/proline-rich region in the mid-portion of the sequence.

In addition to these insertion-associated length differences, quail and chick share multiple amino acid states that diverge from duck within otherwise conserved blocks, including an A → G at the start of a conserved segment (i.e., quail/chick ASAAS versus duck GSAAS), a quail/chick MAY where duck have MTY around ~260, and a shared quail/chick RCTPEC sequence where duck have RCTAEC. Quail and chick also differ from duck near the C-terminal portion, including a PEP segment versus AEP in duck, and a DGAGR segment versus DSAGR in duck. In the hydrophobic C-terminal region corresponding to the GPI-anchor signal, quail and chick share a similar terminal configuration (including a PPL terminus) that differs from duck (which terminates with AGL), and quail and chick lack an arginine present in duck. In contrast, human and mouse GAS1 are longer than the avian proteins (human 345 aa; mouse 384 aa) and share sequence features that differ from birds, including an extended N-terminal segment upstream of the avian start site. Human and mouse also contain a prominent low-complexity insertion in the C-terminal half of the protein present in both human and mouse but absent from duck, quail, and chick, while retaining the same basic domain architecture.

3 | DISCUSSION

3.1 | Early developmental parameter values establish species-specific jaw size

In his influential book *On Growth and Form*, originally published in 1917, D'Arcy Thompson addressed how changes in anatomical size and shape arise.[1,20] Thompson argued that coordinate scaling could alter body plan proportions and drive evolutionary transformations.[1] Since then, allometry and related mathematical approaches (e.g., power law equations) have been used to describe relationships among measured quantities (e.g., morphogen diffusion rates, gene expression levels, rates of maturation), to model differential growth (i.e., changes in size and shape) of parts of one organism, or to compare variation in the same or multiple body parts across species.[2,3,133,134]

Building on Thompson's theoretical framework, our empirical studies on mechanisms underlying avian jaw size provide additional evidence for how changes in developmental parameter values can scale to generate species-specific morphology.[9] Our previously published data, alongside quantitative and molecular analyses

FIGURE 7 Gas1 promoter map and protein domains. (A) Comparative map of *Gas1* promoter regions 1.5 kb upstream of the translation start site (ATG) showing predicted transcription factor binding sites (TFBS) in duck (pink) and quail (green). The promoter is oriented 5′ to 3′ with ATG at +1. Colored boxes represent predicted TFBS for specific transcription factors, with positions scaled relative to ATG. Duck-specific sites are shown as pink boxes, quail-specific sites as green boxes, and polymorphic sites (where SNPs alter TFBS identity between species) as boxes with both pink and green coloring. An approximately 84–90 bp insertion unique to duck is indicated. TFBS for genes known to be regulated by SHH signaling are marked with a star (★). (B) Comparison of GAS1 protein across duck, quail, chick, human, and mouse. Schematics show conserved domain organization including N-terminal signal peptide (light gray), GDNF domain-containing region (dark gray), disordered/flexible linker region (blue gray), and C-terminal GPI anchor signal (black). Protein lengths are indicated in amino acids (AA). Duck GAS1 (337 AA) contains multiple insertions (pink shading) relative to quail and chick (both 314 AA), primarily in low-complexity segments including N-terminal extensions, internal proline/glutamine-rich regions, and expanded glycine/proline-rich segments. Human (345 AA) and mouse (384 AA) GAS1 proteins show mammal-specific sequence features including N- and C-terminal extensions while maintaining the same basic domain architecture. (C) Model illustrating how species-specific *Gas1* levels modulate SHH signaling to regulate jaw size. In duck, elevated *Gas1* extends and buffers SHH signaling to maintain NCM proliferation and produce a larger jaw, whereas in quail, lower *Gas1* limits SHH signaling to promote earlier NCM differentiation and a smaller jaw.

performed here across multiple embryonic stages, indicate that species-specific differences in the mandibular arch emerge early in development. Divergence in these parameter values may compound into substantial morphological differences over extended incubation periods (28 days) of larger species like duck versus smaller species like quail (17 days).[135] These parameter values include initial size of the migratory NCM population allocated to the mandibular primordia (e.g., ~15% greater in duck), absolute time between developmental stages, and length of the cell cycle (e.g., 13.5 h in duck vs. 11 h in quail).[15] Our ability to model relative population size of duck and quail and mathematically replicate patterns observed in vivo supports the conclusion that changes in developmental parameter values are major determinants of species-specific jaw size during evolution.[9,15,33]

Our results align with theoretical and experimental work showing that variation in these parameter values directly affects diffusion, condensation, adhesion, differentiation, and other critical biochemical and cell–cell interactions.[136–141] Such processes are often mediated by morphogens that translate quantitative differences in developmental timing and cell populations into distinct morphological outcomes. From an evolutionary perspective, this provides a mechanistic framework by which relatively modest regulatory changes to genes and signaling pathways can be amplified into significant species-specific size differences. Our findings on the SHH pathway, which is known to pattern and scale organs such as the limb buds, neural tube, and craniofacial primordia by eliciting concentration-dependent proliferation and differentiation responses,[16,37,85,86,142–155] raise the possibility that modulation of individual pathway members can calibrate developmental parameter values underlying species-specific variation in jaw size.

3.2 | NCM may drive species-specific jaw size by modulating SHH signaling

Our study uncovers distinct temporal patterns and differential expression of members and targets of the SHH pathway in duck and quail. The temporal switch in SHH pathway gene expression from higher in duck at early stages (HH15–HH18) to higher in quail at later stages (HH21–HH27) may reflect distinct developmental strategies. During early stages, when NCM is actively migrating into the mandibular arch and proliferating,[15,156] duck may require elevated pathway activity to expand their larger mandibular mesenchyme population. In contrast, during later stages, quail may sustain higher pathway activation due to their accelerated developmental timeline and to promote relatively earlier differentiation. The three genes that do not follow this temporal switch (i.e., *Ptch1*, *Boc*, and *Gas1*) are receptors or co-receptors,[39–42,57,61] implying that receptor-level regulation may follow distinct evolutionary and developmental constraints relative to downstream effectors such as *Gli* transcription factors. Species-specific jaw size may therefore be achieved through regulatory changes at multiple hierarchical levels of the SHH signaling cascade. Notably, *Gas1* expression remains continuously elevated in duck.

Although spatial domains of *Gas1* are similar in both species, *Gas1* levels are up to 75-fold higher in duck than in quail. *Gas1* is expressed predominantly in mesenchyme rather than epithelium, reflecting that NCM is the primary constituent of mandibular mesenchyme.[15,106,107,122] While for technical reasons we were only able to examine *Gas1* at the transcriptional level, previous mouse studies show that GAS1 protein localization closely matches *Gas1* mRNA expression patterns.[67,157,158] Thus, whereas spatial patterns of *Gas1* expression are conserved across species, variation in expression levels may contribute to differences in SHH-mediated growth of the mandibular primordia by tuning the magnitude and range of pathway activity.

In addition, our quck chimeras demonstrate *Gas1* and *Gli1* are regulated by NCM. This contrasts with *Shh*, *Smo*, *Cdon*, and *Boc*, which appear less affected by NCM. Considering our prior work showing NCM controls species-specific size and shape,[14,15,17,19,81,87,107,108,159] this study adds *Gas1* and *Gli1* to the list of genes through which this process may be accomplished. Accordingly, we propose that axes of growth generating species-specific jaw size may be regulated by *Gas1*- and *Gli1*-mediated activation of SHH signaling. Unlike *Gli2* and *Gli3*, which can be processed into either activators or repressors depending on the presence of SHH ligand, *Gli1* lacks the N-terminal repressor domain and only functions as a SHH pathway activator.[49] Other studies show that various aspects of the SHH pathway affect tissue size, including changes in *Shh* enhancers,[160] variation in levels of SHH ligand,[86,155] differential regulation of SHH receptors,[100,102,161] transcriptional activity of target genes,[16,162] and variation in interacting co-factors.[163,164] Given this evidence for species-specific alteration of SHH signaling at multiple hierarchical levels, we tested whether pathway perturbation reveals distinct intrinsic sensitivities in duck versus quail.

3.3 | SHH pathway perturbation reveals species-specific regulatory strategies

Our inhibition and activation experiments uncover species-specific sensitivity to SHH signaling and point to

divergent strategies for pathway regulation. Duck exhibit robust compensatory responses to pathway inhibition, characterized by increased *Shh*, *Cdon*, and *Gas1*. Prior work shows that *Gas1* expression in mandibular mesenchyme is associated with regions where SHH activity is restricted by oral epithelium.[165] Consistent with this spatial relationship, inhibition of SHH signaling increases *Gas1* expression in duck, suggesting *Gas1* responds dynamically to changes in SHH pathway activity in a context-dependent manner likely shaped by local epithelial–mesenchymal interactions and additional regulatory inputs. Duck also show resistance to *Gas1* downregulation, even at high rSHH concentrations. This indicates duck may have evolved buffering mechanisms that not only maintain pathway homeostasis in response to perturbation[166] but also function by keeping *Gas1* elevated during normal development. Such stability likely enables this co-receptor to help propagate SHH ligand from its epithelial source to more cells across relatively longer distances in duck mandibular primordia.[58,167] Conversely, quail show minimal compensatory responses to inhibition but readily downregulate *Gas1* in response to pathway activation, indicating a more sensitive regulatory architecture that may reflect their accelerated maturation and contribute to smaller jaw size through effects on SHH signal range within the mandibular primordia. This shift in cell-intrinsic sensitivity parallels strategies observed in the zebra finch neural tube, where scaling is achieved not by modifying the SHH morphogen gradient alone, but by modulating the ratio of GLI2 and GLI3 to increase target cell responsiveness.[16]

The exceptional species-specific levels and sensitivity of *Gas1* point to this gene as an evolutionary hotspot where minor regulatory changes could calibrate SHH pathway output without disrupting core signaling mechanisms.[168] This developmental modularity is illustrated by genetic ablation of *Gas1* in mice, which selectively impairs structures dependent on low-threshold SHH signals while leaving high-threshold ventral cell types intact.[59–61,99] These threshold-specific effects demonstrate how expression levels can fine-tune morphological outcomes such as jaw size while preserving essential functions of the broader SHH network.[41] *Gas1*-mediated regulation of jaw size also aligns with studies on upper jaw development, where SHH signaling activity contributes to continuous variation in facial morphology.[82,83,86,169] Consistent with the broad suite of pathway members that regulate SHH pathway activity in the midface, including SHH-binding proteins such as CDON, BOC, and HHIP, along with GLI proteins,[59,99,100,102,162] our data suggest the lower jaw operates under a similar regulatory logic. *Gas1* may be required in these domains to potentiate signaling in peripheral regions exposed to low levels of SHH. While scaling in other avian organ systems is achieved by modulating how cells respond to SHH through downstream transcription factors, our results point to species-specific differences in *Gas1* expression as an additional mechanism for modulating SHH pathway output in the lower jaw. Thus, channeling evolutionary change through *Gas1* could facilitate a range of threshold-specific shifts during morphogenesis and expand the repertoire of regulatory strategies that diversify the SHH signaling network such as the ZRS enhancer[170–172] and *Gli* genes, which have undergone functional diversification and can act as context-dependent transcriptional regulators through a combinatorial code.[173–175]

3.4 | Gas1 regulates mandibular growth and is linked to cell cycle regulation

Since its identification in 1988,[176] *Gas1* has been implicated in a variety of biological contexts. For example, *Gas1* inhibits the transition from G0 to S phase, induces growth arrest through p53,[129,177] and functions as a tumor suppressor by regulating apoptosis.[178] During embryogenesis, *Gas1* can also function as a positive regulator of cell proliferation, differentiation, and survival.[157,179–181] Likewise, our overexpression experiments corroborate the importance of *Gas1* in maintaining cell number and the size of the mandibular primordia. Knockdown of *Gas1* also reduces jaw size as evidenced by left–right asymmetry in embryos treated with morpholinos. This is consistent with *Gas1* loss-of-function studies in mice that produce smaller jaws.[61,67] In light of the established role of *Gas1* in cell cycle regulation[129,131,179] and the effects of *Gas1* on cell number, we propose that *Gas1* serves as a conduit for specifying species-specific jaw size.

The apparent paradox that *Gas1* overexpression in duck and quail reduces mandibular cell number and jaw size, while *Gas1* knockdown in quail also leads to smaller jaws, is consistent with the non-linear, threshold-dependent nature of SHH signaling.[86,182,183] In such a threshold-dependent system, small deviations from an optimal signaling range can produce similar phenotypic outcomes.[184,185] Our results imply *Gas1* levels must be precisely calibrated for normal jaw development, with duck and quail occupying different positions along the SHH dose–response curve, potentially reflecting the role of *Gas1* as a co-receptor in helping to shape SHH signaling gradients. In duck, which maintains high *Gas1* expression, overexpression may push the system beyond an upper threshold at which *Gas1* becomes inhibitory through mechanisms such as ligand sequestration or

receptor interference. This could produce inhibitory effects on SHH signaling equivalent to gene expression changes we observe, and consistent with the smaller jaw size reported for chicken and other amniote embryos treated with cyclopamine.[91,186,187] Similarly, *Gas1* overexpression may push quail beyond an optimal range and produce comparable inhibitory effects on mandibular growth, while *Gas1* knockdown may push quail below the threshold required for adequate SHH pathway activation. This explanation is consistent with our SHH pathway perturbation experiments, which demonstrate quail exhibit high sensitivity to both activation and inhibition and lack compensatory mechanisms present in duck. In contrast, higher baseline *Gas1* levels may allow duck to operate closer to an upper inhibitory limit under normal developmental conditions.

Higher *Gas1* expression in duck compared to quail, in conjunction with established roles of *Gas1* in regulating cell proliferation and differentiation, suggests species-specific differences in *Gas1* levels may contribute to distinct patterns of mandibular growth. This interpretation is consistent with previous observations that duck exhibit extended proliferative growth and a longer cell cycle relative to quail,[15,107] as well as studies showing that *Gas1* acts as a negative regulator of growth by reducing cell proliferation[188,189] and promoting cell cycle arrest and differentiation.[181,190] The threshold effects we observe likely arise because proper mandibular development requires precise regulation of *Gas1* activity. Excessive *Gas1* may over-suppress NCM proliferation or promote premature differentiation, whereas insufficient *Gas1* may impair cell cycle progression, with both leading to reduced mandibular growth. This interpretation is further supported by previous work from our lab demonstrating that NCM governs jaw size through differential expression of *Runx2* (with significantly higher levels in quail) and species-specific regulation of the cell cycle, which acts like an autonomous clock controlling the transition from proliferation to osteogenic differentiation.[9,107] Overexpressing *Runx2* augments osteogenesis and reduces jaw size.[191] Our results support a model (Figure 7C) in which species-specific differences in *Gas1* expression and SHH pathway sensitivity contribute to regulation of NCM population size and establishment of distinct growth trajectories within the mandibular primordia.

3.5 | Gas1 dosage reveals species-specific differences in gene network architecture

Species-specific threshold effects and differential responses to *Gas1* perturbation indicate distinct gene regulatory network architecture and buffering capacity between duck and quail. Our RNA-seq analyses confirm these network differences manifest at the transcriptomic level and reveal a clear asymmetry between species. Duck exhibit bidirectional sensitivity to shifts in *Gas1* dosage, where knockdown and overexpression both trigger large, convergent transcriptional responses. This pattern is consistent with duck operating near an optimal *Gas1* baseline in which deviations in either direction induce compensatory regulatory programs. In contrast, quail exhibit a comparatively restricted transcriptional response to *Gas1* perturbation, reflecting differences in buffering capacity and pathway sensitivity.

The differential responses of SHH pathway members to *Gas1* perturbation reveal distinct mechanisms for maintaining signaling homeostasis and provide further molecular evidence for divergent regulatory architectures. These transcriptomic patterns mirror sensitivities observed in our biochemical manipulation experiments in which duck exhibit robust compensatory responses to cyclopamine treatment (upregulating *Shh*, *Cdon*, and *Gas1*) whereas quail show minimal response. In duck, *Gas1* perturbation triggers downregulation of *Shh* and *Boc* under both morpholino and overexpression conditions, with overexpression also increasing *Smo* and *Gli3*. These duck-specific effects on multiple pathway components may reflect the role of *Gas1* in stabilizing SHH signaling across larger mandibular primordia.

In contrast, quail are strongly affected by *Gas1* morpholino treatment, with pronounced downregulation of *Shh* and *Gli* genes. However, quail show minimal transcriptional responses to *Gas1* overexpression, where only *Gas1* itself is significantly increased (reflecting the exogenously overexpressed transgene). This asymmetry parallels the limited responsiveness of quail to cyclopamine and their high sensitivity to rSHH-mediated *Gas1* downregulation, in line with a more constrained regulatory architecture in which reduced *Gas1* disrupts SHH pathway activity whereas increased *Gas1* produces relatively little transcriptional change. Reduction of *Shh* following *Gas1* perturbation in both species further implies *Gas1* may influence *Shh* regulation indirectly through crosstalk with other signaling pathways rather than solely through modulation of downstream SHH pathway components.

Such crosstalk likely involves WNT signaling, supported by recurring GO enrichment of WNT-associated programs across treatment conditions in both species, together with coordinated changes in multiple WNT ligands, receptors, and downstream signaling components. These findings are consistent with known interactions between SHH and WNT signaling networks during craniofacial development,[65,192–197] and evidence that

WNT signaling can directly regulate Shh transcription through TCF/LEF1 binding sites in Shh enhancers.[198,199] The broader reduction of WNT pathway components observed in duck suggests extensive disruption of developmental signaling programs associated with proliferation, differentiation, and fate specification, whereas comparatively targeted WNT responses in quail may reflect differences in signaling network connectivity or compensatory regulation. These broader signaling network changes likely contribute to the smaller jaws observed following *Gas1* perturbation. Collectively, these findings point to *Gas1* as a developmental rheostat, fine-tuning the coordination and magnitude of multiple signaling pathways required for appropriate growth trajectories.

Despite the known role of *Gas1* in regulating cell cycle progression, *Gas1* manipulation only affects a limited number of cell cycle genes, which are distinct in each species. However, the genes affected are important for cell cycle regulation and their disruption may directly relate to smaller jaw size phenotypes we observe. In duck, *Gas1* overexpression upregulates *Ccnb3* and *Ccnk*, which are two cyclins implicated in standard mitotic progression and transcriptional elongation,[200–204] while *Gas1* knockdown increases the checkpoint inhibitor *Cdkn1A* (*p21*). Given *p21* is a well-established cyclin-dependent kinase inhibitor,[205,206] its specific induction following *Gas1* depletion implies baseline *Gas1* activity is required to suppress cell cycle checkpoints and maintain cell proliferation. Conversely, quail seem to bypass these classical checkpoints and instead, *Gas1* knockdown downregulates *Ccni*, which is a cell survival-linked factor,[207] and upregulates *Ccnl2*, which is a pre-mRNA splicing regulator.[208] Thus, *Gas1* disruption triggers standard cell cycle arrest pathways in duck but alters survival and RNA splicing mechanisms in quail, with both species-specific responses ultimately converging to decrease cell numbers required for normal jaw outgrowth.

Multiple factors may explain the small number of canonical cell cycle regulators identified across these treatments. Our RNA-seq analysis at HH24 represents only a limited temporal snapshot and, because transcriptional changes frequently precede cellular and morphological events, this single time point may miss earlier or later waves of gene expression. Also, the cell cycle is extensively controlled at post-transcriptional and post-translational levels,[209,210] which may explain why changes in cell number and jaw size are not accompanied by broader transcriptional changes in cell cycle genes. Thus, *Gas1* likely influences jaw size through developmental and growth-regulatory mechanisms that extend beyond direct transcriptional control of cell cycle genes, as evidenced by GO enrichment of cell cycle-adjacent processes such as p53-mediated DNA damage response and growth control pathways.[177] In addition to altered expression of canonical cell cycle genes, *Gas1* perturbation may influence cell number indirectly through effects on SHH-dependent cell survival signaling,[63] WNT-mediated cell fate specification,[211] and other SHH-independent *Gas1* functions.[67,212,213] Consequently, reductions in mandibular growth may arise through combined effects on processes related to proliferation, apoptosis, specification, cellular stress responses, and metabolic state.

3.6 | Regulatory and coding changes to Gas1 may underlie species-specific jaw size

Our finding that *Gas1* is expressed at substantially higher levels in duck than quail, and that this difference is mediated by NCM, implicates *cis*-regulatory evolution in species-specific expression of *Gas1* within NCM-driven developmental programs. Given the avian lineages containing duck and quail diverged over 100 million years ago,[214] discovery of multiple sequence differences within the proximal ~2 kb upstream region of *Gas1*, including a duck-specific insertion and numerous predicted TFBS differences, is consistent with divergence in *cis*-regulatory architecture. Distal enhancers outside the regions we examined may also contribute to species-specific *Gas1* regulation.

Several TFBS differences map to transcription factor families that are established components of NCM and craniofacial transcriptional programs. For example, quail contain predicted TFAP2A/TFAP2E binding sites not detected in duck. TFAP2A (AP-2α) is required for craniofacial development and NCM-related morphogenesis.[215–220] In addition, one SNP-dependent motif swap between species is predicted to replace SOX-family binding logic (e.g., SOX10/11 in duck) with a RHOXF1-like motif in quail. SOX10/11 affect multiple NCM derivatives and craniofacial development[92,221–223] whereas RHOXF1 is not annotated in the avian genome and is thought to have evolved in the mammalian lineage.[224] This difference may reflect either a prediction artifact (e.g., bias towards mammalian TFBS in the JASPAR database) or a non-functional motif that attenuates SOX10/11-mediated regulation of *Gas1* in quail. Alternatively, even though genes including RHOXF1 (and also ZNF93, ZNF549, ZNF354C, MAZ, and KLF1) are not annotated in birds, the motif may still be biologically meaningful at the level of DNA-binding specificity, potentially recognized by avian transcription factors with similar sequence preferences. Quail also contain predicted motifs for pathway-linked transcriptional regulators active in craniofacial NCM regulatory networks, including

a SMAD2 site consistent with potential TGFβ responsiveness, whereas duck contain species-specific motifs such as OSR2 at one polymorphic locus. *Osr2* is expressed in mandibular NCM and is essential for normal craniofacial development.[225–228]

We also find species-specific differences in how WNT signaling may interact with the *Gas1* promoter. Quail contain a predicted TCF7 binding site, whereas duck harbor multiple motifs for SP5 (including a duck-specific insertion), which function as transcriptional effectors of canonical WNT/β-catenin signaling.[229–233] These features suggest *Gas1* may be differentially responsive to WNT pathway activity between species, either through direct β-catenin–TCF-mediated transcription in quail or through SP5-associated regulatory logic in duck. Duck-specific distal motifs also include multiple ZIC sites (ZIC1, ZIC2, and ZIC3), which modulate WNT/β-catenin transcriptional output in other developmental contexts,[234–236] are regulated by SHH,[237] and interact with GLI proteins.[238–240] These differences indicate that divergence in WNT-associated transcriptional inputs could contribute to species-specific tuning of *Gas1*.

Quail-specific distal motifs also include predicted bHLH binding sites such as HAND2. Conditional *Hand2* perturbations in NCM disrupt mandibular development[241,242] and synergistic interactions between HAND2 and GLI3 affect jaw patterning.[163] Although we do not identify predicted GLI TFBS in the *Gas1* promoter of either species, several putative SHH-responsive transcription factors are present. For example, HES1 and ATOH1 are direct transcriptional targets of GLI proteins, supported by GLI2 occupancy at the *Hes1* promoter[243,244] and GLI2-dependent activation at regulatory regions within the *Atoh1* locus.[245] NKX2-5 is also likely GLI2-responsive, as reporter assays show that multiple predicted GLI-binding sites in its promoter can be activated by GLI2.[246]

Even though *Gas1* promoters in duck and quail share a conserved core of predicted TFBS, they differ in several features, including a duck-specific proximal insertion, distinct motif landscapes, variation in SHH-responsive elements, and SNPs that alter TFBS identities. These *cis*-regulatory differences may provide a basis for SHH sensitivity patterns we observe in *Gas1* expression, including differential responses to cyclopamine and rSHH treatment between species. Because GAS1 functions as a Hedgehog co-receptor that participates in ligand reception and transfer to PTCH receptors,[58,247] differences in promoter architecture and transcription factor inputs could modulate how strongly *Gas1* expression is coupled to SHH-dependent transcriptional states in each species. SHH pathway activation can downregulate *Gas1* (along with other co-receptors) in some contexts, consistent with negative-feedback regulation in Hedgehog signaling.[61,167] Moreover, in the absence of *Gas1*, PTCH1 binds SHH less efficiently, reducing sensitivity of responding cells, particularly at low to intermediate ligand concentrations and over long ranges.[57,60] This context dependence, along with SHH-independent functions of *Gas1*,[213] lends support to the idea that relatively small regulatory changes could fine-tune pathway output during patterned outgrowth.

Although the single-exon structure of *Gas1* may limit splicing-based regulatory complexity, CDS variations we identified, including insertions and substitutions, may influence protein function. For example, duck-specific insertions within low-complexity regions and substitutions within conserved domains, may alter GAS1 protein stability, membrane localization, or binding affinity for SHH ligand, while changes to the C-terminal GPI-anchor region could affect membrane tethering and spatial distribution. Notably, the basic domain architecture of GAS1 is conserved across species, indicating these sequence differences likely modulate rather than disrupt core protein function, and their localization within these regions and the GPI-anchored C-terminal domain suggests potential effects on protein–protein interactions and membrane-associated signaling dynamics. These structural differences represent an additional layer of variation potentially affecting GAS1 activity, acting alongside regulatory differences to shape SHH signaling dynamics in the mandibular primordia.

Taken together, our findings indicate that species-specific variation in jaw size emerges through quantitative tuning of signaling across multiple hierarchical levels of regulation, similar to what we previously identified for the TGFβ pathway at later embryonic stages when bone is being deposited and resorbed in the jaw skeleton.[107,108,159] Although SHH and TGFβ signaling act during distinct periods of development, in both cases species-specific differences in jaw size are associated with modulation of signaling components at the levels of ligands, receptors, and downstream effectors. In this context, *Gas1*-mediated SHH signaling influences proliferation and the transition to differentiation within early mandibular mesenchyme, whereas TGFβ signaling affects later growth and remodeling of the jaw skeleton. These effects build upon species-specific differences in NCM allocation to the mandibular arch at early stages and subsequent proliferation dynamics that progressively expand the jaw progenitor population.[15] An important next step for understanding *Gas1*-mediated effects on jaw size will be determining how these multiple levels of regulation interact dynamically during development to shape SHH signaling output and establish distinct growth trajectories within the mandibular primordia. Defining mechanisms through

which NCM integrates these interacting processes across species may ultimately explain how subtle quantitative changes in developmental signaling translate into evolutionary transformations in scaling and form.

4 | EXPERIMENTAL PROCEDURES

4.1 | Use of avian embryos

For all experiments, we adhered to accepted practices for humane treatment of avian embryos as described in S3.4.4 of the *AVMA Guidelines for the Euthanasia of Animals: 2013 Edition*[248] and S5.3 of the *AVMA Guidelines for the Euthanasia of Animals: 2020 Edition*.[248] Embryos were not allowed to hatch, and no live vertebrate animals were used in this study. Fertilized eggs from white Pekin duck (*Anas platyrhynchos*), Japanese quail (*Coturnix coturnix japonica*), and Rhode Island red chicken (*Gallus gallus*) were obtained from commercial suppliers (AA Labs, Westminster, CA and Petaluma Farms, Petaluma, CA) and incubated at 37.8°C and 85 to 87% humidity until reaching stages appropriate for surgery, manipulations, collection, and/or analysis.

To visualize embryos at early stages, a small amount of sterile 0.5% Neutral Red solution (N4638, Sigma-Aldrich, MilliporeSigma, St. Louis, MO) was brushed lightly over the embryo with a blunt glass rod. Embryos were staged using the Hamburger and Hamilton (HH) staging system, a well-established standard that is based on external morphological characters and that is independent of body size and incubation time.[109,113,114,119,135] Absolute times of incubation to reach a particular embryonic stage for duck and quail are in Figure 1A and Table S1.

4.2 | Isolation of mandibular primordia

Using forceps, mandibular primordia were cut along the proximal junction at each side of the maxillary primordia and placed into RNase-free ice-cold 1x phosphate buffered saline (PBS; BP3991, Fisher Scientific, Hanover Park, IL). For RNA extraction, isolated mandibular primordia were transferred into 1.5 mL microcentrifuge tubes with as little 1x PBS as possible. Samples for RNA extraction were flash frozen on dry ice in 100% ethanol and stored at −80°C until ready to process.

4.3 | Quantification of mandibular mesenchyme

Mandibular mesenchyme was quantified in HH18, HH21, HH24, and HH27 duck and quail embryos. To separate mandibular mesenchyme from overlying epithelium,[249] trypsin-pancreatin solution was made at room temperature by dissolving (i.e., stirring for 15 min) 2.25 g of trypsin (T7409-100G, Lot # 029 K7012, Sigma-Aldrich, MilliporeSigma, St. Louis, MO) and 0.75 g of pancreatin (P1625-100G, Lot # SLBP2575V, Sigma-Aldrich, MilliporeSigma, St. Louis, MO) in Hanks' Balanced Salt Solution (HBSS; 14,175,095, ThermoFisher Scientific by Life Technologies Corporation, Grand Island, NY). Pre-made trypsin-pancreatin solution was stored at −20°C in 5 mL single use aliquots. The solution was thawed prior to dissection, filter sterilized using a 5 mL syringe (309646, BD Vacutainer Labware Medical, Fisher Scientific, Hanover Park, IL) with 0.2 μm filter (431219, Corning Life Sciences Plastic, Lowell, MA) and kept on ice until ready for use.

Isolated mandibular primordia were incubated in 0.5 mL trypsin-pancreatin solution at 4°C on a rocker. Incubation length varied for each stage and species due to differences in size. Incubation times are listed in Table S19. Trypsin-pancreatin solution was replaced with 1 mL of ice-cold HBSS to stop the enzymatic reaction. Samples were washed for 5 min at 4°C on rocker. The solution was replaced with 1 mL of ice-cold Dulbecco's Modified Eagle's Medium (DMEM; 11965092, ThermoFisher Scientific by Life Technologies Corporation, Grand Island, NY); samples were kept on ice.

Mandibular epithelium was removed using two pairs of sharp forceps. Isolated mandibular mesenchyme was transferred into 1.5 mL microcentrifuge tubes containing 200 μL for HH18, 500 μL for HH21 and HH24, and 900 μL for HH27 of DMEM; homogenized by pipetting until all clumps were separated into single cells; and kept on ice. Mandibular mesenchymal cells (i.e., cell number per mandibular primordium) were counted using a hemacytometer (1492, Hausser Scientific Partnership, Fisher Scientific, Hanover Park, IL) in combination with MIPAR image analysis software (Version 3.0, Columbus, OH).[250]

4.4 | Modeling relative population size

To model cell counts per mandibular primordia, the size of the cell population, cell cycle length, and absolute developmental time were considered. Relative cell population size at HH13, HH15, HH18, HH21, HH24, and HH27 in duck and quail was calculated as ax^b, where x represents cell division (i.e., doubling event when a mother cell divides in two daughter cells) and is equal to 2, b represents the number of cell cycles that the cell population for a particular species is able to go through

within a period of time (e.g., from HH18 to HH21) and is calculated as follows $\frac{absolute\ time\ [hours]\ from\ earlier\ stage\ to\ next\ stage}{cell\ cycle\ length}$, and a is relative cell population at a previous developmental time point (i.e., earlier stage). Starting relative population size at HH13 was set to 1 for quail and calculated for duck by dividing the duck *Sox10*-positive cell population by that in quail using published values.[15]

4.5 | Extraction of RNA

Total RNA was extracted from mandibula primordia at HH15, HH18, HH21, HH24, and HH27; and from mandibular mesenchyme, mandibular epithelium, explant tissue cultures, whole heads, and forelimbs at HH24 using the Arcturus PicoPure RNA Isolation kit (KIT0214, Applied Biosystems, Life Technologies Corporation, Grand Island, NY) following the manufacturer's protocol with the following modifications: For whole mandibular primordia and explant tissue culture, 85 μL of extraction buffer was added to each sample. Sample homogenization was carried out in a Bead Mill 24 Homogenizer (15-340-163, Fisher Scientific, Hanover Park, IL) at 4 m/s for 15 s for 1 cycle. Samples were spun down for 2 min at 16,000 RCF then incubated in a water bath at 42°C for 30 min. Samples were vortexed for 2 s in the middle of the incubation.

Extraction tubes were pre-treated following manufacturer's directions. 85 μL of RNase-free 70% ethanol, made by diluting 100% ethanol (BP28184, Fisher Scientific, Hanover Park, IL), was added to tissue extract and mixed by pipetting 20 times up and down. Extract was transferred into a pre-conditioned purification column and centrifuged following manufacturer's directions. 180 μL of RNase-free 70% ethanol was added onto the column and centrifuged for 1 min at 16,000 RCF. The remaining protocol was carried out following manufacturer's directions. Residual genomic DNA was removed in on-column step using RNase-free DNase Set (79254, Qiagen, Germantown, MD), 5 μL of DNase I mixed with 35 μL of RDD buffer. Total RNA was eluted in 21 μL of elution buffer for whole mandibular primordia at HH18, 21, 24, and 27 and explant tissue culture; and in 16 μL of elution buffer for whole mandibular primordia at HH15.

Concentration and purity of RNA were assessed using a NanoDrop spectrophotometer (ND-1000, ThermoFisher Scientific by Life Technologies Corporation, Grand Island, NY) and/or Qubit 4 fluorometer (Q33222, Invitrogen, Hanover Park, IL) according to the manufacturer's instructions. Total RNA extracted in elution buffer was stored at −80°C.

4.6 | Preparation of cDNA libraries

Depending on total RNA amount per sample, 100, 200, or 400 ng of total RNA were reverse transcribed to cDNA in a 20 μL reverse transcription reaction using 5 μL of iScript reverse transcription supermix (1708841, Bio-Rad Laboratories, Hercules, CA), a corresponding volume of total RNA template (calculated with the formula: $\frac{100,\ 200\ or\ 400\ [ng]}{total\ RNA\ concentration\ \left[\frac{ng}{\mu L}\right]}$), and sufficient nuclease-free water to bring total volume to 20 μL.

The cDNA synthesis reaction involved four steps: 25°C for 5 min, 42°C for 30 min, 85°C for 5 min, and 4°C hold in a thermocycler (C1000 Touch Thermal Cycler, Bio-Rad Laboratories, Hercules, CA). Lid temperature was set to 105°C. cDNA libraries were stored at −20°C.

4.7 | Designing and validating primers for RT-qPCR

Species-specific primers were designed for *r18s*, *Shh*, *Ptc1*, *Cdon*, *Boc*, *Smo*, *Gas1*, *Gli1*, *Gli2*, and *Gli3* using Geneious Prime (Biomatters, San Francisco, CA) (i.e., bioinformatics suite that incorporates Primer 3[251,252]). Primer sequences are listed in Table S20. Design criteria for primers included a product size between 70 and 200 bp (with optimal being 150 bp); a primer size minimum of 18 bp and maximum of 27 bp (with optimal being 20 bp); a T_m minimum of 50°C and maximum of 65°C (with optimal being 60°C); a GC content minimum of 45% and maximum of 60% (with optimal being 50%); a maximum Tm difference for primer pair of 5°C; a maximum dimer Tm of 40°C; a maximum 3′ stability of 9; a GC clamp of 1; and a maximum Poly-X of 3. The Santa-Lucia 1988 formula and salt concentration were set for Tm calculation with concentration settings of 50 mM for monovalent cations, 3 mM for divalent cations, 500 nM for oligos, and 0.8 mM for dNTPs. Gene sequences were checked for SNPs and those regions were avoided. Primer pairs for all genes spanned the same region for both species. For genes with multiple splice variants, primers were designed to regions present in all known isoforms. To prevent potential amplification of genomic DNA, all primer pairs, except for *Gas1* (which has a single exon), were designed to span exon-exon junctions. All potential primer pairs were blasted using Primer Blast[253] against genomes of duck and quail to avoid cross reactivity and amplification of unintended target sequences. Selected primer pairs were ordered from IDT (Integrated DNA Technologies, Coralville, IA) with standard desalting. Lyophilized primers were diluted in an appropriate amount of RNase/DNase free

water to make a stock concentration of 100 μM, which was stored at −20°C. Prior to use, stock solution was diluted 1:10 (i.e., working concentration).

To validate pan- and species-specific primers, RNA was extracted from whole heads and forelimbs of HH24 duck and quail as described above. 400 ng of RNA were reverse transcribed to cDNA and cDNA was diluted to a concentration of 2 ng/μL (1×). Standard curves with five serial dilutions (1:4, 1:16, 1:64, and 1:256) for each species-specific primer pair were generated from a 25 μL reaction mixture (1.5 μL of forward primer at working concentration, 1.5 μL of reverse primer at working concentration, 4 μL of cDNA, 6 μL of RNase/DNase free water, and 12.5 μL of iQ SYBR-Green Supermix [1708884BUN, Bio-Rad Laboratories, Hercules, CA]), run in technical triplicates on hard-shell PCR white 96-well plates (HSP9601, Bio-Rad Laboratories, Hercules, CA), sealed with optically clear microseal film for PCR plates (MSB1001, Bio-Rad Laboratories, Hercules, CA), and following the protocol described below. Controls for each run included no reverse transcription and no cDNA. Melt curves were checked for primer specificity (i.e., single product) and for excluding samples with potential genomic DNA contamination. To confirm correct product size, 1x samples were run on a 1% Agarose gel (BP1356-500, Fisher Bioreagent, Fisher Scientific, Hanover Park, IL) in 1x TAE buffer at 110 V for 30 min. Quick-Load 100 bp Ladder (N0467S, New England BioLabs, Ipswich, MA) was used as a size reference.

For selected primers, products were amplified in a 25 μL PCR reaction mixture using a thermocycler (C1000 Touch Thermal Cycler, Bio-Rad Laboratories, Hercules, CA). PCR reaction reagents included 2.5 μL of 10x Buffer (42-800B3, Apex Bioresearch Products, Genesee Scientific, El Cajon, CA), 0.5 μL of dNTPs (17-106, PCR Biosystems), 0.75 μL of $MgCl_2$ (42-800B3, Apex Bioresearch Products), 1.25 μL of DMSO (D128-500, Fisher Chemical, Fisher Scientific, Hanover Park, IL), 0.125 μL of Taq (42-800B3, Apex Bioresearch Products), 1.25 μL of forward primer at working concentration, 1.25 μL of reverse primer at working concentration, 13.0 μL of DNase/RNase-free water, and 4.375 μL of cDNA at the concentration of 2 ng/μL. The protocol for product amplification was: Step 1, 94°C for 2 min; step 2, 94°C for 2 min; step 3, 57.5°C for 30 s; step 4, 72°C for 1 min; steps 2 to 4 were repeated 39 times; step 5, hold at 4°C. Lid temperature was set to 105°C. To verify primer pairs, PCR products were cleaned and sequenced (Molecular Cloning Laboratories, South San Francisco, CA).

4.8 | Analysis of gene expression by RT-qPCR

4.6 μL aliquots of cDNA (1 ng/μL) were prepared and stored in 0.2 mL snap strip PCR tubes with dome caps (490003-692, GeneMate – BioExpress, VWR International, Brisbane, CA) at −20°C prior to RT-qPCR plates preparation. Only a portion (i.e., volume necessary to run RT-qPCR for selected genes and primer pairs) of total volume of working solution for each sample was aliquoted and the remaining volume stored in 0.5- or 1.5-mL microcentrifuge tubes at −20°C until ready for next usage to prevent the number of freeze–thaw cycles.

RT-qPCR was performed in a C1000 Touch Thermal Cycler with a CFX96 Real-Time System (1855196, Bio-Rad Laboratories, Hercules, CA). Reaction mixture for each well contained 1.25 μL of forward primer at working concentration, 1.25 μL of reverse primer at working concentration, 2 μg of cDNA (i.e., 2 μL at the concentration of 1 ng/μL), 10 μL of iQ SYBR-Green Supermix (1708884BUN, Bio-Rad Laboratories, Hercules, CA), containing dNTPs, iTaq DNA polymerase, $MgCl_2$, SYBR Green I, enhancers, stabilizers, and fluorescein, and 5 μL of RNase-free water. Samples were run in technical duplicates on hard-shell PCR white 96-well plates (HSP9601, Bio-Rad Laboratories, Hercules, CA) sealed with optically clear microseal film for PCR plates (MSB1001, Bio-Rad Laboratories, Hercules, CA) using tested protocol. Protocol steps were: step 1, 95°C for 3 min; step 2, 95°C for 10 s; step 3, 60°C for 30 s and a plate read; steps 2 and 3 were repeated 39 times; step 4, 95°C for 10 s; step 5, melt curve of 60–90°C for 5 s at each 0.5°C with a plate read. Lid temperature was set to 105°C. Melt curves were used to assess specificity of primers and to exclude samples with potential genomic DNA contamination. Gene expression levels were quantified using the Pfaffl method.[254] Levels were normalized to *r18s*.

4.9 | Generating probes for in situ hybridization

PCR primers were designed against the coding region of *Gas1* using Primer3[252] targeting a conserved region in duck and quail that would generate a ~ 650 bp probe. Primers were synthesized with and without T7 RNA polymerase promoter consensus sequence 5′-TAA TAC GAC TCA CTA TAG GG −3′ as a primer tail. The forward primer with the T7 RNA polymerase promoter was used to generate sense template and the reverse primer with T7 RNA polymerase promoter was used to generate antisense template. Q5 Hot Start High-Fidelity DNA Polymerase (M0493L, New England BioLabs, Ipswich, MA) was used to amplify templates for in vitro transcription. In vitro transcription was carried out using T7 RNA polymerase (M0251S, New England BioLabs) following the manufacturer's directions with digoxigenin (DIG) RNA Labeling Mix (11277073910, Roche, Basel, Switzerland) to generate DIG labeled probe. RNaseOUT

(10777019, Invitrogen, Carlsbad, CA) was used to protect RNA from degradation during synthesis. In vitro transcription was carried out at 37°C for 2 h. Following in vitro transcription, DNA was degraded using DNase I (4716728001, Roche, Basel, Switzerland). RNA probes were precipitated with LiCl and ethanol. RNA probes were resuspended in RNAse free MilliQ water and then mixed with an equal volume of formamide (VWRV0606-100ML, VWR, Radnor, PA) to stabilize RNA. Probes were stored at −20°C until ready for use. Primer sequences for duck and quail *Gas1* probes are listed in Table S21.

4.10 | Analysis of Gas1 expression by in situ hybridization

Mandibular primordia were isolated from duck and quail embryos at HH21 and HH27 using forceps and placed in RNase-free ice-cold 1x PBS. Samples were transferred into 15 mL conical tubes and fixed at 4°C for 2 h in 4% paraformaldehyde (PFA) generated from 32% PFA and diluted with 1X PBS. Samples were washed three times for 30 min at room temperature in 1x PBS followed by 30 min washes in 25%, 50%, and 75% methanol in 1x PBS and three times in 100% methanol (A412-4, Fisher Chemical, Fisher Scientific, Hanover Park, IL). Samples were stored at −20°C in 100% methanol until processing.

Whole mount in situ hybridization was performed following published protocols.[15,106] Proteinase K (P6556, Sigma-Aldrich, MilliporeSigma, St. Louis, MO) in 1x PBS was used at a concentration of 10 μg/mL for HH21 embryos and 20 μg/mL for HH27 embryos. Incubation times were 25 min for HH21 embryos and 15 min for HH27 embryos. Following the color reaction, developed for 2 h at room temperature then for 14 h at 4°C, mandibular primordia were imaged on a stereo dissecting microscope under brightfield illumination (MZFLIII-TS, Leica Microsystems, Buffalo Grove, IL).

4.11 | Generation of chimeric embryos

Quail and duck were incubated until stage matched at HH9.5 (about 32 h for quail and 55 h for duck) (Figure 1A). To generate chimeric "quck" embryos, bilateral grafts of neural folds containing presumptive NCM from the anterior hindbrain and midbrain (Figure 3A) were excised from quail donors and transplanted into duck hosts with a comparable region of tissue removed using flame-sharpened tungsten needles (Tungsten wire, 7190, A-M Systems, Sequim, WA) and hand-made Spemann pipettes.[255] Orthotopic control grafts were performed as done previously.[77,85,104,256,257] After surgery, eggs were sealed with tape (3 M Scotch Transparent Film Tape 600, 3 M United States, St. Paul, MN) and placed in the incubator until reaching stages for collection and analysis.

4.12 | Culture of mandibular primordia and biochemical treatments

For explant cultures, dissected mandibular primordia were processed as described previously.[14,106] Briefly, isolated mandibular primordia were placed onto a small circular piece of nitrocellulose membrane filter (AAWP04700, MilliporeSigma, St. Louis, MO), which was then transferred to a 50 mm Petri dish containing DMEM (11965092, ThermoFisher Scientific by Life Technologies Corporation, Grand Island, NY). Nitrocellulose membrane filters were cut prior to use with a sterilized metal 6 mm pore diameter punch pliers. Mandibular primordia were positioned into the center of the membrane filter, which was then placed into a transwell plate (3413, Corning Life Sciences Plastic, Lowell, MA) containing 325 μL of complete media (75% DMEM, 10% horse serum (16050122, ThermoFisher Scientific by Life Technologies Corporation, Grand Island, NY), 15% chick embryo extract ultrafiltrate (C3999, US Biological Life Sciences, Salem, MA)), 10% horse serum (16050122, Thermo Fisher Scientific, Waltham, MA), and incubated at 37°C with 5% CO_2.

To make cyclopamine stock solution, lyophilized Cyclopamine-KAAD (Lot # 2944661, 239,804, MilliporeSigma, Burlington, MA) was reconstituted following the manufacturer's instructions to a concentration of 4 ng/μL and stored at −20°C in 20 μL aliquots. To make SHH stock solution lyophilized human rSHH protein (SHH-005/SHH-100, Lot #1362, StemRD, Burlingame, CA) was reconstituted in sterile water to 100 ng/μL. Stock solution was stored at −80°C in 7.15 μL aliquots. 45 μL aliquots of rSHH protein were diluted in complete media for final concentrations of 0.1, 1, 10, 100, or 1000 ng/mL.

Mandibular primordia were placed with the aboral side down on the membrane for cyclopamine treatments and oral side down for rSHH and control treatments. For cyclopamine treatment, 40 μL of complete media were added to the side of each well and 5 μL of cyclopamine stock solution were pipetted on top of the mandibular primordia. For rSHH treatments, 45 μL of protein at each concentration were added to the side of each well. rSHH protein was mixed into complete media by rotating the 24-well plate. For control samples, 45 μL complete media were added to the side of each well. The final volume per well, after adding cyclopamine, rSHH protein at each concentration, or complete media (i.e., controls) was 370 μL.

After 24 h, explants were removed from transwell plates and transferred into 50 mm Petri dishes containing RNase-free ice-cold 1x PBS. Explants were carefully detached from the cellulose membrane using a pair of forceps and a 1 mL syringe (329654, BD Vacutainer Labware Medical, Fisher Scientific, Hanover Park, IL) with a 30 gauge by 0.5-inch needle (305106, BD Vacutainer Labware Medical, Fisher Scientific, Hanover Park, IL). Each explant was transferred into a 1.5 mL microcentrifuge tube with snap cap with as little 1x PBS as possible, flash frozen on dry ice, and stored at −80°C. Harvested explants were processed for RT-qPCR as described above.

4.13 | Cloning full-length Gas1

Full-length cDNA synthesis from RNA was performed using Maxima H Minus reverse transcriptase (K1651, Thermo Scientific, Fisher Scientific, Hanover Park, IL) following the manufacturer's directions with 2 μg of total RNA and 100 pmol of d(T)20 VN primer. The cDNA synthesis reaction was carried out at 50°C for 30 min, 55°C for 10 min, 60°C for 10 min, 65°C for 10 min, and 85°C for 5 min. Full-length duck and quail *Gas1* was amplified by PCR in a thermocycler (2720 Thermal Cycler Applied Biosystems, Carlsbad, CA) using Q5 Hot Start High-Fidelity DNA Polymerase (M0493L, New England BioLabs, Ipswich, MA) and cloned using CloneJET PCR Cloning Kit (K1231, Thermo Scientific, Fisher Scientific, Hanover Park, IL). Primer sequences are in Table S22. Duck and quail *Gas1* were confirmed by Sanger sequencing.

Gas1 was cloned into pPIDNB plasmid, which integrates into the genome and is doxycycline (dox)-inducible,[126] using AflII (R0520S, New England BioLabs, Ipswich, MA), PstI (R3140S, New England BioLabs, Ipswich, MA), and NEBuilder HiFi DNA Assembly Master Mix (E2621L, New England BioLabs, Ipswich, MA). All constructs were verified by Sanger sequencing and midi-prepped for electroporation and/or transfection using PureLink Fast Low-Endotoxin Midi Kit (A36227, Invitrogen, Fisher Scientific, Hanover Park, IL).[126] Empty pPIDNB plasmid was used as a control.

4.14 | Preparation of micropipettes

Micropipettes for DNA injection were generated using a micropipette puller (P-87 Flaming/Brown, Sutter Instrument Co., Novato, CA). Borosilicate capillary glass without a filament and with an outside diameter of 1 mm and an inner diameter of 0.75 mm (B100–75 – 10, Sutter Instrument Co., Novato, CA) was used. Program settings were as follows: Heat = 693, Velocity = 50, Pull = 100, Time = 250, Press = 300.

4.15 | Electroporation

A DNA solution containing 3 μg/μL pPIDNB (empty or containing *Gas1*), 1 μg/μL pNano-hyPBase plasmid, and 0.5 μL of 1% Fast Green were loaded into a glass micropipette (described above) and delivered with a picospritzer fluid injector (PV830 Pneumatic PicoPump, SYS-PV830, World Precision Instruments, Sarasota, FL). To target presumptive NCM of the mandibular primordia,[15] DNA solution was injected into the lumen of dorsal neural folds from the anterior hindbrain to midbrain of HH8.5 duck and quail. Homemade platinum electrodes mounted in an Adjustatrode holder (01-925-09, Intracel by Abbotsbury Engineering Ltd., St Ives, UK) were positioned on each side of the area pellucida, centered on the midbrain-hindbrain boundary. The distance between electrodes was set to 5 mm. Electrodes were overlayed with albumin to prevent drying and facilitate conductivity.

In ovo electroporation was performed using a BEX CUY21EDITII Pulse Generator (CUY21EDIT2, BEX CO., LTD, Tokyo, Japan). Unilateral electroporations involved three square pulses delivered at 50 V with 10% decay for 1 ms spaced 50 ms apart followed by five square pluses at 10 V with 20% decay for 50 ms spaced 50 ms apart. Bilateral electroporations involved three square pulses at 50 V with 10% decay for 1 ms spaced 50 ms apart, three square pulses at 50 V with 10% decay for 1 ms spaced 50 ms apart in reverse polarity, three five-square pluses at 10 V with 20% decay for 50 ms spaced 50 ms apart followed by five square pluses at 10 V with 20% decay for 50 ms spaced 50 ms apart in reverse polarity.

After electroporation, a small amount of albumin was added on top of the embryo to prevent desiccation. Eggs were sealed with tape and incubated at 37.8°C. After 24 h, electroporation efficiency was confirmed by visualizing fluorescence *in ovo* of constitutively active mNeonGreen (GFP) in pPIDNB plasmid[126] on a Nikon AZ100 C2+ Macro Confocal Microscope (Nikon Instrument, Inc., Melville, NY). Eggs were re-sealed with tape, incubated until reaching HH15, and treated with dox (see below).

4.16 | Treatment with doxycycline

Stock solution of doxycycline hyclate (dox) (446060250, Acros Organics, Fisher Scientific, Hanover Park, IL) was made up to final concentration of 1 mg/mL in filter

sterilized water. Single use 200 μL aliquots of stock solution were stored at −20°C. For *in ovo* dox treatments, egg volumes were estimated to be 75 mL for duck and 8 mL for quail. A dox working solution was made up by mixing 7.5 μL for duck and 0.8 μL for quail of stock (i.e., 1 mg/mL) dox solution with 750 μL for duck and 200 μL for quail of HBSS. Prepared working solution was gently pipetted through the egg window onto the vitelline membrane adjacent to the embryo and allowed to diffuse. Final dox concentration was 100 ng/mL. Eggs were sealed with tape and incubated until collection at HH18, HH21, HH24, and HH27. Duck mandibular primordia were isolated and imaged on a stereo dissecting microscope (MZFLIII-TS, Leica Microsystems, Buffalo Grove, IL) under brightfield illumination or epifluorescent illumination to assess distribution of *Gas1* overexpression as indicated by mScarlet (RFP) fluorescence. Heads of quail at HH27 were stained with Hoechst 33342 Dye (see below) and imaged on a stereo dissection microscope under epifluorescent illumination (MZFLIII-TS, Leica Microsystems, Buffalo Grove, IL).

4.17 | Injections with vivo-Morpholinos

In ovo Vivo-Morpholino injections were performed using a 0.5 mM solution of Vivo-Morpholino (quail anti-*Gas1* or control anti-GFP) (Gene Tools, LLC, Philomath, OR) in HBSS containing 0.01% Phenol Red (417240050, Acros Organics, Fisher Scientific, Hanover Park, IL). Vivo-Morpholino sequences are listed in Table S23. To validate the specificity of duck and quail Vivo-Morpholino, *Gas1* target sequences or morpholino scramble sequences used were cloned directly upstream of the mScarlet CDS in the pPIDNB plasmid (Figure S1C). Duck scramble sequence was generated by symmetrically swapping bases of the morpholino so the sequence would be different, but the base composition would not change. Embryonic chick fibroblasts (DF-1) (CRL-12203, ATCC, Manassas, VA) were cultured in Dulbecco's Modified Eagle's Medium (10-013-CV, DMEM, Corning, NY) supplemented with 10% FBS (97068-085, Lot# 283K18, VWR, Radnor, PA) and 1× penicillin–streptomycin (15140122, Thermo Fisher Scientific, Waltham, MA) at 37°C with 5% CO2. pPIDNB morpholino constructs were transfected into DF-1 cells using X-tremeGENE 360 Transfection Reagent (8724121001, MilliporeSigma, Burlington, MA) following the manufacturer's instructions. DF-1 cells were transfected for 14 h and then the medium was replaced with complete medium. Cells were allowed to recover for 8 h. Cells were treated with 0, 10 or 20 μM *Gas1* MO in complete medium for 14 h and induced with 2 ng/mL dox. After 26 h of dox induction, GFP and RFP were measured using a SpectraMax M5 plate reader (Molecular Devices, San Jose, CA). To normalize for transfection efficiency the ratio of RFP (under the control of MO) and GFP (constitutively expressed) was used.

Vivo-Morpholino solution was injected into the right side of duck and quail mandibular primordia at HH18 with pulled glass micropipettes loaded into a PicoNozzle (5430-10) and a picospritzer fluid injector (PV830, World Precision Instruments, Sarasota, FL). After injection, eggs were sealed with tape and incubated until reaching HH27. Heads of treated embryos were either stained with Hoechst 33342 Dye and imaged on a stereo microscope under epifluorescent illumination (MZFLIII-TS, Leica Microsystems, Buffalo Grove, IL); or mandibular primordia were dissected for RNA-seq analyses.

4.18 | RNA-seq

Control and treated mandibular primordia were harvested at HH24 and flash frozen in a dry ice ethanol bath and stored at −80°C. Total RNA was extracted from mandibular primordia using TriplePrep Kit (28942544, Cytiva, Marlborough, MA) following the manufacturer's instructions and eluted with 50 μL of H_2O. RNA was submitted to Novogene for 150 bp paired end Illumina mRNA sequencing. RNA sequencing reads for duck and quail were aligned to duck genome assembly GCA_015476345.1[258] or quail genome assembly GCA_001577835.2,[259] respectively, using Geneious RNA assembler[260] applying the medium-low sensitivity/fast setting. The duck genome assembly does not contain Smo, thus, Smo (NCBI Gene ID: 101798413) was manually added to the reference sequence. To prevent clustering based on embryonic sex in duck, the W chromosome (female specific sex chromosome) was removed from the reference sequence. The quail reference genome is based on a male, so no W chromosome sequence was present. Read counts for each gene were based on mRNA annotations. Reads aligning to different isoforms for a single gene were combined to generate read counts for each gene. Library normalization factors were calculated by inputting the read counts for each gene into the edgeR Bioconductor package.[261] Statistical analysis was carried out using the edgeR LRT model. Unannotated LOC entries were batch-queried using the MyGene.info API to retrieve Entrez and Ensembl gene identifiers, and genes with assigned Ensembl IDs were evaluated for human orthologs via the Ensembl REST homology endpoint. Protein sequences corresponding to LOC-associated Ensembl gene identifiers were extracted from Ensembl proteomes derived from the *Anas platyrhynchos* assembly ASM874695v1 (duck) and the *Coturnix japonica* assembly Coturnix_japonica_2.0 (quail). BLASTP searches were performed using BLAST+ v2.17.0 against a

locally formatted SwissProt database. For each query, the top hit was selected by highest bitscore (ties resolved by lowest e-value), and percent query coverage was calculated from alignment length and query length. Hits were classified as high (≥65% identity and ≥70% coverage), moderate (≥40% identity and ≥50% coverage but not high), or low confidence. For LOCs with multiple protein isoforms, candidate hits were ranked by confidence tier, then bitscore, percent identity, and coverage (all descending), and the top-ranked hit was retained. Final selection was based solely on sequence similarity metrics, independent of species origin. Annotated LOCs were merged with RNA-seq expression tables by exact LOC matching. DE gene lists for GO analysis were generated using the criteria of FDR <0.05 and log fold-change >1. DE gene lists were inputted into DAVID[128] selecting OFFICIAL_GENE_SYMBOL and either *Anas platyrhynchos* or *Coturnix japonica* for the species. GO terms were taken from GOTERM BP DIRECT list.

4.19 | Gas1 promoter analysis

Genomic DNA from duck and quail embryos was extracted using PureLink Genomic DNA Mini Kit (K1820-01, Thermo Fisher Scientific, Waltham, MA) following the manufacturer's instructions. 1.5 kb of *Gas1* promoter sequences were amplified by PCR using KOD Xtreme Hot Start DNA Polymerase (71975-3, Millipore-Sigma, Burlington, MA) following the manufacturer's instructions. *Gas1* promotor PCR products were purified using NucleoSpin Gel and PCR Clean-Up (740609.250, Takara Bio, Mountain View, CA). Sequencing adapters were added to the *Gas1* promoter PCR products using Native Barcoding Kit 24 V14 (SQK-NBD114.24, Oxford, United Kingdom) following the manufacturer's instructions and then run on a Flongle flow cell (FLO-FLG114, Oxford, United Kingdom) following the manufacturer's instructions. Three embryos per species were sequenced. Base calling was performed using Dorado high accuracy base caller (dna_r10.4.1_e8.2_400bps_sup@v4.1.0). Consensus sequences were generated for each embryo, and those consensus sequences were used to generate consensus sequences for each species.

To identify transcription factor-binding sites, we used the JASPAR 2024 database, which contains transcription factor-binding profiles stored as position frequency matrices.[262] To map transcription factor-binding sites on the *Gas1* promoter of duck and quail, we used the TFBSTools[263] R/bioconductor package.[264] Position-frequency matrices were converted to position-weighted matrices by setting pseudocounts to 0.8[265] and background frequencies of nucleotides to 0.25. Minimum threshold score was set to 98%.

4.20 | GAS1 protein structure

GAS1 protein sequences were derived from the full-length duck and quail CDS. We previously published chick *Gas1* CDS,[126] which is available on NCB1 (MW036691). Human GAS1 (NP_002039.2) and mouse GAS1 protein sequences (NP_032112.1) were downloaded from NCBI. InterProScan[266] was used to identify domains in the translated protein sequences and PrDOS[267] was used to identify disordered regions with a threshold of 5%. Duck and quail glycophosphatidylinositol (GPI) anchor sequences were identified by alignment to the previously identified mouse and human GAS1 GPI sequences.[130–132]

4.21 | Staining with Hoechst dye

To enhance contrast for phenotypic analysis, whole mount duck and quail embryos were stained with Hoechst 33342 Dye (62249, Lot# RF22228410, Thermo-Fisher Scientific, Hanover Park, IL). Briefly, a 20 mM stock solution was diluted 1:1000 in 1x PBS to a working solution of 1 μg/mL. Samples were incubated in working solution for 48 h at 4°C on a rocker.

4.22 | Capture and adjustment of images

Brightfield and epifluorescent images were acquired with SPOT Insight 2.0 Firewire Color Mosaic camera (IN1820, 18.2) and SPOT image capture software (SPOT Imag3ing, Diagnostic Instrument, Inc., Sterling Heights, MI). Multiple image planes were combined in Helicon Focus (version 7.6.1 Pro, Helicon Soft Ltd., 2000, Kharkiv, Ukraine). Images were adjusted in Adobe Photoshop 2026 (version 27.2.0) to normalize for exposure, brightness, contrast, saturation, and color balance across samples. Figures were assembled in Adobe Illustrator 2026 (Version 30.1).

4.23 | Methods for determining statistical significance

Prism (v.10.6.1) software (GraphPad, San Diego, CA) was used to perform statistical tests and determine significance. Unpaired multiple t-tests were performed at each time point for analysis of mandibular mesenchyme population size, gene expression levels in vivo, as well as gene expression ratios. The Holm-Šídák method was used to correct for multiple comparisons. Ordinary one-way ANOVA was performed for analysis of gene expression and gene expression ratios between duck, quail, and quck

at quck embryonic stage HH21 and HH24 and for analysis of gene expression following treatments in mandibular primordia explants. The Dunnett's multiple comparison test was used to correct for multiple comparisons.

Error bars denote SEM. Multiplicity adjusted p-values were used to determine significance, and p-values are indicated on the data points and/or legends of each figure. In all figures, $p < 0.05$ was considered statistically significant, although some statistical comparisons reached significance below $p < 0.01$, $p < 0.001$, or $p < 0.0001$ as noted. Exact p-values are reported in the Supplemental Tables. Formal power analyses were not conducted. The number of biological replicates for each data point and/or treatment group are listed in the Supplemental Tables.

4.24 | Use of artificial intelligence tools

An Enterprise version of ChatGPT (5.2 Pro) was used to help build a LOC annotation pipeline, analyze datasets we generated from our RNA-seq experiments, evaluate our maps of TFBS on the *Gas1* promoter and the *Gas1* CDS that we cloned from duck, chick, and quail. Sections of the manuscript were also checked by Claude Sonnet 4 for accuracy and clarity especially with regard to the Figures, Tables, and citations.

ACKNOWLEDGMENTS

We thank Sophie E. Creuzet, Katherine C. Woronowicz, Tamara Alliston, Ralph S. Marcucio, Spenser S. Smith, Jessye Aggleton, and Evelyn E. Schwager for technical support and early comments on the manuscript; Banjot Saini, Ganesan Kandapillai, Angeline K Chemel, Hugo Sugier, and Nicolas Rose for laboratory assistance; Thomas Dam at AA Lab Eggs for fertilized avian eggs; the UCSF Biological Imaging Development CoLab (BIDC) for microscopy and data analysis support; and the UCSF Parnassus Flow Cytometry Core (PFCC, RRID:SCR_018206) for assistance with Flow/Mass Cytometry.

FUNDING INFORMATION

This study was supported in part, by the UCSF Biological Imaging Development Core (BIDC); by the National Institute of Arthritis and Musculoskeletal and Skin Diseases (NIAMS) P30 AR075055 to the UCSF Core Center for Musculoskeletal Biology and Medicine (CCMBM); by the National Institute of Diabetes and Digestive and Kidney Diseases (NIDDK) P30 DK063720 to the UCSF Diabetes Research Center (DRC); by the National Institutes of Health (NIH) Office of the Director S10 OD021822 to the Parnassus Flow Cytometry Core (PFCC); by the National Institute of Dental and Craniofacial Research (NIDCR) F30 DE027616 to An Nguyen; and by NIDCR R01 DE016402, NIDCR R01 DE025668, and NIH Office of the Director S10 OD021664 to Richard A. Schneider. The content is solely the responsibility of the authors and does not necessarily represent the official views of the NIH. The funders had no role in study design, data collection and analysis, manuscript preparation, or decision to publish.

CONFLICT OF INTEREST STATEMENT

The authors declare no conflict of interest.

DATA AVAILABILITY STATEMENT

Datasets supporting the results of this study that are not presented in the Supplemental Tables are available upon request from the corresponding author (Richard A. Schneider). The GenBank (INSDC) accession number for chick (*Gallus gallus*) *Gas1* CDS is MW036691; PZ065757 for quail (*Coturnix japonica*); and PZ065756 for duck (*Anas platyrhynchos*). The GenBank accession number for *Gas1* promoter sequence for quail is PZ065759 and PZ065758 for duck. The stable and inducible overexpression pPIDNB plasmid used in this study is available at Addgene (https://www.addgene.org/browse/article/28216052). The RNA-seq datasets for duck and quail (i.e., control, *Gas1* morpholino treatments, and *Gas1* overexpression) are available in Dryad (https://doi.org/10.5061/dryad.1g1jwsvc5).

ORCID

Richard A. Schneider https://orcid.org/0000-0002-2626-3111

REFERENCES

1. Thompson DW. *On Growth and Form*. Cambridge [Eng.]: University press; 1917:xv, 793 p. 1917.
2. Huxley JS. *Problems of relative growth*. Methuen; 1932.
3. Huxley JS, Teissier G. Terminology of relative growth. *Nature*. 1936;137:780-781.
4. Woodger J. On biological transformations. In: Clark WELG, Medawar PB, eds. *Essays on Growth and Form Presented to D'Arcy Wentworth Thompson*. Clarendon Press; 1945:95-120.
5. Gould SJ. Allometry and size in ontogeny and phylogeny. *Biol Rev Camb Philos Soc*. 1966;41:587-640.
6. Stern DL, Emlen DJ. The developmental basis for allometry in insects. *Development*. 1999;126(6):1091-1101.
7. Gayon J. History of the concept of Allometry. *Am Zool*. 2000; 40(5):748-758.
8. Young NM, Hu D, Lainoff AJ, et al. Embryonic bauplans and the developmental origins of facial diversity and constraint. *Development*. 2014;141(5):1059-1063. doi:10.1242/dev.099994
9. Schneider RA. Chapter 7: Cellular control of time, size, and shape in development and evolution. In: Hall BK, Moody S, eds. *Cells in Evolutionary Biology: Translating Genotypes into Phenotypes—Past, Present, Future*. CRC Press, Taylor & Francis Group; 2018:167-212.

10. Russell ES. *Form and Function: A Contribution to the History of Animal Morphology*. John Murray Publishers Ltd.; 1916.
11. Haldane JBS. On being the right size. Harper's Magazine 1926. 1926.
12. Smith FJ, Percival CJ, Young NM, et al. Divergence of craniofacial developmental trajectories among avian embryos. *Dev Dyn*. 2015;244:1158-1167. doi:10.1002/dvdy.24262
13. Leevers SJ, McNeill H. Controlling the size of organs and organisms [review]. *Curr Opin Cell Biol*. 2005;17(6):604–609. doi:10.1016/j.ceb.2005.09.008
14. Eames BF, Schneider RA. The genesis of cartilage size and shape during development and evolution. *Development*. 2008;135(23):3947-3958.
15. Fish JL, Sklar RS, Woronowicz KC, Schneider RA. Multiple developmental mechanisms regulate species-specific jaw size. *Development*. 2014;141(3):674-684. doi:10.1242/dev.100107
16. Uygur A, Young J, Huycke TR, Koska M, Briscoe J, Tabin CJ. Scaling pattern to variations in size during development of the vertebrate neural tube. *Dev Cell*. 2016;37(2):127-135. doi:10.1016/j.devcel.2016.03.024
17. Schneider RA. Neural crest and the origin of species-specific pattern. *Genesis*. 2018;56(6–7):e23219. doi:10.1002/dvg.23219
18. Allard P, Tabin CJ. Achieving bilateral symmetry during vertebrate limb development. *Semin Cell Dev Biol*. 2009;20(4):479-484. doi:10.1016/j.semcdb.2008.10.011
19. Schneider RA. Regulation of jaw length during development, disease, and evolution. *Curr Top Dev Biol*. 2015;115:271-298. doi:10.1016/bs.ctdb.2015.08.002
20. Woronowicz KC, Schneider RA. Molecular and cellular mechanisms underlying the evolution of form and function in the amniote jaw. *EvoDevo*. 2019;10(1):17. doi:10.1186/s13227-019-0131-8
21. Goldschmidt R. *Physiological Genetics*. McGraw Hill; 1938.
22. Goldschmidt R. *The Material Basis of Evolution*. 1982nd ed. Yale University Press; 1940.
23. de Beer GR. Embryos and Ancestors. Revised ed. Oxford: Clarendon Press; 1954:XII, 159, [1] s. 1954.
24. Gould SJ. *Ontogeny and Phylogeny*. Harvard University Press; 1977:501.
25. Alberch P, Gould SJ, Oster GF, Wake DB. Size and shape in ontogeny and phylogeny. *Paleobiology*. 1979;5(3):296-317.
26. Hall BK. Developmental processes underlying heterochrony as an evolutionary mechanism. *Can J Zool*. 1984;62:1-7.
27. McKinney ML. Classifying heterochrony: Allometry, size, and time. In: McKinney ML, ed. *Heterochrony in Evolution: A Multidisciplinary Approach*. Plenum Press; 1988:17-34.
28. Klingenberg CP. Heterochrony and allometry: the analysis of evolutionary change in ontogeny. *Biol Rev*. 1998;73(1):79-123. doi:10.1111/j.1469-185X.1997.tb00026.x
29. Smith KK. Time's arrow: heterochrony and the evolution of development. *Int J Dev Biol*. 2003;47(7–8):613-621.
30. Keyte AL, Smith KK. Heterochrony and developmental timing mechanisms: changing ontogenies in evolution. *Semin Cell Dev Biol*. 2014;34:99-107. doi:10.1016/j.semcdb.2014.06.015
31. Gurdon JB, Standley H, Dyson S, et al. Single cells can sense their position in a morphogen gradient. *Development*. 1999;126(23):5309-5317.
32. Gurdon JB, Bourillot PY. Morphogen gradient interpretation. *Nature*. 2001;413(6858):797-803.
33. Oster GF, Shubin N, Murray JD, Alberch P. Evolution and morphogenetic rules - the shape of the vertebrate limb in ontogeny and phylogeny. *Evolution*. 1988;42(5):862-884.
34. Tostevin F, ten Wolde PR, Howard M. Fundamental limits to position determination by concentration gradients. *PLoS Comput Biol*. 2007;3(4):e78. doi:10.1371/journal.pcbi.0030078
35. Ben-Zvi D, Barkai N. Scaling of morphogen gradients by an expansion-repression integral feedback control. *Proc Natl Acad Sci U S A*. 2010;107(15):6924-6929. doi:10.1073/pnas.0912734107
36. Cheung D, Miles C, Kreitman M, Ma J. Adaptation of the length scale and amplitude of the Bicoid gradient profile to achieve robust patterning in abnormally large Drosophila melanogaster embryos. *Development*. 2014;141(1):124-135. doi:10.1242/dev.098640
37. Dessaud E, Yang LL, Hill K, et al. Interpretation of the sonic hedgehog morphogen gradient by a temporal adaptation mechanism. *Nature*. 2007;450(7170):717-720. doi:10.1038/nature06347
38. Ribes V, Briscoe J. Establishing and interpreting graded sonic hedgehog signaling during vertebrate neural tube patterning: the role of negative feedback. *Cold Spring Harb Perspect Biol*. 2009;1(2):a002014-a002014. doi:10.1101/cshperspect.a002014
39. Tenzen T, Allen BL, Cole F, Kang JS, Krauss RS, McMahon AP. The cell surface membrane proteins Cdo and Boc are components and targets of the hedgehog signaling pathway and feedback network in mice. *Dev Cell*. 2006;10(5):647-656. doi:10.1016/j.devcel.2006.04.004
40. Beachy PA, Hymowitz SG, Lazarus RA, Leahy DJ, Siebold C. Interactions between hedgehog proteins and their binding partners come into view. *Genes Dev*. 2010;24(18):2001-2012. doi:10.1101/gad.1951710
41. Izzi L, Levesque M, Morin S, et al. Boc and Gas1 each form distinct Shh receptor complexes with Ptch1 and are required for Shh-mediated cell proliferation. *Dev Cell*. 2011;20(6):788-801. doi:10.1016/j.devcel.2011.04.017
42. Choudhry Z, Rikani AA, Choudhry AM, et al. Sonic hedgehog signalling pathway: a complex network. *Ann Neurosci*. 2014;21(1):28-31. doi:10.5214/ans.0972.7531.210109
43. van den Heuvel M, Ingham PW. Smoothened encodes a receptor-like serpentine protein required for hedgehog signalling. *Nature*. 1996;382(6591):547-551.
44. Alcedo J, Noll M. Hedgehog and its patched-smoothened receptor complex: a novel signalling mechanism at the cell surface. *Biol Chem*. 1997;378(7):583-590.
45. Quirk J, van den Heuvel M, Henrique D, et al. The smoothened gene and hedgehog signal transduction in drosophila and vertebrate development. *Cold Spring Harb Symp Quant Biol*. 1997;62(4):217-226.
46. Murone M, Rosenthal A, de Sauvage FJ. Sonic hedgehog signaling by the patched-smoothened receptor complex. *Curr Biol*. 1999;9(2):76-84.
47. Taipale J, Cooper MK, Maiti T, Beachy PA. Patched acts catalytically to suppress the activity of smoothened. *Nature*. 2002;418(6900):892-897.

48. Wilson CW, Chuang PT. Mechanism and evolution of cytosolic hedgehog signal transduction. *Development*. 2010; 137(13):2079-2094. doi:10.1242/dev.045021
49. Hui CC, Angers S. Gli proteins in development and disease. *Annu Rev Cell Dev Biol*. 2011;27:513-537. doi:10.1146/annurev-cellbio-092910-154048
50. Bai CB, Auerbach W, Lee JS, Stephen D, Joyner AL. Gli2, but not Gli1, is required for initial Shh signaling and ectopic activation of the Shh pathway. *Development*. October 15, 2002 2002;129(20):4753–4761.
51. Bai CB, Joyner AL. Gli1 can rescue the in vivo function of Gli2. *Development*. 2001;128(24):5161-5172.
52. Wang B, Fallon JF, Beachy PA. Hedgehog-regulated processing of Gli3 produces an anterior/posterior repressor gradient in the developing vertebrate limb. *Cell*. 2000;100(4):423-434.
53. Matise MP, Joyner AL. Gli genes in development and cancer. *Oncogene*. 1999;18(55):7852-7859.
54. Mo R, Freer AM, Zinyk DL, et al. Specific and redundant functions of Gli2 and Gli3 zinc finger genes in skeletal patterning and development. *Development*. 1997;124(1):113-123.
55. Lee J, Platt KA, Censullo P, Ruiz i Altaba A. Gli1 is a target of sonic hedgehog that induces ventral neural tube development. *Development*. 1997;124(13):2537-2552.
56. Marigo V, Johnson RL, Vortkamp A, Tabin CJ. Sonic hedgehog differentially regulates expression of GLI and GLI3 during limb development. *Dev Biol*. 1996;180(1):273-283.
57. Allen BL, Song JY, Izzi L, et al. Overlapping roles and collective requirement for the coreceptors GAS1, CDO, and BOC in SHH pathway function. *Dev Cell*. 2011;20(6):775-787. doi:10.1016/j.devcel.2011.04.018
58. Wierbowski BM, Petrov K, Aravena L, Gu G, Xu Y, Salic A. Hedgehog pathway activation requires Coreceptor-catalyzed, lipid-dependent relay of the sonic hedgehog ligand. *Dev Cell*. 2020;55(4):450-467 e8. doi:10.1016/j.devcel.2020.09.017
59. Seppala M, Depew MJ, Martinelli DC, Fan CM, Sharpe PT, Cobourne MT. Gas1 is a modifier for holoprosencephaly and genetically interacts with sonic hedgehog. *J Clin Invest*. 2007; 117(6):1575-1584. doi:10.1172/jci32032
60. Martinelli DC, Fan CM. Gas1 extends the range of hedgehog action by facilitating its signaling. *Genes Dev*. 2007;21(10): 1231-1243. doi:10.1101/gad.1546307
61. Allen BL, Tenzen T, McMahon AP. The hedgehog-binding proteins Gas1 and Cdo cooperate to positively regulate Shh signaling during mouse development. *Genes Dev*. 2007;21(10): 1244-1257. doi:10.1101/gad.1543607
62. Martinelli DC, Fan C-M. The role of Gas1 in embryonic development and its implications for human disease. *Cell Cycle*. 2007;6(21):2650–2655. doi:10.4161/cc.6.21.4877
63. Delloye-Bourgeois C, Rama N, Brito J, Le Douarin N, Mehlen P. Sonic hedgehog promotes the survival of neural crest cells by limiting apoptosis induced by the dependence receptor CDON during branchial arch development. *Biochem Biophys Res Commun*. 2014;452(3):655-660. doi:10.1016/j.bbrc.2014.08.134
64. Echevarria-Andino ML, Franks NE, Schrader HE, Hong M, Krauss RS, Allen BL. CDON contributes to hedgehog-dependent patterning and growth of the developing limb. *Dev Biol*. 2023;493:1-11. doi:10.1016/j.ydbio.2022.09.011
65. Xu J, Iyyanar PPR, Lan Y, Jiang R. Sonic hedgehog signaling in craniofacial development. *Differentiation*. 2023;133:60-76. doi:10.1016/j.diff.2023.07.002
66. Qiu T, Huteckova B, Seppala M, et al. Molecular profiling of the vestibular lamina highlights a key role for Hedgehog signalling. *Development*. 2023;150(7):1-13. doi:10.1242/dev.201464
67. Audu GC, Rohan SY, Kumari A. Gas1 regulates embryonic tongue muscle proliferation, differentiation and maturation via alternative pathways to hedgehog signaling. *Development*. 2025;152(19):1-17. doi:10.1242/dev.204868
68. Jeong J, Mao J, Tenzen T, Kottmann AH, McMahon AP. Hedgehog signaling in the neural crest cells regulates the patterning and growth of facial primordia. *Genes Dev*. 2004;18(8): 937-951.
69. Marcucio RS, Cordero DR, Hu D, Helms JA. Molecular interactions coordinating the development of the forebrain and face. *Dev Biol*. 2005;284(1):48-61.
70. Moore-Scott BA, Manley NR. Differential expression of sonic hedgehog along the anterior-posterior axis regulates patterning of pharyngeal pouch endoderm and pharyngeal endoderm-derived organs. *Dev Biol*. 2005;278(2):323-335.
71. Haworth KE, Wilson JM, Grevellec A, et al. Sonic hedgehog in the pharyngeal endoderm controls arch pattern via regulation of Fgf8 in head ectoderm. *Dev Biol*. 2007;303(1):244-258. doi:10.1016/j.ydbio.2006.11.009.
72. Billmyre KK, Klingensmith J. Sonic hedgehog from pharyngeal arch 1 epithelium is necessary for early mandibular arch cell survival and later cartilage condensation differentiation. *Dev Dyn*. 2015;244(4):564-576. doi:10.1002/dvdy.24256
73. Le Lièvre CS. Participation of neural crest-derived cells in the genesis of the skull in birds. *J Embryol Exp Morphol*. 1978;47: 17-37.
74. Noden DM. The control of avian cephalic neural crest cytodifferentiation. I. Skeletal and connective tissues. *Dev Biol*. 1978; 67(2):296-312.
75. Jheon AH, Schneider RA. The cells that fill the bill: neural crest and the evolution of craniofacial development. *J Dent Res*. 2009;88(1):12–21. doi:10.1177/0022034508327757
76. Couly G, Creuzet S, Bennaceur S, Vincent C, Le Douarin NM. Interactions between Hox-negative cephalic neural crest cells and the foregut endoderm in patterning the facial skeleton in the vertebrate head. *Development*. 2002;129(4):1061-1073.
77. Helms JA, Schneider RA. Cranial skeletal biology. *Nature*. 2003;423(6937):326-331.
78. Abzhanov A, Tabin CJ. Shh and Fgf8 act synergistically to drive cartilage outgrowth during cranial development. *Dev Biol*. 2004;273(1):134-148.
79. Graham A, Okabe M, Quinlan R. The role of the endoderm in the development and evolution of the pharyngeal arches [review]. *J Anat*. 2005;207(5):479-487. doi:10.1111/j.1469-7580.2005.00472.x
80. Brito JM, Teillet MA, Le Douarin NM. An early role for sonic hedgehog from foregut endoderm in jaw development: ensuring neural crest cell survival. *Proc Natl Acad Sci U S A*. 2006; 103(31):11607-11612. doi:10.1073/pnas.0604751103
81. Fish JL, Schneider RA. Chapter 6 - neural crest-mediated tissue interactions during craniofacial development: the origins of species-specific pattern. In: Trainor PA, ed. *Neural Crest Cells*. Academic Press; 2014:101-124.

82. Hu D, Young NM, Li X, Xu Y, Hallgrimsson B, Marcucio RS. A dynamic Shh expression pattern, regulated by SHH and BMP signaling, coordinates fusion of primordia in the amniote face. *Development*. 2015;142(3):567-574. doi:10.1242/dev.114835
83. Hu D, Young NM, Xu Q, et al. Signals from the brain induce variation in avian facial shape. *Dev Dyn*. 2015;244:1133-1143. doi:10.1002/dvdy.24284
84. Hu D, Marcucio RS. Neural crest cells pattern the surface cephalic ectoderm during FEZ formation. *Dev Dyn*. 2012;241(4):732-740. doi:10.1002/dvdy.23764
85. Schneider RA, Hu D, Rubenstein JL, Maden M, Helms JA. Local retinoid signaling coordinates forebrain and facial morphogenesis by maintaining FGF8 and SHH. *Development*. 2001;128(14):2755-2767.
86. Young NM, Chong HJ, Hu D, Hallgrimsson B, Marcucio RS. Quantitative analyses link modulation of sonic hedgehog signaling to continuous variation in facial growth and shape. *Development*. 2010;137(20):3405–3409. doi:10.1242/dev.052340
87. Schneider RA, Helms JA. The cellular and molecular origins of beak morphology. *Science*. 2003;299(5606):565-568.
88. Eames BF, Schneider RA. Quail-duck chimeras reveal spatiotemporal plasticity in molecular and histogenic programs of cranial feather development. *Development*. 2005;132(7):1499-1509.
89. Cole F, Krauss RS. Microform Holoprosencephaly in mice that lack the Ig superfamily member Cdon. *Curr Biol*. 2003;13(5):411-415.
90. Cordero D, Marcucio R, Hu D, Gaffield W, Tapadia M, Helms JA. Temporal perturbations in sonic hedgehog signaling elicit the spectrum of holoprosencephaly phenotypes. *J Clin Invest*. 2004;114(4):485-494.
91. Melnick M, Witcher D, Bringas P Jr, Carlsson P, Jaskoll T. Meckel's cartilage differentiation is dependent on hedgehog signaling. *Cells Tissues Organs*. 2005;179(4):146-157. doi:10.1159/000085950
92. Zhang W, Kang JS, Cole F, Yi MJ, Krauss RS. Cdo functions at multiple points in the sonic hedgehog pathway, and Cdo-deficient mice accurately model human holoprosencephaly. *Dev Cell*. 2006;10(5):657-665. doi:10.1016/j.devcel.2006.04.005
93. Roessler E, Muenke M. The molecular genetics of holoprosencephaly. *Am J Med Genet C Semin Med Genet*. 2010;154C(1):52-61. doi:10.1002/ajmg.c.30236
94. Ribeiro LA, Quiezi RG, Nascimento A, Bertolacini CP, Richieri-Costa A. Holoprosencephaly and holoprosencephaly-like phenotype and GAS1 DNA sequence changes: report of four Brazilian patients. *Am J Med Genet A*. 2010;152A(7):1688-1694. doi:10.1002/ajmg.a.33466
95. Zhang W, Hong M, Bae GU, Kang JS, Krauss RS. Boc modifies the holoprosencephaly spectrum of Cdo mutant mice. *Dis Model Mech*. 2011;4(3):368-380. doi:10.1242/dmm.005744
96. Bae GU, Domené S, Roessler E, et al. Mutations in CDON, encoding a hedgehog receptor, result in holoprosencephaly and defective interactions with other hedgehog receptors. *Am J Hum Genet*. 2011;89(2):231-240. doi:10.1016/j.ajhg.2011.07.001
97. Dennis JF, Kurosaka H, Iulianella A, et al. Mutations in hedgehog acyltransferase (Hhat) perturb hedgehog signaling, resulting in severe acrania-holoprosencephaly-agnathia craniofacial defects. *PLoS Genet*. 2012;8(10):e1002927. doi:10.1371/journal.pgen.1002927
98. Pineda-Alvarez DE, Roessler E, Hu P, et al. Missense substitutions in the GAS1 protein present in holoprosencephaly patients reduce the affinity for its ligand, SHH *Hum Genet*. 2012;131(2):301-310. doi:10.1007/s00439-011-1078-6
99. Seppala M, Xavier GM, Fan CM, Cobourne MT. Boc modifies the spectrum of holoprosencephaly in the absence of Gas1 function. *Biol Open*. 2014;3(8):728-740. doi:10.1242/bio.20147989
100. Xavier GM, Seppala M, Barrell W, Birjandi AA, Geoghegan F, Cobourne MT. Hedgehog receptor function during craniofacial development. *Dev Biol*. 2016;415(2):198-215. doi:10.1016/j.ydbio.2016.02.009
101. Hong M, Srivastava K, Kim S, et al. BOC is a modifier gene in holoprosencephaly. *Hum Mutat*. 2017;38(11):1464-1470. doi:10.1002/humu.23286
102. Echevarría-Andino ML, Allen BL. The hedgehog co-receptor BOC differentially regulates SHH signaling during craniofacial development. *Development*. 2020;147(23):dev.189076. doi:10.1242/dev.189076
103. Schneider RA, Hu D, Helms JA. From head to toe: conservation of molecular signals regulating limb and craniofacial morphogenesis. *Cell Tissue Res*. 1999;296(1):103-109.
104. Lwigale PY, Schneider RA. Other chimeras: quail-duck and mouse-chick. *Methods Cell Biol*. 2008;87:59-74.
105. Schneider RA. Developmental mechanisms facilitating the evolution of bills and quills. *J Anat*. 2005;207(5):563-573.
106. Merrill AE, Eames BF, Weston SJ, Heath T, Schneider RA. Mesenchyme-dependent BMP signaling directs the timing of mandibular osteogenesis. *Development*. 2008;135(7):1223-1234.
107. Hall J, Jheon AH, Ealba EL, et al. Evolution of a developmental mechanism: species-specific regulation of the cell cycle and the timing of events during craniofacial osteogenesis. *Dev Biol*. 2014;385(2):380-395. doi:10.1016/j.ydbio.2013.11.011
108. Ealba EL, Jheon AH, Hall J, Curantz C, Butcher KD, Schneider RA. Neural crest-mediated bone resorption is a determinant of species-specific jaw length. *Dev Biol*. 2015;408:151-163. doi:10.1016/j.ydbio.2015.10.001
109. Hamburger V, Hamilton HL. A series of normal stages in the development of the chick embryo. *J Morphol*. 1951;88:49-92.
110. Tokita M, Schneider RA. Developmental origins of species-specific muscle pattern. *Dev Biol*. 2009;331(2):311–325. doi:10.1016/j.ydbio.2009.05.548
111. Solem RC, Eames BF, Tokita M, Schneider RA. Mesenchymal and mechanical mechanisms of secondary cartilage induction. *Dev Biol*. 2011;356(1):28–39. doi:10.1016/j.ydbio.2011.05.003
112. Woronowicz KC, Gline SE, Herfat ST, Fields AJ, Schneider RA. FGF and TGFbeta signaling link form and function during jaw development and evolution. *Dev Biol*. 2018;444(Suppl 1):S219-S236. doi:10.1016/j.ydbio.2018.05.002
113. Hamilton HL. *Lillie's Development of the Chick: an Introduction to Embryology*. 3rd ed. Holt, Rinehart and Winston; 1965.
114. Starck JM, Ricklefs RE. *Avian Growth and Development: Evolution within the Altricial-Precocial Spectrum*. Oxford University Press; 1998:441.

115. Koecke H. Normalstadien der Embryonalentwicklung bei der Hausente (*Anas boschas domestica*). *Embryologia*. 1958;4(1): 55-78.
116. Padgett CS, Ivey WD. The normal embryology of the Coturnix quail. *Anat Rec*. 1960;137:1-11.
117. Zacchei AM. The embryonic development of the Japanese quail (*Coturnix coturnix japonica*). *Arch Ital Anat Embriol*. 1961;66:36-62.
118. Nakane Y, Tsudzuki M. Development of the skeleton in Japanese quail embryos. *Dev Growth Differ*. 1999;41(5): 523-534.
119. Ainsworth SJ, Stanley RL, Evans DJ. Developmental stages of the Japanese quail. *J Anat*. 2010;216(1):3–15. doi:10.1111/j.1469-7580.2009.01173.x
120. Yamashita T, Sohal GS. Embryonic origin of skeletal muscle cells in the iris of the duck and quail. *Cell Tissue Res*. 1987; 249(1):31-37.
121. Le Douarin NM, Dieterlen-Lievre F, Teillet M. Quail-Chick transplantations. In: Bronner-Fraser M, ed. *Methods in Avian Embryology*. Vol 51. Academic Press; 1996:23-59.
122. Noden DM, Schneider RA. Neural crest cells and the community of plan for craniofacial development: historical debates and current perspectives. *Adv Exp Med Biol*. 2006;589:1-23.
123. Brito JM, Teillet MA, Le Douarin NM. Induction of mirror-image supernumerary jaws in chicken mandibular mesenchyme by sonic hedgehog-producing cells. *Development*. 2008; 135(13):2311-2319. doi:10.1242/dev.019125
124. Roper RJ, VanHorn JF, Cain CC, Reeves RH. A neural crest deficit in down syndrome mice is associated with deficient mitotic response to sonic hedgehog [research support, N.I.H., extramural]. *Mech Dev*. 2009;126(3–4):212–219. doi:10.1016/j.mod.2008.11.002
125. ten Berge D, Brouwer A, Korving J, et al. Prx1 and Prx2 are upstream regulators of sonic hedgehog and control cell proliferation during mandibular arch morphogenesis. *Development*. 2001;128(15):2929-2938.
126. Chu D, Nguyen A, Smith SS, Vavrusova Z, Schneider RA. Stable integration of an optimized inducible promoter system enables spatiotemporal control of gene expression throughout avian development. *Biology Open*. 2020;9:9(bio055343). doi:10.1242/bio.055343
127. Coordinators NR. Database resources of the National Center for biotechnology information. *Nucleic Acids Res*. 2018;46(D1): D8-D13. doi:10.1093/nar/gkx1095
128. Huang DW, Sherman BT, Lempicki RA. Systematic and integrative analysis of large gene lists using DAVID bioinformatics resources. *Nat Protoc*. 2009;4(1):44-57.
129. Del Sal G, Ruaro ME, Philipson L, Schneider C. The growth arrest-specific gene, gas1, is involved in growth suppression. *Cell*. 1992;70(4):595-607. doi:10.1016/0092-8674(92)90429-g
130. Ruaro ME, Stebel M, Vatta P, Marzinotto S, Schneider C. Analysis of the domain requirement in Gas1 growth suppressing activity. *FEBS Lett*. 2000;481(2):159-163. doi:10.1016/s0014-5793(00)02005-6
131. Stebel M, Vatta P, Ruaro ME, Del Sal G, Parton RG, Schneider C. The growth suppressing gas1 product is a GPI-linked protein. *FEBS Lett*. 2000;481(2):152-158. doi:10.1016/s0014-5793(00)02004-4
132. Cabrera JR, Sanchez-Pulido L, Rojas AM, et al. Gas1 is related to the glial cell-derived neurotrophic factor family receptors alpha and regulates ret signaling. *J Biol Chem*. 2006;281(20): 14330-14339. doi:10.1074/jbc.M509572200
133. Huxley JS. Constant differential growth-ratios and their significance. *Nature*. 1924;114(20 December):895-896. doi:10.1038/114895a0
134. Longo G, Montévil M. Scaling and scale symmetries in biological systems. *Perspectives on Organisms: Biological Time, Symmetries and Singularities*. Springer Berlin Heidelberg; 2014: 23-73.
135. Ricklefs RE, Starck JM. Embryonic growth and development. In: Starck JM, Ricklefs RE, eds. *Avian Growth and Development: Evolution within the Altricial-Precocial Spectrum*. Oxford University Press; 1998:31-58.
136. Alberch P. Developmental constraints: why St. Bernards often have an extra digit and poodles never do. *American Naturalist*. 1985;126(3):430-433.
137. Alberch P. The logic of monsters: evidence for internal constraint in development and evolution. *Geobios*. 1989;22(Suppl 2):21–57. doi:10.1016/S0016-6995(89)80006-3
138. Oster G, Alberch P. Evolution and bifurcation of developmental programs. *Evolution*. 1982;36:444-459.
139. Hall BK, Miyake T. The membranous skeleton: the role of cell condensations in vertebrate skeletogenesis. *Anat Embryol (Berl)*. 1992;186(2):107-124.
140. Hall BK, Miyake T. Divide, accumulate, differentiate: cell condensation in skeletal development revisited. *Int J Dev Biol*. 1995;39(6):881-893.
141. Hall BK, Miyake T. All for one and one for all: condensations and the initiation of skeletal development. *Bioessays*. 2000; 22(2):138-147.
142. Summerbell D, Lewis JH, Wolpert L. Positional information in chick limb morphogenesis. *Nature*. 1973;244(5417):492-496.
143. Riddle RD, Johnson RL, Laufer E, Tabin C. Sonic hedgehog mediates the polarizing activity of the ZPA. *Cell*. 1993;75(7): 1401-1416.
144. Echelard Y, Epstein DJ, St-Jacques B, et al. Sonic hedgehog, a member of a family of putative signaling molecules, is implicated in the regulation of CNS polarity. *Cell*. 1993;75(7):1417-1430.
145. Laufer E, Nelson CE, Johnson RL, Morgan BA, Tabin C. Sonic hedgehog and Fgf-4 act through a signaling cascade and feedback loop to integrate growth and patterning of the developing limb bud. *Cell*. 1994;79(6):993-1003.
146. Ericson J, Muhr J, Placzek M, Lints T, Jessell TM, Edlund T. Sonic hedgehog induces the differentiation of ventral forebrain neurons: a common signal for ventral patterning within the neural tube [published erratum appears in cell 1995 Jul 14;82(1):following 165]. *Cell*. 1995;81(5):747–756.
147. López-Martínez A, Chang DT, Chiang C, et al. Limb-patterning activity and restricted posterior localization of the amino-terminal product of sonic hedgehog cleavage. *Curr Biol*. 1995;5(7):791-796.
148. Ericson J, Briscoe J, Rashbass P, van Heyningen V, Jessell TM. Graded sonic hedgehog signaling and the specification of cell fate in the ventral neural tube. *Cold Spring Harb Symp Quant Biol*. 1997;62(1):451-466.

149. Yang Y, Drossopoulou G, Chuang PT, et al. Relationship between dose, distance and time in sonic hedgehog-mediated regulation of anteroposterior polarity in the chick limb. *Development*. 1997;124(21):4393-4404.
150. Zeng X, Goetz JA, Suber LM, Scott WJ Jr, Schreiner CM, Robbins DJ. A freely diffusible form of sonic hedgehog mediates long-range signalling. *Nature*. 2001;411(6838):716-720.
151. Briscoe J, Chen Y, Jessell TM, Struhl G. A hedgehog-insensitive form of patched provides evidence for direct long-range morphogen activity of sonic hedgehog in the neural tube. *Mol Cell*. 2001;7(6):1279-1291.
152. McLellan JS, Zheng X, Hauk G, Ghirlando R, Beachy PA, Leahy DJ. The mode of hedgehog binding to Ihog homologues is not conserved across different phyla. *Nature*. 2008;455(7215):979-983. doi:10.1038/nature07358
153. Dessaud E, McMahon AP, Briscoe J. Pattern formation in the vertebrate neural tube: a sonic hedgehog morphogen-regulated transcriptional network. *Development*. 2008;135(15):2489-2503. doi:10.1242/dev.009324
154. Hu D, Marcucio RS. A SHH-responsive signaling center in the forebrain regulates craniofacial morphogenesis via the facial ectoderm. *Development*. 2009;136(1):107–116. doi:10.1242/dev.026583
155. Xu Q, Jamniczky H, Hu D, et al. Correlations between the morphology of sonic hedgehog expression domains and embryonic craniofacial shape. *Evol Biol*. 2015;42(3):379-386. doi:10.1007/s11692-015-9321-z
156. Tosney KW. The segregation and early migration of cranial neural crest cells in the avian embryo. *Dev Biol*. 1982;89(1):13-24.
157. Lee CS, Fan CM. Embryonic expression patterns of the mouse and chick Gas1 genes. *Mech Dev*. 2001;101(1–2):293-297. doi:10.1016/s0925-4773(01)00283-0
158. Zarco N, Bautista E, Cuellar M, et al. Growth arrest specific 1 (GAS1) is abundantly expressed in the adult mouse central nervous system. *J Histochem Cytochem*. 2013;61(10):731-748. doi:10.1369/0022155413498088
159. Smith SS, Chu D, Qu T, Aggleton JA, Schneider RA. Species-specific sensitivity to TGFbeta signaling and changes to the Mmp13 promoter underlie avian jaw development and evolution. *Elife*. 2022;11:e66005. doi:10.7554/eLife.66005
160. Kvon EZ, Kamneva OK, Melo US, et al. Progressive loss of function in a limb enhancer during Snake evolution. *Cell*. 2016;167(3):633-642.e11. doi:10.1016/j.cell.2016.09.028
161. Lopez-Rios J, Duchesne A, Speziale D, et al. Attenuated sensing of SHH by Ptch1 underlies evolution of bovine limbs. *Nature*. 2014;511(7507):46-51. doi:10.1038/nature13289
162. Chang C-F, Chang Y-T, Millington G, Brugmann SA. Craniofacial ciliopathies reveal specific requirements for GLI proteins during development of the facial midline. *PLoS Genet*. 2016;12(11):e1006351. doi:10.1371/journal.pgen.1006351
163. Elliott KH, Chen X, Salomone J, et al. Gli3 utilizes Hand2 to synergistically regulate tissue-specific transcriptional networks. *Elife*. 2020;9:e56450. doi:10.7554/eLife.56450
164. Swartz ME, Lovely CB, Eberhart JK. Variation in phenotypes from a bmp-Gata3 genetic pathway is modulated by Shh signaling. *PLoS Genet*. 2021;17(5):e1009579. doi:10.1371/journal.pgen.1009579
165. Cobourne MT, Miletich I, Sharpe PT. Restriction of sonic hedgehog signalling during early tooth development. *Development*. 2004;131(12):2875-2885. doi:10.1242/dev.01163
166. Wagner A. Robustness and evolvability: a paradox resolved. *Proc Biol Sci*. 2008;275(1630):91-100. doi:10.1098/rspb.2007.1137
167. Kang JS, Zhang W, Krauss RS. Hedgehog signaling: cooking with Gas1. *Sci STKE*. 2007;2007(403):pe50. doi:10.1126/stke.4032007pe50
168. Martin A, Orgogozo V. The loci of repeated evolution: a catalog of genetic hotspots of phenotypic variation. *Evolution*. 2013;67(5):1235-1250. doi:10.1111/evo.12081
169. Swartz ME, Nguyen V, McCarthy NQ, Eberhart JK. Hh signaling regulates patterning and morphogenesis of the pharyngeal arch-derived skeleton. *Dev Biol*. 2012;369(1):65-75. doi:10.1016/j.ydbio.2012.05.032
170. Lettice LA, Heaney SJ, Purdie LA, et al. A long-range Shh enhancer regulates expression in the developing limb and fin and is associated with preaxial polydactyly. *Hum Mol Genet*. 2003;12(14):1725-1735. doi:10.1093/hmg/ddg180
171. Sagai T, Masuya H, Tamura M, et al. Phylogenetic conservation of a limb-specific, cis-acting regulator of sonic hedgehog (Shh). *Mamm Genome*. 2004;15(1):23-34. doi:10.1007/s00335-033-2317-5
172. Sagai T, Hosoya M, Mizushina Y, Tamura M, Shiroishi T. Elimination of a long-range cis-regulatory module causes complete loss of limb-specific Shh expression and truncation of the mouse limb. *Development*. 2005;132(4):797-803. doi:10.1242/dev.01613
173. Karlstrom RO, Tyurina OV, Kawakami A, et al. Genetic analysis of zebrafish gli1 and gli2 reveals divergent requirements for gli genes in vertebrate development. *Development*. 2003;130(8):1549-1564. doi:10.1242/dev.00364
174. Ruiz i Altaba A, Mas C, Stecca B. The Gli code: an information nexus regulating cell fate, stemness and cancer. *Trends Cell Biol*. 2007;17(9):438-447. doi:10.1016/j.tcb.2007.06.007
175. Abbasi AA, Goode DK, Amir S, Grzeschik KH. Evolution and functional diversification of the GLI family of transcription factors in vertebrates. *Evol Bioinform Online*. 2009;5:5-13. doi:10.4137/ebo.s2322
176. Schneider C, King RM, Philipson L. Genes specifically expressed at growth arrest of mammalian cells. *Cell*. 1988;54(6):787-793. doi:10.1016/s0092-8674(88)91065-3
177. Del Sal G, Ruaro EM, Utrera R, Cole CN, Levine AJ, Schneider C. Gas1-induced growth suppression requires a transactivation-independent p53 function. *Mol Cell Biol*. 1995;15(12):7152-7160. doi:10.1128/mcb.15.12.7152
178. Zamorano A, Mellström B, Vergara P, Naranjo JR, Segovia J. Glial-specific retrovirally mediated gas1 gene expression induces glioma cell apoptosis and inhibits tumor growth in vivo. *Neurobiol Dis*. 2004;15(3):483-491. doi:10.1016/j.nbd.2003.11.022
179. Lee KK, Leung AK, Tang MK, et al. Functions of the growth arrest specific 1 gene in the development of the mouse embryo. *Dev Biol*. 2001;234(1):188-203. doi:10.1006/dbio.2001.0249
180. Liu Y, May NR, Fan CM. Growth arrest specific gene 1 is a positive growth regulator for the cerebellum. *Dev Biol*. 2001;236(1):30-45. doi:10.1006/dbio.2000.0146

181. Bautista E, Zarco N, Aguirre-Pineda N, et al. Expression of Gas1 in mouse brain: release and role in neuronal differentiation. *Cell Mol Neurobiol*. 2018;38(4):841-859. doi:10.1007/s10571-017-0559-0
182. Balaskas N, Ribeiro A, Panovska J, et al. Gene regulatory logic for reading the sonic hedgehog signaling gradient in the vertebrate neural tube. *Cell*. 2012;148(1–2):273-284. doi:10.1016/j.cell.2011.10.047
183. Jacobs CT, Dominguez J, Devine J, Vidal-García M, David Aponte J, da Silva C, Marcucio RS, Hallgrímsson B A nonlinear response to hedgehog Signalling provides a mechanism for novel directions of shape change during development. *Evolutionary Biology*. 2026;53:103-117. doi:10.1007/s11692-026-09667-0.
184. Green RM, Fish JL, Young NM, et al. Developmental nonlinearity drives phenotypic robustness. *Nat Commun*. 2017;8(1):1970. doi:10.1038/s41467-017-02037-7
185. Mosby LS, Bowen AE, Hadjivasiliou Z. Morphogens in the evolution of size, shape and patterning. *Development*. 2024;151(18):1-14. doi:10.1242/dev.202412
186. Ahlgren SC, Bronner-Fraser M. Inhibition of sonic hedgehog signaling in vivo results in craniofacial neural crest cell death. *Curr Biol*. 1999;9(22):1304-1314.
187. Marchini M, Keller G, Khan N, et al. Sonic hedgehog and fibroblast growth factor 8 regulate the evolution of amniote facial proportions. *Commun Biol*. 2025;8(1):84. 10.1038/s42003-025-07522-0
188. Sacilotto N, Castillo J, Riffo-Campos ÁL, et al. Growth arrest specific 1 (Gas1) gene overexpression in liver reduces the in vivo progression of murine hepatocellular carcinoma and partially restores gene expression levels. *PLoS One*. 2015;10(7):e0132477. doi:10.1371/journal.pone.0132477
189. Sarkar S, Poon CC, Mirzaei R, et al. Microglia induces Gas1 expression in human brain tumor-initiating cells to reduce tumorigenecity. *Sci Rep*. 2018;8(1):15286. doi:10.1038/s41598-018-33306-0
190. Leem YE, Han JW, Lee HJ, et al. Gas1 cooperates with Cdo and promotes myogenic differentiation via activation of p38MAPK. *Cell Signal*. 2011;23(12):2021-2029. doi:10.1016/j.cellsig.2011.07.016
191. Eames BF, Sharpe PT, Helms JA. Hierarchy revealed in the specification of three skeletal fates by Sox9 and Runx2. *Dev Biol*. 2004;274(1):188-200.
192. Sarkar L, Cobourne M, Naylor S, Smalley M, Dale T, Sharpe PT. Wnt/Shh interactions regulate ectodermal boundary formation during mammalian tooth development. *Proc Natl Acad Sci U S A*. 2000;97(9):4520-4524.
193. Kurosaka H, Iulianella A, Williams T, Trainor PA. Disrupting hedgehog and WNT signaling interactions promotes cleft lip pathogenesis. *J Clin Invest*. 2014;124(4):1660-1671. doi:10.1172/JCI72688
194. Kurosaka H, Trainor PA, Leroux-Berger M, Iulianella A. Cranial nerve development requires co-ordinated Shh and canonical Wnt signaling. *PLoS One*. 2015;10(3):e0120821. doi:10.1371/journal.pone.0120821
195. Marchini M, Hu D, Lo Vercio L, et al. Wnt signaling drives correlated changes in facial morphology and brain shape. *Front Cell Dev Biol*. 2021;9:644099. doi:10.3389/fcell.2021.644099
196. Seppala M, Thivichon-Prince B, Xavier GM, et al. Gas1 regulates patterning of the murine and human dentitions through sonic hedgehog. *J Dent Res*. 2022;101(4):473-482. doi:10.1177/00220345211049403
197. Sun L, Wang J, Chen S, He Y. Crosstalk between Wnt/beta-catenin and hedgehog supports Gli1+ lineage Osteogenesis in cranial sutures. *Int J Mol Sci*. 2025;26(8):5308. doi:10.3390/ijms26083508
198. Sagai T, Amano T, Maeno A, et al. SHH signaling directed by two oral epithelium-specific enhancers controls tooth and oral development. *Sci Rep*. 2017;7(1):13004. doi:10.1038/s41598-017-12532-y
199. Seo H, Amano T, Seki R, et al. Upstream enhancer elements of Shh regulate Oral and dental patterning. *J Dent Res*. 2018;97(9):1055-1063. doi:10.1177/0022034518758642
200. Truman AW, Kitazono AA, Fitz Gerald JN, Kron SJ. Cell Cycle: Regulation by Cyclins. *eLS*. John Wiley & Sons, Ltd; 2001.
201. Kohoutek J, Blazek D. Cyclin K goes with Cdk12 and Cdk13. *Cell Div*. 2012;7:12. doi:10.1186/1747-1028-7-12
202. Yuan K, O'Farrell PH. Cyclin B3 is a mitotic cyclin that promotes the metaphase-anaphase transition. *Curr Biol*. 2015;25(6):811-816. doi:10.1016/j.cub.2015.01.053
203. Xiao Y, Dong J. Coming of age: targeting cyclin K in cancers. *Cells*. 2023;12(16):2044. doi:10.3390/cells12162044
204. Lara-Gonzalez P, Variyar S, Moghareh S, et al. Cyclin B3 is a dominant fast-acting cyclin that drives rapid early embryonic mitoses. *J Cell Biol*. 2024;223(11):1-13. doi:10.1083/jcb.202308034
205. Dutto I, Tillhon M, Cazzalini O, Stivala LA, Prosperi E. Biology of the cell cycle inhibitor p21(CDKN1A): molecular mechanisms and relevance in chemical toxicology. *Arch Toxicol*. 2015;89(2):155-178. doi:10.1007/s00204-014-1430-4
206. Shamloo B, Usluer S. p21 in cancer research. *Cancers (Basel)*. 2019;11(8):1178. doi:10.3390/cancers11081178
207. Brinkkoetter PT, Pippin JW, Shankland SJ. Cyclin I-Cdk5 governs survival in post-mitotic cells. *Cell Cycle*. 2010;9(9):1729-1731. doi:10.4161/cc.9.9.11471
208. Loyer P, Trembley JH, Grenet JA, et al. Characterization of cyclin L1 and L2 interactions with CDK11 and splicing factors: influence of cyclin L isoforms on splice site selection. *J Biol Chem*. 2008;283(12):7721-7732. doi:10.1074/jbc.M708188200
209. Morgan DO. Principles of CDK regulation. *Nature*. 1995;374(6518):131-134. doi:10.1038/374131a0
210. Vermeulen K, Van Bockstaele DR, Berneman ZN. The cell cycle: a review of regulation, deregulation and therapeutic targets in cancer. *Cell Prolif*. 2003;36(3):131-149. doi:10.1046/j.1365-2184.2003.00266.x
211. Lee CS, Buttitta L, Fan CM. Evidence that the WNT-inducible growth arrest-specific gene 1 encodes an antagonist of sonic hedgehog signaling in the somite. *Proc Natl Acad Sci U S A*. 2001;98(20):11347-11352.
212. Marczenke M, Sunaga-Franze DY, Popp O, et al. GAS1 is required for NOTCH-dependent facilitation of SHH signaling in the ventral forebrain neuroepithelium. *Development*. 2021;148(21):1-14. doi:10.1242/dev.200080
213. Franks NE, Allen BL. Hedgehog-dependent and hedgehog-independent roles for growth arrest specific 1 in mammalian

kidney morphogenesis. *Development*. 2024;151(24):1-15. doi:10.1242/dev.203012

214. Pereira SL, Baker AJ. A molecular timescale for galliform birds accounting for uncertainty in time estimates and heterogeneity of rates of DNA substitutions across lineages and sites. *Mol Phylogenet Evol*. 2006;38(2):499-509. doi:10.1016/j.ympev.2005.07.007
215. Mitchell PJ, Timmons PM, Hébert JM, Rigby PWJ, Tjian R. Transcription factor *AP-2* is expressed in neural crest cell lineages during mouse embryogenesis. *Genes Dev*. 1991;5:105-119.
216. Chazaud C, Oulad-Abdelghani M, Bouillet P, Décimo D, Chambon P, Dollé P. AP-2.2, a novel gene related to AP-2, is expressed in the forebrain, limbs and face during mouse embryogenesis. *Mech Dev*. 1996;54(1):83-94.
217. Schorle H, Meier P, Buchert M, Jaenisch R, Mitchell PJ. Transcription factor *AP-2* essential for cranial closure and craniofacial development. *Nature*. 1996;381(6579):235-238.
218. Shen H, Wilke T, Ashique AM, et al. Chicken transcription factor AP-2: cloning, expression and its role in outgrowth of facial prominences and limb buds. *Dev Biol*. 1997;188(2):248-266.
219. Brewer S, Feng W, Huang J, Sullivan S, Williams T. Wnt1-Cre-mediated deletion of AP-2alpha causes multiple neural crest-related defects. *Dev Biol*. 2004;267(1):135-152. doi:10.1016/j.ydbio.2003.10.039
220. Van Otterloo E, Milanda I, Pike H, et al. AP-2alpha and AP-2beta cooperatively function in the craniofacial surface ectoderm to regulate chromatin and gene expression dynamics during facial development. *Elife*. 2022;11:e70511. doi:10.7554/eLife.70511
221. Southard-Smith EM, Kos L, Pavan WJ. Sox10 mutation disrupts neural crest development in Dom Hirschsprung mouse model. *Nat Genet*. 1998;18(1):60-64. doi:10.1038/ng0198-60
222. Mollaaghababa R, Pavan WJ. The importance of having your SOX on: role of SOX10 in the development of neural crest-derived melanocytes and glia [review]. *Oncogene*. 2003;22(20):3024-3034. doi:10.1038/sj.onc.1206442
223. Britsch S, Goerich DE, Riethmacher D, et al. The transcription factor Sox10 is a key regulator of peripheral glial development. *Genes Dev*. 2001;15(1):66-78. doi:10.1101/gad.186601
224. Le Beulze M, Daubech C, Balde-Camara A, Ghieh F, Vialard F. Mammal reproductive Homeobox (Rhox) genes: an update of their involvement in reproduction and development. *Genes (Basel)*. 2023;14(9):1685. doi:10.3390/genes14091685
225. Lan Y, Kingsley PD, Cho ES, Jiang R. Osr2, a new mouse gene related to drosophila odd-skipped, exhibits dynamic expression patterns during craniofacial, limb, and kidney development. *Mech Dev*. 2001;107(1–2):175-179. doi:10.1016/s0925-4773(01)00457-9
226. Lan Y, Ovitt CE, Cho ES, Maltby KM, Wang Q, Jiang R. Odd-skipped related 2 (Osr2) encodes a key intrinsic regulator of secondary palate growth and morphogenesis. *Development*. 2004;131(13):3207-3216. doi:10.1242/dev.01175
227. Stricker S, Brieske N, Haupt J, Mundlos S. Comparative expression pattern of odd-skipped related genes Osr1 and Osr2 in chick embryonic development. *Gene Expr Patterns*. 2006;6(8):826-834. doi:10.1016/j.modgep.2006.02.003
228. Gao Y, Lan Y, Ovitt CE, Jiang R. Functional equivalence of the zinc finger transcription factors Osr1 and Osr2 in mouse development. *Dev Biol*. 2009;328(2):200-209. doi:10.1016/j.ydbio.2009.01.008.
229. Weise A, Bruser K, Elfert S, et al. Alternative splicing of Tcf7l2 transcripts generates protein variants with differential promoter-binding and transcriptional activation properties at Wnt/beta-catenin targets. *Nucleic Acids Res*. 2010;38(6):1964-1981. doi:10.1093/nar/gkp1197
230. Cadigan KM, Waterman ML. TCF/LEFs and Wnt Signaling in the Nucleus. *Cold Spring Harb Perspect Biol*. 2012;4(11):a007906. doi:10.1101/cshperspect.a007906
231. Wallmen B, Schrempp M, Hecht A. Intrinsic properties of Tcf1 and Tcf4 splice variants determine cell-type-specific Wnt/beta-catenin target gene expression. *Nucleic Acids Res*. 2012;40(19):9455-9469. doi:10.1093/nar/gks690
232. Kennedy MW, Chalamalasetty RB, Thomas S, Garriock RJ, Jailwala P, Yamaguchi TP. Sp5 and Sp8 recruit beta-catenin and Tcf1-Lef1 to select enhancers to activate Wnt target gene transcription. *Proc Natl Acad Sci U S A*. 2016;113(13):3545-3550. doi:10.1073/pnas.1519994113
233. Huggins IJ, Bos T, Gaylord O, et al. The WNT target SP5 negatively regulates WNT transcriptional programs in human pluripotent stem cells. *Nat Commun*. 2017;8(1):1034. doi:10.1038/s41467-017-01203-1
234. Pourebrahim R, Houtmeyers R, Ghogomu S, et al. Transcription factor Zic2 inhibits Wnt/beta-catenin protein signaling. *J Biol Chem*. 2011;286(43):37732-37740. doi:10.1074/jbc.M111.242826
235. Fujimi TJ, Hatayama M, Aruga J. Xenopus Zic3 controls notochord and organizer development through suppression of the Wnt/beta-catenin signaling pathway. *Dev Biol*. 2012;361(2):220-231. doi:10.1016/j.ydbio.2011.10.026
236. Ali RG, Bellchambers HM, Warr N, et al. WNT-responsive SUMOylation of ZIC5 promotes murine neural crest cell development, having multiple effects on transcription. *J Cell Sci*. 2021;134(9):1-13. doi:10.1242/jcs.256792
237. Aruga J, Tohmonda T, Homma S, Mikoshiba K. Zic1 promotes the expansion of dorsal neural progenitors in spinal cord by inhibiting neuronal differentiation. *Dev Biol*. 2002;244(2):329-341. doi:10.1006/dbio.2002.0598
238. Mizugishi K, Aruga J, Nakata K, Mikoshiba K. Molecular properties of Zic proteins as transcriptional regulators and their relationship to GLI proteins. *J Biol Chem*. 2001;276(3):2180-2188. doi:10.1074/jbc.M004430200
239. Koyabu Y, Nakata K, Mizugishi K, Aruga J, Mikoshiba K. Physical and functional interactions between Zic and Gli proteins. *J Biol Chem*. 2001;276(10):6889-6892. doi:10.1074/jbc.C000773200
240. Quinn ME, Haaning A, Ware SM. Preaxial polydactyly caused by Gli3 haploinsufficiency is rescued by Zic3 loss of function in mice. *Hum Mol Genet*. 2012;21(8):1888-1896. doi:10.1093/hmg/dds002
241. Funato N, Kokubo H, Nakamura M, Yanagisawa H, Saga Y. Specification of jaw identity by the Hand2 transcription factor. *Sci Rep*. 2016;6:28405. doi:10.1038/srep28405
242. Barron F, Woods C, Kuhn K, Bishop J, Howard MJ, Clouthier DE. Downregulation of Dlx5 and Dlx6 expression

by Hand2 is essential for initiation of tongue morphogenesis. *Development*. 2011;138(11):2249-2259. doi:10.1242/dev.056929
243. Wall DS, Wallace VA. Hedgehog to Hes1: the heist of a Notch target. *Cell Cycle*. 2009;8(9):1301-1302. doi:10.4161/cc.8.9.8284
244. Wall DS, Mears AJ, McNeill B, et al. Progenitor cell proliferation in the retina is dependent on Notch-independent sonic hedgehog/Hes1 activity. *J Cell Biol*. 2009;184(1):101-112. doi:10.1083/jcb.200805155
245. Yin WC, Satkunendran T, Mo R, et al. Dual regulatory functions of SUFU and Targetome of GLI2 in SHH subgroup Medulloblastoma. *Dev Cell*. 2019;48(2):167-183 e5. doi:10.1016/j.devcel.2018.11.015
246. Voronova A, Al Madhoun A, Fischer A, Shelton M, Karamboulas C, Skerjanc IS. Gli2 and MEF2C activate each other's expression and function synergistically during cardiomyogenesis in vitro. *Nucleic Acids Res*. 2012;40(8):3329-3347. doi:10.1093/nar/gkr1232
247. Kim Y, Lee J, Seppala M, Cobourne MT, Kim SH. Ptch2/Gas1 and Ptch1/Boc differentially regulate hedgehog signalling in murine primordial germ cell migration. *Nat Commun*. 2020;11(1):1994. doi:10.1038/s41467-020-15897-3
248. Leary S, Underwood W, Anthony R, et al. *AVMA Guidelines for the Euthanasia of Animals: 2020 Edition*. American Veterinary Medical Association. Schaumburg, IL2020.
249. Tyler MS, Hall BK. Epithelial influences on skeletogenesis in the mandible of the embryonic chick. *Anat Rec*. 1977;188:229-240.
250. Sosa JM, Huber DE, Welk B, Fraser HL. Development and application of MIPAR™: a novel software package for two- and three-dimensional microstructural characterization. *Integr Mater Manuf Innov*. 2014;3(1):123–140. doi:10.1186/2193-9772-3-10
251. Koressaar T, Remm M. Enhancements and modifications of primer design program Primer3. *Bioinformatics*. 2007;23(10):1289-1291. doi:10.1093/bioinformatics/btm091
252. Untergasser A, Cutcutache I, Koressaar T, et al. Primer3--new capabilities and interfaces. *Nucleic Acids Res*. 2012;40(15):e115. doi:10.1093/nar/gks596
253. Ye J, Coulouris G, Zaretskaya I, Cutcutache I, Rozen S, Madden TL. Primer-BLAST: a tool to design target-specific primers for polymerase chain reaction. *BMC Bioinform*. 2012;13:134. doi:10.1186/1471-2105-13-134
254. Pfaffl MW. A new mathematical model for relative quantification in real-time RT-PCR. *Nucleic Acids Res*. 2001;29(9):e45. doi:10.1093/nar/29.9.e45
255. Fish JL, Schneider RA. Assessing species-specific contributions to craniofacial development using quail-duck chimeras. *J Vis Exp*. 2014;87:e51534. doi:10.3791/51534
256. Noden DM. The role of the neural crest in patterning of avian cranial skeletal, connective, and muscle tissues. *Dev Biol*. 1983;96:144-165.
257. Schneider RA. Neural crest can form cartilages normally derived from mesoderm during development of the avian head skeleton. *Dev Biol*. 1999;208(2):441-455.
258. Li J, Zhang J, Liu J, et al. A new duck genome reveals conserved and convergently evolved chromosome architectures of birds and mammals. *Gigascience*. 2021;10(1):1-15. doi:10.1093/gigascience/giaa142
259. Morris KM, Hindle MM, Boitard S, et al. The quail genome: insights into social behaviour, seasonal biology and infectious disease response. *BMC Biol*. 2020;18(1):14. doi:10.1186/s12915-020-0743-4
260. Prime G. v2021. 0.1. Biomatters, Ltd, Auckland, New Zealand; 603. 2021.
261. Robinson MD, McCarthy DJ, Smyth GK. edgeR: a Bioconductor package for differential expression analysis of digital gene expression data. *Bioinformatics*. 2010;26(1):139-140. doi:10.1093/bioinformatics/btp616
262. Rauluseviciute I, Riudavets-Puig R, Blanc-Mathieu R, et al. JASPAR 2024: 20th anniversary of the open-access database of transcription factor binding profiles. *Nucleic Acids Res*. 2024;52(D1):D174-D182. doi:10.1093/nar/gkad1059
263. Tan G, Lenhard B. TFBSTools: an R/bioconductor package for transcription factor binding site analysis. *Bioinformatics*. 2016;32(10):1555-1556. doi:10.1093/bioinformatics/btw024
264. Team RC. R: A Language and Environment for Statistical Computing. 2013.
265. Nishida K, Frith MC, Nakai K. Pseudocounts for transcription factor binding sites. *Nucleic Acids Res*. 2009;37(3):939-944. doi:10.1093/nar/gkn1019
266. Jones P, Binns D, Chang HY, et al. InterProScan 5: genome-scale protein function classification. *Bioinformatics*. 2014;30(9):1236-1240. doi:10.1093/bioinformatics/btu031
267. Ishida T, Kinoshita K. PrDOS: prediction of disordered protein regions from amino acid sequence. *Nucleic Acids Res*. 2007;35:W460-W464. doi:10.1093/nar/gkm363

SUPPORTING INFORMATION

Additional supporting information can be found online in the Supporting Information section at the end of this article.

How to cite this article: Vavrušová Z, Chu DB, Nguyen A, Ta Y, Fish JL, Schneider RA. Differential sensitivity to SHH signaling and neural crest-mediated *Gas1* expression regulate jaw size during development and evolution. *Developmental Dynamics*. 2026;1-36. doi:10.1002/dvdy.70177

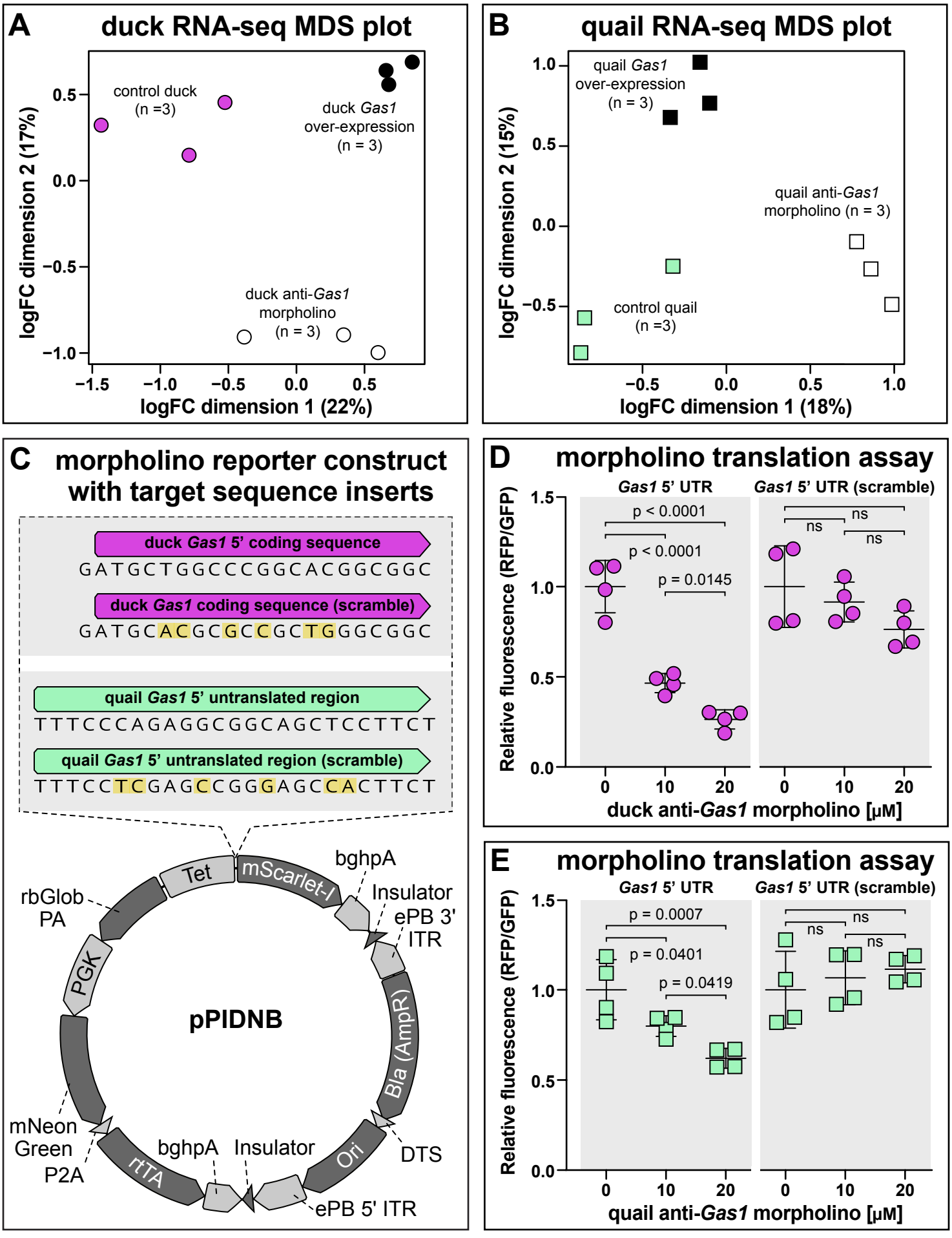
A
duck RNA-seq MDS plot
control duck
(n =3)
duck Gas1
over-expression
(n = 3)
duck anti-Gas1
morpholino
(n = 3)
logFC dimension 2 (17%)
logFC dimension 1 (22%)
B
quail RNA-seq MDS plot
quail Gas1
over-expression
(n = 3)
quail anti-Gas1
morpholino (n = 3)
control quail
(n =3)
logFC dimension 2 (15%)
logFC dimension 1 (18%)
C
morpholino reporter construct
with target sequence inserts
duck Gas1 5' coding sequence
GATGCTGGCCCGGCACGGCGGC
duck Gas1 coding sequence (scramble)
GATGCACGCGCCGCTGGGCGGC
quail Gas1 5' untranslated region
TTTCCCAGAGGCGGCAGCTCCTTCT
quail Gas1 5' untranslated region (scramble)
TTTCCTCGAGCCGGGAGCCACTTCT
pPIDNB
Tet
mScarlet-I
bghpA
Insulator
ePB 3'
ITR
Bla (AmpR)
DTS
Ori
ePB 5' ITR
Insulator
bghpA
rtTA
P2A
mNeon
Green
PA
rbGlob
PGK
D
morpholino translation assay
Gas1 5' UTR
Gas1 5' UTR (scramble)
p < 0.0001
p < 0.0001
p = 0.0145
ns
ns
ns
Relative fluorescence (RFP/GFP)
duck anti-Gas1 morpholino [μM]
E
morpholino translation assay
Gas1 5' UTR
Gas1 5' UTR (scramble)
p = 0.0007
p = 0.0401
p = 0.0419
ns
ns
ns
Relative fluorescence (RFP/GFP)
quail anti-Gas1 morpholino [μM]


Consensus
Identity
1. GAS1 Quail protein
2. GAS1 Duck protein
3. GAS1 Chick protein
4. GAS1 Human protein
5. GAS1 Mouse protein

Supplemental Table 1. Duck and quail incubation times

stage	approximate incubation [days]	
	duck	quail
HH8.5	2.4	1.2
HH9.5	2.5	1.3
HH15	3.5	2.2
HH18	4.5	2.7
HH21	5.5	3.4
HH24	6.5	4.2
HH27	7.5	5

Supplemental Table 2. Mandibular mesenchyme population size in duck and quail

stage	duck			quail			duck versus quail
	mean	SEM	n	mean	SEM	n	p-values
HH18	68206.8	10378.0	9	18574.7	3991.7	9	3.92E-04
HH21	279777.8	24087.8	12	59793.2	4784.6	9	5.11E-07
HH24	638656.6	26323.9	11	163454.6	14439.6	11	3.56E-12
HH27	2105453.7	74286.0	18	505857.1	42977.0	7	1.41E-11

Supplemental Table 3. Mandibular mesenchyme population size modeling in duck and quail embryos

stage	duck			quail		
	hours	population	n° cell cycles	hours	population	n° cell cycles
HH13	0	1.26	0	0	1.00	0
HH15	24	4.31	1.78	12	2.13	1.09
HH18	26	16.37	1.93	12	4.54	1.09
HH21	26	62.19	1.93	18	14.11	1.64
HH24	24	213.26	1.78	20	49.74	1.82
HH27	24	731.28	1.78	20	175.40	1.82

Supplemental Table 4. Duck/quail mandibular mesenchyme population size ratios

stage	HH18	HH21	HH24	HH27
in vivo	3.67	4.68	3.91	4.16
model	3.61	4.41	4.29	4.17

Supplemental Table 5. SHH pathway members mRNA levels and p-values in duck and quail mandibular primordia

gene	stage	duck			quail			duck vs. quail
		mean	SEM	n	mean	SEM	n	p-value
Shh	HH15	21.52	1.88	13	1.03	0.08	11	< 0.000001
	HH18	4.27	0.63	8	1.42	0.23	11	0.000361
	HH21	1.35	0.17	10	9.56	1.48	8	0.000040
	HH24	0.94	0.10	10	6.38	0.79	9	0.000006
	HH27	0.82	0.09	8	0.96	0.26	6	0.577145
Ptch1	HH15	36.58	2.32	13	1.03	0.09	11	< 0.000001
	HH18	17.55	1.10	8	1.08	0.08	11	< 0.000001
	HH21	6.84	0.69	10	8.20	0.75	8	0.490391
	HH24	6.55	0.44	10	6.92	0.64	9	0.867551
	HH27	4.79	0.70	8	4.81	0.62	6	0.979494
Smo	HH15	9.28	0.25	13	1.01	0.04	11	< 0.000001
	HH18	1.96	0.15	8	0.55	0.03	11	< 0.000001
	HH21	0.73	0.09	10	7.19	0.68	8	< 0.000001
	HH24	0.82	0.08	10	7.68	0.60	9	< 0.000001
	HH27	0.73	0.05	8	8.44	0.57	6	< 0.000001
Cdon	HH15	22.20	1.36	13	1.01	0.03	11	< 0.000001
	HH18	8.93	1.02	8	0.60	0.05	11	< 0.000001
	HH21	1.71	0.18	10	6.12	0.55	8	< 0.000001
	HH24	2.14	0.24	10	7.22	0.46	9	< 0.000001
	HH27	1.99	0.14	8	9.85	0.50	6	< 0.000001
Boc	HH15	76.15	2.47	13	1.11	0.18	11	< 0.000001
	HH18	32.98	4.06	8	1.46	0.28	11	< 0.000001
	HH21	10.60	1.18	10	15.21	2.73	8	0.306173
	HH24	20.48	1.80	10	26.34	3.43	9	0.306173
	HH27	32.32	3.09	8	35.90	2.27	6	0.399275
Gas1	HH15	19.77	1.68	11	1.09	0.17	8	< 0.000001
	HH18	15.17	1.54	10	0.53	0.04	8	< 0.000001
	HH21	19.50	2.27	8	0.55	0.06	10	< 0.000001
	HH24	39.97	3.56	8	0.54	0.07	10	< 0.000001
	HH27	85.33	31.66	10	1.53	0.04	10	0.016400
Gli1	HH15	12.37	0.85	13	1.01	0.04	11	< 0.000001
	HH18	6.10	0.64	8	0.80	0.06	11	< 0.000001
	HH21	1.79	0.18	10	5.00	0.61	8	0.000091
	HH24	2.10	0.17	10	5.56	0.35	9	< 0.000001
	HH27	2.34	0.35	8	4.53	0.51	6	0.003356
Gli2	HH15	8.91	0.38	13	1.01	0.04	11	< 0.000001
	HH18	5.55	0.48	8	0.72	0.06	11	< 0.000001
	HH21	3.90	0.24	9	6.90	0.78	8	0.002999
	HH24	6.23	0.17	8	8.04	0.51	9	0.005630
	HH27	6.25	0.23	8	8.27	0.40	6	0.001758
Gli3	HH15	17.21	0.55	13	1.00	0.02	11	< 0.000001
	HH18	4.47	0.31	8	0.82	0.05	11	< 0.000001
	HH21	5.53	0.35	10	11.34	1.26	8	0.000160
	HH24	5.73	0.58	10	13.29	1.24	9	0.000050
	HH27	8.40	0.56	8	15.47	0.46	6	0.000002

Supplemental Table 6. Gas1 mRNA levels in duck mandibular mesenchyme versus epithelium at HH24 and HH27

stage	tissue	duck			
		mean	SEM	n	p-value
HH24	mesenchyme	0.8735	0.0951	9	—
HH24	epithelium	0.1086	0.0110	7	<0.0001
HH27	mesenchyme	1.1804	0.1970	9	—
HH27	epithelium	0.0517	0.0057	9	<0.0001

Supplemental Table 7. Mean, SEM, n, and p-values for quck

Shh mRNA level					
stage	mean	SEM	n	duck vs quck p value	quail vs quck p value
HH21	1.81	0.13	11	0.083217	0.000012
HH24	0.95	0.09	13	0.931297	0.949962

Ptch1 mRNA level					
stage	mean	SEM	n	duck vs quck p value	quail vs quck p value
HH21	3.85	0.38	11	0.000925	0.000855
HH24	2.75	0.19	13	< 0.000001	0.000855

Smo mRNA level					
stage	mean	SEM	n	duck vs quck p value	quail vs quck p value
HH21	1.064	0.07	11	0.007648	< 0.000001
HH24	1.181	0.06	13	0.002275	< 0.000001

Cdon mRNA level					
stage	mean	SEM	n	duck vs quck p value	quail vs quck p value
HH21	2.54	0.11	11	0.001593	< 0.000001
HH24	2.60	0.09	13	0.066077	< 0.000001

Boc mRNA level					
stage	mean	SEM	n	duck vs quck p value	quail vs quck p value
HH21	10.31	0.98	11	0.850456	0.000114
HH24	14.17	0.63	13	0.002994	< 0.000001

Gas1 mRNA level					
stage	mean	SEM	n	duck vs quck p value	quail vs quck p value
HH21	11.74	2.62	10	0.045359	0.000461
HH24	9.07	1.01	13	< 0.000001	0.000004

Gli1 mRNA level					
stage	mean	SEM	n	duck vs quck p value	quail vs quck p value
HH21	5.53	0.84	7	0.000246	0.969634
HH24	4.90	0.73	13	0.003425	0.935326

Gli2 mRNA level					
stage	mean	SEM	n	duck vs quck p value	quail vs quck p value
HH21	1.65	0.06	11	< 0.000001	< 0.000001
HH24	2.06	0.07	13	< 0.000001	< 0.000001

Gli3 mRNA level					
stage	mean	SEM	n	duck vs quck p value	quail vs quck p value
HH21	2.57	0.13	11	< 0.000001	< 0.000001
HH24	2.87	0.08	13	0.000017	< 0.000001

Supplemental Table 8. mRNA levels for SHH pathway members in treated duck and quail mandibular primordia explant cultures

gene	treatment	duck			vs control	quail			vs control
		mean	SEM	n	p-value	mean	SEM	n	p-value
Shh	ctrl	1.14	0.14	17	—	1.06	0.10	14	—
	cycl	1.78	0.25	8	0.0305	1.55	0.23	8	0.0793
	0.1	0.76	0.27	4	0.6530	0.71	0.07	7	0.3810
	1	0.54	0.06	6	0.0869	1.14	0.28	7	0.9980
	10	0.47	0.04	6	0.0437	0.84	0.11	6	0.8537
	100	0.53	0.09	6	0.0786	0.66	0.07	7	0.2547
	1000	0.57	0.16	13	0.0216	0.47	0.13	8	0.0212
Ptch1	ctrl	1.04	0.08	17	—	1.04	0.08	14	—
	cycl	0.23	0.02	8	0.0024	0.15	0.01	8	< 0.0001
	0.1	0.83	0.18	4	0.9654	0.77	0.09	7	0.1629
	1	0.83	0.10	6	0.9305	0.84	0.13	7	0.4649
	10	0.87	0.13	6	0.9709	0.86	0.04	6	0.6256
	100	1.39	0.14	6	0.5849	1.17	0.13	7	0.8329
	1000	2.46	0.25	13	< 0.0001	1.47	0.12	8	0.0039
Smo	ctrl	1.01	0.04	17	—	1.04	0.08	14	—
	cycl	1.01	0.06	8	0.9999	0.82	0.08	8	0.2321
	0.1	1.16	0.11	4	0.5995	0.71	0.07	7	0.0306
	1	1.12	0.08	6	0.7395	0.84	0.07	7	0.3457
	10	1.04	0.06	6	0.9997	0.80	0.06	6	0.2463
	100	1.05	0.09	6	0.9976	0.83	0.06	7	0.3299
	1000	1.16	0.05	13	0.1816	0.77	0.13	8	0.0786
Cdon	ctrl	1.02	0.06	17	—	1.02	0.05	14	—
	cycl	1.48	0.10	8	0.0001	1.13	0.08	8	0.6230
	0.1	1.16	0.08	4	0.8307	0.95	0.07	7	0.9590
	1	1.08	0.07	6	0.9932	0.92	0.04	7	0.8030
	10	1.17	0.10	6	0.6535	0.88	0.05	6	0.5450
	100	1.13	0.12	6	0.8993	0.75	0.08	7	0.0189
	1000	0.94	0.06	13	0.8708	0.48	0.07	8	< 0.0001
Boc	ctrl	1.02	0.05	17	—	1.04	0.08	14	—
	cycl	1.06	0.08	8	0.9968	0.87	0.08	8	0.4507
	0.1	1.32	0.10	4	0.0815	0.97	0.06	7	0.9841
	1	1.12	0.05	6	0.8595	0.97	0.08	7	0.9779
	10	1.11	0.10	6	0.9095	0.71	0.07	6	0.0273
	100	0.91	0.14	6	0.8580	0.61	0.06	7	0.0012
	1000	1.00	0.05	13	0.9997	0.54	0.09	8	< 0.0001
Gas1	ctrl	1.08	0.11	17	—	1.07	0.11	14	—
	cycl	1.93	0.21	8	< 0.0001	1.14	0.10	8	0.9917
	0.1	1.28	0.05	4	0.9278	0.68	0.08	7	0.0143
	1	1.18	0.14	6	0.9940	0.68	0.05	7	0.0133
	10	1.09	0.24	6	> 0.9999	0.55	0.07	6	0.0012
	100	0.95	0.11	6	0.9760	0.55	0.04	7	0.0007
	1000	0.95	0.05	13	0.9405	0.24	0.02	8	< 0.0001
Gli1	ctrl	1.03	0.06	17	—	1.04	0.08	14	—
	cycl	0.21	0.03	8	< 0.0001	0.17	0.02	8	< 0.0001
	0.1	1.42	0.33	4	0.3716	0.78	0.10	7	0.0792
	1	1.33	0.13	6	0.4607	0.76	0.05	7	0.0502
	10	1.26	0.13	6	0.7449	0.89	0.05	6	0.6649
	100	1.57	0.19	6	0.0306	0.83	0.05	7	0.2399
	1000	1.84	0.16	13	< 0.0001	1.07	0.11	8	0.9995
Gli2	ctrl	1.01	0.04	17	—	1.02	0.05	14	—
	cycl	0.81	0.06	8	0.0796	0.69	0.03	8	< 0.0001
	0.1	1.24	0.06	4	0.1507	0.98	0.07	7	0.9938
	1	1.12	0.06	6	0.7471	0.90	0.05	7	0.3284
	10	1.06	0.08	6	0.9922	0.95	0.02	6	0.8536
	100	1.10	0.07	6	0.8780	0.84	0.03	7	0.0320
	1000	1.18	0.07	13	0.0999	0.70	0.04	8	< 0.0001
Gli3	ctrl	1.03	0.06	17	—	1.02	0.05	14	—
	cycl	1.27	0.08	8	0.0690	0.79	0.05	8	0.0064
	0.1	1.30	0.22	4	0.1549	0.94	0.06	7	0.7736
	1	1.08	0.07	6	0.9951	0.89	0.05	7	0.3560
	10	1.09	0.03	6	0.9893	0.81	0.04	6	0.0452
	100	0.97	0.05	6	0.9923	0.73	0.02	7	0.0009
	1000	0.89	0.05	13	0.3985	0.53	0.06	8	< 0.0001

Supplemental Table 9. Mandibular mesenchyme population size in duck and quail embryos following Gas1 over-expression

stage	duck Gas1 over-expression				quail Gas1 over-expression			
	mean	SEM	n	p-value	mean	SEM	n	p-value
HH18	62888.90	23888.90	2	0.8335	5222.20	1206.98	4	0.0614
HH21	131523.81	15732.72	21	0.0000	29722.25	833.35	2	0.0570
HH24	408268.52	30175.12	6	0.0002	106277.78	14040.04	4	0.0614

Supplemental Table 10. Differentially expressed genes in duck mandibular primordia following *Gas1* morpholino knockdown

gene name	LOC match	confidence	logFC	logCPM	p-value	FDR (0.05)
Col17A1			-1.56	6.64	3.51E-24	4.94E-20
Ap1M2			-1.68	4.69	2.14E-23	1.51E-19
Ptprf			-1.40	8.11	1.32E-21	6.22E-18
Tp63			-1.52	5.64	2.25E-16	7.94E-13
LOC101790824	*Dynll1*	*high*	1.17	5.54	9.55E-16	2.69E-12
Esrp2			-1.27	6.50	2.13E-15	5.01E-12
Gpat2			-1.65	4.65	3.14E-15	6.32E-12
LOC101804915	*no match*		-1.48	5.84	1.29E-14	2.27E-11
Cdh1			-1.18	6.42	2.16E-14	3.38E-11
Agrn			-1.26	6.51	3.45E-14	4.87E-11
Adamts17			-1.05	6.87	6.51E-14	8.33E-11
Pak1			-1.46	5.38	1.24E-13	1.46E-10
LOC101799763	*no match*		-1.77	4.23	1.55E-13	1.56E-10
Tp53I11			-1.28	6.83	4.44E-13	3.92E-10
Sulf1			-1.20	5.05	4.45E-13	3.92E-10
Vit			-1.29	5.35	7.75E-13	6.06E-10
Foxa1			-2.51	1.72	1.32E-12	9.77E-10
Grhl2			-1.42	4.92	2.16E-12	1.45E-09
Arl4C			-1.13	6.19	6.03E-12	3.54E-09
Lamb4			-1.37	4.97	6.67E-12	3.76E-09
Fat2			-1.99	3.35	8.15E-12	4.11E-09
St14			-1.21	6.00	8.17E-12	4.11E-09
LOC101791569	*no match*		2.87	1.36	9.03E-12	4.24E-09
LOC101790207	*no match*		-1.02	6.34	1.07E-11	4.80E-09
Znf385C			-1.47	4.89	1.86E-11	7.71E-09
Tp73			-1.40	4.71	2.08E-11	8.39E-09
LOC101793739	*no match*		3.09	0.46	2.88E-11	1.13E-08
Psat1			1.15	5.19	3.27E-11	1.21E-08
Dtl			1.32	6.81	4.37E-11	1.54E-08
Pkp3			-1.94	3.32	5.11E-11	1.71E-08
Ppm1H			-1.31	3.75	7.20E-11	2.36E-08
Asns			1.40	6.88	1.19E-10	3.72E-08
Shh			-1.88	3.50	1.24E-10	3.80E-08
Ripk4			-2.27	2.68	1.86E-10	5.56E-08
Igfbp2			-1.06	6.26	4.57E-10	1.24E-07
Anxa5			-1.00	6.41	4.53E-10	1.24E-07
Nptx2			-1.37	3.56	6.97E-10	1.75E-07
Pkp2			-1.29	5.81	8.96E-10	2.14E-07
Dmrt2			-2.55	1.47	9.75E-10	2.29E-07
Prom2			-1.16	3.97	1.07E-09	2.44E-07
Pkp1			-1.48	3.14	1.23E-09	2.75E-07
LOC101799848	*no match*		-1.35	6.75	1.62E-09	3.52E-07

Supplemental Table 10. Differentially expressed genes in duck mandibular primordia following *Gas1* morpholino knockdown

gene name	LOC match	confidence	logFC	logCPM	p-value	FDR (0.05)
LOC101805062	*Adap1*	*high*	-1.57	3.42	1.84931E-09	3.89877E-07
Phgdh			2.24	6.04	1.85405E-09	3.89877E-07
Id1			1.90	6.30	2.16842E-09	4.49278E-07
Hsd17B2			-1.05	4.48	2.3225E-09	4.65956E-07
Fam83F			-2.16	1.25	2.97579E-09	5.74327E-07
Ppl			-1.34	3.93	3.05265E-09	5.812E-07
Pdlim1			-1.16	4.92	3.24923E-09	6.02347E-07
LOC101797494	*no match*		-1.54	3.34	3.42727E-09	6.27101E-07
LOC119713017	*no match*		4.14	-1.27	3.91834E-09	6.90069E-07
Myo5B			-1.68	4.18	4.6714E-09	7.93399E-07
Dlx4			1.35	4.62	5.56864E-09	9.12286E-07
Eya2			-1.13	4.57	5.78186E-09	9.36329E-07
Akap6			-1.44	2.62	6.88389E-09	1.07764E-06
LOC101797091	*no match*		3.03	-0.61	7.4032E-09	1.13374E-06
Sox2			-1.75	2.64	7.81257E-09	1.18356E-06
Il8			3.87	-0.74	8.48448E-09	1.25829E-06
Xbp1			1.03	6.66	9.22208E-09	1.33948E-06
Sh3Bp4			-1.13	5.34	1.08208E-08	1.49465E-06
Pak6			-1.90	1.80	1.10065E-08	1.50553E-06
Lad1			-1.32	3.36	1.15205E-08	1.56069E-06
Plk3			1.10	4.33	1.39794E-08	1.87576E-06
Actc1			-1.81	4.30	1.5545E-08	2.06617E-06
LOC101791703	*Klf8*	*moderate*	-1.78	3.80	1.63753E-08	2.13621E-06
LOC119712989	*no match*		1.85	5.05	1.63351E-08	2.13621E-06
Sfn			-1.99	1.55	1.79429E-08	2.31924E-06
Gbx2			1.02	5.25	1.91965E-08	2.43657E-06
Plk2			-1.12	6.34	2.28202E-08	2.84525E-06
Myl10			-3.12	-0.09	2.63801E-08	3.2319E-06
Wnt10A			-1.52	2.74	2.70288E-08	3.25477E-06
Kiaa1217			-1.05	6.43	2.68696E-08	3.25477E-06
Plcl1			-1.82	1.79	2.83239E-08	3.36631E-06
Fam83H			-1.57	3.23	3.2014E-08	3.72765E-06
Acacb			-1.42	2.96	3.19483E-08	3.72765E-06
Prag1			-1.27	3.60	3.64693E-08	4.17737E-06
LOC101794808	*Anxa8*	*high*	-1.24	5.60	4.69801E-08	5.09156E-06
Tnnt2			-1.88	3.36	5.24865E-08	5.60214E-06
Nkx2-3			-1.42	2.90	5.39124E-08	5.71107E-06
Fndc1			-1.26	3.95	8.40666E-08	8.4001E-06
Rassf7			-1.24	3.87	1.07624E-07	1.01766E-05
Map7D2			-1.12	5.45	1.33863E-07	1.21677E-05
Ccdc88C			-1.04	4.70	1.43515E-07	1.28789E-05
Klf5			-1.16	4.95	1.77471E-07	1.53398E-05

Supplemental Table 10. Differentially expressed genes in duck mandibular primordia following *Gas1* morpholino knockdown

gene name	LOC match	confidence	logFC	logCPM	p-value	FDR (0.05)
Sox14			-2.63	-0.38	1.79292E-07	1.54028E-05
LOC101797666	*no match*		5.33	-1.58	1.82074E-07	1.55469E-05
LOC101794703	*no match*		-1.90	2.67	2.16921E-07	1.81917E-05
Septin4			-1.33	4.14	2.26194E-07	1.87462E-05
Foxa2			-2.21	1.26	2.73983E-07	2.21847E-05
Sowaha			-1.73	2.31	2.9747E-07	2.38128E-05
LOC119713220	*Myh1b*	*high*	-1.54	3.21	3.22644E-07	2.52662E-05
Myot			-1.85	1.49	3.3532E-07	2.61013E-05
Vill			-1.04	4.97	3.41305E-07	2.62786E-05
Foxe1			-1.47	5.47	4.12533E-07	3.05088E-05
Cobl			-1.12	3.57	4.13598E-07	3.05088E-05
Tnni2			-2.81	1.39	4.36916E-07	3.17305E-05
Slc2A3			1.06	4.28	4.48327E-07	3.22269E-05
Cavin1			-1.19	3.16	4.75709E-07	3.33446E-05
Nlrc5			-3.60	0.62	5.36613E-07	3.72431E-05
Fkbp11			1.02	4.30	5.47873E-07	3.78381E-05
Myl9			-1.16	5.09	6.21273E-07	4.22856E-05
Tmem132E			-2.24	0.38	6.41652E-07	4.34627E-05
Stk17A			-1.04	5.13	6.85848E-07	4.62341E-05
LOC101793706	*no match*		-1.91	2.22	7.34659E-07	4.85944E-05
LOC101794100	*no match*		1.72	3.90	7.4083E-07	4.87736E-05
Lix1			-1.79	1.40	1.00057E-06	6.09626E-05
Aldob			-1.88	5.09	1.05314E-06	6.36811E-05
Ahnak2			-1.72	2.69	1.23459E-06	7.15807E-05
Hspa2			-1.09	5.63	1.46143E-06	8.30246E-05
Hhla1			-4.71	-1.90	1.49027E-06	8.43232E-05
Ngef			-1.25	4.11	1.79366E-06	9.895E-05
Kcnk5			-1.05	4.45	1.80967E-06	9.895E-05
Gucy1A2			1.12	4.44	1.81199E-06	9.895E-05
Ankrd22			-1.59	1.99	1.93056E-06	0.000103815
LOC101799146	*no match*		-2.21	1.79	1.98216E-06	0.000106185
Hspa12A			-1.14	3.23	2.01339E-06	0.000107223
LOC101800358	*Exfabp*	*high*	3.09	2.88	2.02437E-06	0.000107223
Irf6			-1.00	4.80	2.08493E-06	0.000110017
LOC101799613	*Serpinb1*	*high*	-1.83	0.94	2.25724E-06	0.00011692
Grm8			-2.09	-0.02	2.26827E-06	0.000117061
Rbm47			-1.36	2.48	2.30275E-06	0.000118407
Palmd			-1.31	2.74	2.69826E-06	0.000134332
Irx1			-1.71	3.05	2.71889E-06	0.000134409
Otx1			-1.15	3.89	3.03254E-06	0.000148352
Litaf			-1.04	3.13	3.39181E-06	0.000162541
Ddx43			-2.21	-0.20	3.65608E-06	0.000171702

Supplemental Table 10. Differentially expressed genes in duck mandibular primordia following *Gas1* morpholino knockdown

gene name	LOC match	confidence	logFC	logCPM	p-value	FDR (0.05)
Slitrk6			-1.14	3.33	3.98401E-06	0.00018525
Garem1			-1.09	3.46	4.36425E-06	0.000199636
Cdkl2			-1.26	3.25	4.4793E-06	0.000204236
Nhsl2			-1.10	4.00	4.58818E-06	0.000207189
Prkch			-1.11	3.22	4.71109E-06	0.000211384
Mafb			-1.31	2.64	4.83725E-06	0.000216229
Fzd10			-1.21	4.14	5.12636E-06	0.000227124
LOC101803782	*no match*		-2.07	2.35	5.52414E-06	0.00024246
LOC113839978	*no match*		-1.44	6.17	5.59519E-06	0.000244713
LOC113841948	*no match*		6.48	-2.27	5.61022E-06	0.000244713
LOC101794001	*no match*		1.71	5.39	5.71734E-06	0.000247712
Kcnip1			-1.72	0.95	6.05175E-06	0.000258247
Rspo2			1.19	3.65	6.05754E-06	0.000258247
Elfn1			-1.67	2.11	6.25359E-06	0.000264585
Trib1			-1.32	2.45	7.18262E-06	0.000294174
LOC106020456	*no match*		-2.30	0.43	8.08142E-06	0.000324448
Ackr3			-1.20	3.82	8.39002E-06	0.000332042
LOC101804508	*Akr1b10*	*high*	-1.95	4.41	9.69125E-06	0.000365176
LOC101792808	*no match*		-1.24	3.29	9.6938E-06	0.000365176
LOC101797182	*no match*		-1.38	1.22	1.02355E-05	0.000381503
LOC113841364	*no match*		3.16	-0.60	1.06991E-05	0.000393577
Pgap4			-1.71	2.66	1.09891E-05	0.000401101
LOC101798440	*Gpd1l*	*high*	-1.12	3.10	1.11482E-05	0.000404813
Tns4			-1.03	3.76	1.16079E-05	0.000417204
LOC101790005	*no match*		-2.08	0.44	1.21245E-05	0.00043356
Rnf32			-2.19	-0.44	1.23914E-05	0.000437548
LOC101802140	*no match*		1.13	9.89	1.25156E-05	0.000439732
LOC101794275	*no match*		2.70	-1.02	1.31017E-05	0.000453537
Nkx2-5			-2.15	1.13	1.41817E-05	0.000480304
Acsl6			-1.63	2.53	1.44671E-05	0.000487623
LOC113841481	*no match*		2.35	-0.97	1.47016E-05	0.000494344
LOC101801165	*no match*		-1.81	0.34	1.62974E-05	0.000541544
Wnt3			-2.20	1.85	1.67645E-05	0.000551858
Npw			1.32	1.06	1.81354E-05	0.000580705
Unc13B			-1.06	3.63	1.82212E-05	0.000582127
LOC101799867	*no match*		-3.38	-1.88	2.13966E-05	0.000669905
LOC101790251	*no match*		-1.35	2.38	2.23985E-05	0.000694125
LOC119713030	*no match*		3.58	-0.63	2.24166E-05	0.000694125
Wnt9B			-1.33	4.59	2.28568E-05	0.000704658
LOC101804201	*no match*		-1.17	4.26	2.3813E-05	0.00072935
Ntn4			-1.21	2.15	2.66624E-05	0.000799247
Foxq1			-1.86	0.51	2.67227E-05	0.000799355

Supplemental Table 10. Differentially expressed genes in duck mandibular primordia following *Gas1* morpholino knockdown

gene name	LOC match	confidence	logFC	logCPM	p-value	FDR (0.05)
LOC119713066	*no match*		3.24	1.06	2.86553E-05	0.000848162
Saa2			2.92	-0.88	3.02132E-05	0.00088314
Malrd1			-2.48	-0.25	3.22259E-05	0.00093039
Lgr6			-1.04	3.12	3.42404E-05	0.00096676
Lypd6			-1.22	2.45	3.45421E-05	0.000973329
Fam83G			-2.01	0.14	3.47602E-05	0.000975571
Wnt7B			-1.16	2.32	3.47599E-05	0.000975571
LOC119718666	*no match*		2.94	-0.44	3.58068E-05	0.001000955
Clec19A			1.12	3.88	3.76227E-05	0.001039346
Papss2			-1.17	3.21	3.9697E-05	0.001079714
Pdzk1Ip1			-2.31	-0.13	4.09828E-05	0.001104028
Arhgef5			-1.06	3.87	4.24067E-05	0.001133715
C3H2Orf50			-2.81	-1.48	4.44998E-05	0.001180713
S100A16			-1.09	3.27	4.5668E-05	0.0012049
Dmrta2			-1.35	1.01	4.77033E-05	0.001253901
Exoc3L4			-4.21	-1.90	4.81761E-05	0.001261623
LOC119715024	*no match*		5.03	-1.67	5.05688E-05	0.001316939
Dock8			-2.50	2.54	5.28242E-05	0.001355954
Pthlh			-1.62	0.11	6.03077E-05	0.00150385
LOC101797203	*no match*		-1.13	8.79	6.22787E-05	0.001542083
Scin			-1.21	3.41	6.2922E-05	0.001545296
Lratd2			-1.01	3.23	6.73127E-05	0.001625026
Best4			1.54	0.47	6.95377E-05	0.001666185
LOC101797113	*Perp*	*moderate*	-1.17	4.40	6.9714E-05	0.001667573
Trim55			-2.28	0.92	7.00728E-05	0.001672726
Bcat1			1.09	5.28	7.27142E-05	0.00170461
LOC119715857	*no match*		-2.23	-0.89	7.30087E-05	0.001708671
LOC113842216	*no match*		-1.96	-0.44	7.4996E-05	0.001746476
LOC101792780	*no match*		2.30	0.88	7.91764E-05	0.001813847
Blvra			-1.81	3.23	8.20618E-05	0.001869439
Srrm4			-1.70	0.44	8.32221E-05	0.001884443
LOC119715040	*no match*		-3.27	-1.53	8.49348E-05	0.001917701
Prss35			-1.37	1.44	8.65957E-05	0.001948956
Col8A2			-1.18	2.56	8.96247E-05	0.002004322
Drd4			2.10	-0.15	9.34752E-05	0.002080525
LOC101802994	*Fbp1*	*high*	-1.32	3.61	9.49966E-05	0.002111052
Hoxa1			-2.08	-0.03	9.76157E-05	0.002159039
LOC119714385	*no match*		-1.14	2.26	0.000100731	0.002214028
LOC110351183	*no match*		2.20	0.89	0.00010343	0.002262783
Cish			-1.38	2.06	0.000104954	0.002289
Myl1			-2.36	1.66	0.000106481	0.002318714
Cd3E			-1.45	1.75	0.00010843	0.00235389

Supplemental Table 10. Differentially expressed genes in duck mandibular primordia following *Gas1* morpholino knockdown

gene name	LOC match	confidence	logFC	logCPM	p-value	FDR (0.05)
LOC101805317	*Ccm1*	*high*	-1.74	1.29	0.000116274	0.002491089
Ank1			-2.37	4.56	0.000117962	0.002518127
Six3			-2.62	-0.33	0.000121714	0.002574819
Nrn1			-2.33	-1.37	0.000125642	0.002632813
Obsl1			-1.80	0.50	0.000128997	0.002680595
Scara5			1.31	4.44	0.000139575	0.002845555
Gfi1B			-3.16	0.45	0.000144287	0.002920777
LOC101800522	*Zkscan7*	*low*	1.41	0.85	0.000146062	0.002952466
LOC101804267	*Cyp2w1*	*moderate*	-1.06	3.85	0.000163073	0.003226884
LOC119713219	*Myh1b*	*high*	-1.27	1.74	0.000169444	0.003324927
Ascl2			-1.11	2.50	0.000170369	0.003333795
Cdkn1A			1.13	3.44	0.000172563	0.003362719
LOC101792365	*no match*		2.05	-0.08	0.000178066	0.003446121
Bcl11A			-1.15	5.25	0.000180814	0.003484929
Foxi2			-1.05	5.08	0.000181502	0.003493423
Hivep3			-1.75	0.47	0.000182067	0.003493451
Ush2A			1.39	1.33	0.000182248	0.003493451
Wnt16			-1.76	0.53	0.000185131	0.003524753
Rest			-1.10	5.36	0.000190302	0.003613432
LOC119718673	*no match*		-2.84	1.88	0.000194533	0.003678898
Sptb			-2.66	5.64	0.00019843	0.003737535
LOC101800252	*Rab11a*	*low*	-1.45	2.98	0.000198763	0.003738821
Lrrc4C			-1.31	0.85	0.00020255	0.003794859
LOC101799683	*no match*		-1.38	2.32	0.000207951	0.003862005
LOC101791691	*no match*		-2.09	-0.03	0.000208724	0.003869362
Pjvk			1.03	1.66	0.000219188	0.004010565
Ntn1			-1.02	3.19	0.000222349	0.004043089
Grik3			-2.13	-0.34	0.00022527	0.004079461
Ada			-1.60	4.20	0.000226136	0.004084659
LOC119715258	*no match*		2.35	2.78	0.000232185	0.004167205
Rnd1			1.23	2.59	0.000237896	0.004248059
Ccnd3			-1.40	4.59	0.00025434	0.004473649
LOC119713562	*no match*		2.93	-1.30	0.000264005	0.00460342
Eps8L2			-1.50	1.13	0.00027257	0.004715855
LOC119714450	*no match*		2.89	-1.66	0.000272796	0.004715855
LOC113844783	*no match*		-3.15	5.00	0.0002739	0.00472374
LOC113839608	*no match*		-2.34	5.04	0.000273923	0.00472374
LOC113842226	*no match*		-2.03	0.04	0.000298152	0.005054955
Rgs4			-1.31	2.15	0.00030121	0.005077091
C2H7Orf57			1.57	0.24	0.000301138	0.005077091
Kcnj16			-1.55	0.70	0.000313256	0.005235433
LOC119718708	*no match*		1.44	1.84	0.000315854	0.005253917

Supplemental Table 10. Differentially expressed genes in duck mandibular primordia following *Gas1* morpholino knockdown

gene name	LOC match	confidence	logFC	logCPM	p-value	FDR (0.05)
Gja4			1.16	1.68	0.00033284	0.005465487
LOC101804044	*no match*		-1.78	-0.35	0.000334338	0.005483696
Wipf3			-1.26	1.62	0.000338425	0.005531402
Nrbp2			-1.06	5.72	0.000341754	0.0055536
Obscn			-1.42	0.81	0.00034744	0.005613622
LOC119715041	*no match*		-2.72	-1.70	0.000349866	0.005639892
Hps6			-1.04	3.06	0.000355001	0.0057096
Vwa3B			2.41	-0.39	0.000357709	0.005740042
Hs3St4			-1.47	0.54	0.000359466	0.005761673
LOC119715319	*no match*		8.07	3.41	0.000361416	0.005779783
LOC101803823	*no match*		-1.01	2.86	0.000364388	0.005814121
LOC101802274	*Myh6*	*high*	-1.51	2.54	0.000367761	0.005854673
Prdm1			-1.60	1.44	0.000369566	0.005870142
Klhdc8A			-1.52	1.66	0.000373067	0.005899154
LOC101798148	*no match*		-1.44	1.62	0.000376824	0.005951062
Mgll			-1.16	3.19	0.000400264	0.00622441
LOC101797680	*no match*		2.29	0.80	0.000423809	0.00649026
Srcin1			-1.16	2.11	0.000427026	0.006511216
Alox5			1.34	0.87	0.000444259	0.006715849
Myl2			-2.44	-0.42	0.000447118	0.006737371
Diras2			-1.48	0.92	0.000447097	0.006737371
Hnf4G			-2.46	-1.48	0.000463045	0.00691085
LOC101799764	*no match*		-1.56	0.75	0.000465098	0.006934138
Tmem182			-2.99	-0.53	0.000476218	0.007077647
Slc25A37			-1.87	5.76	0.000477805	0.007078646
LOC110352716	*no match*		-1.79	0.00	0.00048295	0.007139849
LOC119715364	*no match*		-3.67	-1.33	0.000503477	0.007365677
LOC101805050	*no match*		-2.52	-1.04	0.00051636	0.007502221
LOC101804496	*no match*		-1.09	2.59	0.000539948	0.007733766
LOC101800520	*Hbad*	*high*	-2.37	9.27	0.000610709	0.00853599
LOC101793992	*no match*		2.18	-0.20	0.000612247	0.008544775
Sox21			-1.21	1.74	0.000623602	0.008669423
Hemgn			-2.62	3.22	0.000658269	0.00910143
Epas1			-1.13	4.83	0.000667512	0.009211144
LOC101790335	*no match*		1.80	1.54	0.000679281	0.009355213
Ascl4			-2.04	-0.31	0.000686211	0.009413854
LOC101790094	*no match*		3.63	-0.64	0.0006935	0.009495358
Trim63			-2.86	-0.56	0.000706955	0.009632777
Capn6			-1.28	1.77	0.000721952	0.009780373
Pcdh10			-1.12	3.08	0.000721941	0.009780373
Daw1			-1.50	1.42	0.000727193	0.009823035
LOC119715605	*no match*		1.23	6.29	0.000769638	0.010278129

Supplemental Table 10. Differentially expressed genes in duck mandibular primordia following *Gas1* morpholino knockdown

gene name	LOC match	confidence	logFC	logCPM	p-value	FDR (0.05)
Slc7A3			1.04	5.05	0.000779259	0.010377111
LOC119718590	*no match*		1.18	0.99	0.00085301	0.011076553
LOC101798820	*no match*		-2.25	-1.38	0.00086531	0.011174471
LOC113840537	*no match*		-2.46	2.95	0.000875693	0.011277548
Plekhn1			-1.21	2.59	0.000877012	0.011284217
Myocd			-1.03	2.64	0.000879487	0.011295439
Dhrs13			1.08	2.89	0.000883034	0.01132035
Pik3C2G			-1.25	0.94	0.000889418	0.011381484
Phlda3			-1.14	1.93	0.000891852	0.011402277
LOC101793000	*Maoa*	*high*	-1.39	2.38	0.000895701	0.011430733
Meiob			-2.79	-1.83	0.000896987	0.011436789
Fam163B			-2.53	-0.73	0.000905431	0.011503957
Steap3			-2.22	3.70	0.000914678	0.011547394
LOC101802038	*no match*		-1.29	2.22	0.000935906	0.011783715
LOC119715492	*no match*		1.56	-0.60	0.000945875	0.011845712
Slc30A3			1.07	1.14	0.000967632	0.012032624
LOC101791385	*no match*		1.56	2.46	0.00101177	0.012320512
Trim29			-1.13	2.69	0.0010731	0.012955365
LOC101793418	*no match*		-1.24	1.28	0.001078331	0.012996242
LOC119718656	*no match*		-2.70	0.32	0.001086445	0.013060514
Tdo2			-1.42	0.46	0.001094798	0.013138511
Ptgr1			-1.20	3.16	0.00111825	0.01334041
Col20A1			-1.54	2.42	0.001135574	0.013508039
Sstr4			-1.91	2.34	0.001152655	0.013612543
LOC101790820	*no match*		-1.79	4.32	0.00120576	0.014093879
LOC119713856	*no match*		2.03	1.20	0.001207418	0.014093879
Endod1			-1.05	0.97	0.001211794	0.01412296
Atp6V1B1			1.89	0.67	0.001228746	0.014247947
Gap43			-1.45	1.02	0.001246203	0.014368051
Cep126			-1.77	0.51	0.001248419	0.014381832
LOC101801043	*no match*		-2.12	5.86	0.001272959	0.014604818
Brpf3			-1.02	3.77	0.001304695	0.014932446
Hoxa2			-1.21	1.32	0.001335814	0.015177652
Astn2			-1.09	3.62	0.001338255	0.015184239
Spp1			1.96	-0.57	0.001341082	0.015200731
Cracdl			-1.01	3.03	0.001381841	0.015525328
Fzd5			-1.11	0.98	0.001415321	0.015816541
Plcg2			-1.06	2.08	0.001416891	0.015816541
LOC106016928	*no match*		1.24	0.07	0.001423385	0.015840504
LOC119716851	*no match*		-1.63	2.42	0.001446364	0.016058168
Mtnr1A			1.28	0.37	0.001453727	0.016114521
Gcnt4			-1.25	0.56	0.001462412	0.016159943

Supplemental Table 10. Differentially expressed genes in duck mandibular primordia following *Gas1* morpholino knockdown

gene name	LOC match	confidence	logFC	logCPM	p-value	FDR (0.05)
Fos			1.37	0.71	0.001484876	0.016331314
Trpa1			1.22	1.57	0.001489037	0.016364306
LOC101793040	*no match*		1.40	-0.19	0.001491564	0.016366545
Gdf15			1.65	-1.24	0.001490458	0.016366545
Tal1			-2.11	4.13	0.001588815	0.017148103
Frmd7			1.53	-0.17	0.001591645	0.017148103
Smim31			-1.33	0.44	0.00161938	0.017336962
Fabp3			-1.26	2.35	0.001634212	0.01741115
LOC113841747	*no match*		-2.53	3.39	0.001645091	0.017505811
LOC101792412	*Hbad*	*high*	-2.18	10.09	0.001669903	0.017663106
Colca2			-1.25	0.63	0.001675126	0.017705062
Serpinb5			-2.59	1.35	0.001678594	0.017728421
Grip2			-1.13	2.59	0.001734373	0.018194773
Met			-1.30	2.53	0.001767869	0.018477382
LOC101796186	*no match*		3.04	-1.95	0.001812573	0.018832847
Mmd2			-2.01	-1.14	0.001823238	0.018915762
Cltrn			-1.26	-0.28	0.00186225	0.019249627
Adh1C			-2.31	0.86	0.001904647	0.019516055
Jph2			-1.63	-0.25	0.001904282	0.019516055
Tspo2			-1.93	5.62	0.001909454	0.019551092
Fam167A			-1.02	1.07	0.001939825	0.019804491
LOC113840437	*no match*		-2.47	2.65	0.001986044	0.020093899
Xk			-1.10	0.27	0.001989246	0.020093899
LOC101801682	*l-2*	*low*	-1.63	0.34	0.002004348	0.020214218
Exoc1L			1.03	1.44	0.002040135	0.020490248
LOC119715173	*no match*		-2.83	3.88	0.00207802	0.020808258
Zc2Hc1B			1.55	-0.83	0.002105071	0.020974786
Kcnh7			-1.95	-1.26	0.002110714	0.020993533
LOC119718661	*no match*		3.57	1.38	0.002111423	0.020993533
LOC113841622	*no match*		2.04	1.31	0.002132392	0.021131462
Myo18B			-1.44	1.37	0.002217659	0.021818854
Pp2D1			1.29	0.95	0.002231299	0.021891906
Myom1			-2.11	-0.02	0.002255653	0.02206937
Fech			-1.30	7.14	0.002289746	0.022274932
Stk10			-1.63	2.75	0.00234567	0.022651235
Alx1			-1.01	2.92	0.002359754	0.02272717
Slc39A8			-1.99	3.81	0.00237691	0.022843302
Grid1			-1.58	-0.71	0.002414821	0.02311305
LOC101803845	*no match*		-1.61	-0.60	0.002430004	0.023211069
Cabcoco1			-1.50	0.04	0.002446038	0.02333259
Lpar5			-1.31	-0.38	0.002493856	0.023692474
LOC119713878	*no match*		-1.53	-0.31	0.00252277	0.023934882

Supplemental Table 10. Differentially expressed genes in duck mandibular primordia following *Gas1* morpholino knockdown

gene name	LOC match	confidence	logFC	logCPM	p-value	FDR (0.05)
Cntnap2			-1.12	1.61	0.002547926	0.024124823
Tnni1			-1.28	3.32	0.002565731	0.024228276
Tmem268			-1.34	1.29	0.002621739	0.024641551
LOC106016000	*Sbspon*	*moderate*	1.09	2.15	0.002633165	0.02473244
Rsph1			-1.15	0.12	0.002646822	0.024833
Lamp3			-1.59	-0.46	0.002706086	0.025249037
Igfbp1			-1.07	0.58	0.002771162	0.025710288
LOC101798290	*Hbe*	*high*	-2.00	11.06	0.002774831	0.025720128
Ppdpfl			-3.31	-1.84	0.002819526	0.025980581
LOC119718657	*no match*		-1.43	0.88	0.002876203	0.026319999
Tm4Sf1			1.31	0.80	0.002881116	0.026324283
LOC119714959	*no match*		-1.21	0.62	0.002896504	0.026430602
Smyd1			-1.26	1.06	0.002916393	0.026509068
LOC110354175	*no match*		-1.88	-0.38	0.002923799	0.026542142
Ghrh			2.84	0.12	0.002945947	0.026708786
LOC119715269	*no match*		1.41	-0.88	0.002951053	0.02673787
Ppef1			-1.05	0.86	0.002980189	0.026898066
Nmnat3			-1.78	-0.89	0.003047165	0.02734491
Entpd8			-1.28	-0.29	0.003045497	0.02734491
Edn1			-1.23	1.57	0.003093088	0.027692405
Capsl			-1.51	-0.05	0.003152617	0.028076624
Casq2			-1.21	0.07	0.003196721	0.028376642
LOC101797540	*no match*		-1.69	0.32	0.003207997	0.028420655
Cebpa			-1.01	1.48	0.003234528	0.028517691
Tfrc			-1.22	7.45	0.003296161	0.028911978
Hnf4A			-2.20	-1.58	0.00335532	0.029198948
Minar1			-1.07	1.05	0.003384378	0.02937924
Baalc			-1.41	-0.68	0.003391026	0.029407137
LOC113842171	*no match*		-1.76	1.27	0.003444121	0.029688477
LOC119718691	*no match*		-3.12	-0.29	0.003507216	0.030111614
LOC106020099	*no match*		1.12	0.10	0.003579026	0.030654278
LOC113843545	*no match*		-1.47	2.49	0.003600202	0.030797354
C1Qb			1.09	0.36	0.003626012	0.030942992
Adra1B			-1.70	-1.24	0.003759929	0.031777825
LOC119714958	*no match*		-1.94	0.34	0.003876242	0.032434935
Wdr31			-1.03	0.20	0.003894092	0.032540845
Tent5A			-1.13	2.28	0.003963438	0.033002883
Penk			-1.77	-0.04	0.00402012	0.033414133
Cdkn2C			-2.71	-0.87	0.004054674	0.033603708
Dmtn			-1.46	5.12	0.004070572	0.033676035
Slc30A10			-1.62	3.91	0.004088655	0.033746372
Cacna1I			-1.79	-1.47	0.004123348	0.03397301

Supplemental Table 10. Differentially expressed genes in duck mandibular primordia following *Gas1* morpholino knockdown

gene name	LOC match	confidence	logFC	logCPM	p-value	FDR (0.05)
Fxyd2			-1.30	0.44	0.004268675	0.034804027
Abcb11			1.03	1.60	0.004370969	0.035453419
Cfap52			-1.31	-0.23	0.004397281	0.035623315
LOC101795354	*no match*		-2.70	-0.83	0.00443653	0.035840751
Psph			1.30	3.31	0.00448613	0.03618689
LOC119716581	*no match*		1.61	3.38	0.004491184	0.03618689
Rusc2			-1.17	0.00	0.004653594	0.036979402
Mybph			-2.03	-0.40	0.004683497	0.037154161
Stat4			1.04	3.10	0.00468338	0.037154161
Aqp9			-1.10	0.87	0.004689811	0.037183312
LOC119715374	*no match*		-1.08	2.52	0.00476618	0.03768278
Susd1			-1.32	3.41	0.004777858	0.037753919
Hspb1			-1.55	-0.25	0.004868152	0.03824872
LOC101798111	*Hbe*	*high*	-1.93	11.49	0.004907738	0.038499511
Alpk3			-1.08	1.99	0.004946967	0.038742536
Nkain2			-1.02	1.43	0.00506414	0.039265106
LOC113844492	*no match*		-2.19	0.51	0.005115282	0.039429041
Jakmip1			-2.07	-1.40	0.005179105	0.039764799
Fshb			1.10	0.32	0.005204055	0.039912861
Drp2			1.55	0.04	0.005209298	0.039924724
LOC101803770	*no match*		1.61	-0.63	0.005229827	0.040023377
LOC113841284	*no match*		-1.97	0.24	0.005275209	0.040325118
Prr15			-1.34	0.65	0.005426812	0.041187858
Lrrc31			-1.12	2.11	0.005459715	0.041378766
LOC101800713	*no match*		-1.90	11.61	0.005516253	0.041689814
Otx2			-1.48	1.24	0.005520344	0.041689814
Igsf11			-1.57	-0.87	0.005579502	0.041947493
Klf17			-2.04	2.78	0.00561443	0.04212018
LOC101794820	*no match*		-1.91	2.09	0.005703353	0.042696356
LOC113840276	*no match*		-1.50	0.30	0.005923902	0.043973579
Bcl2L15			1.39	-0.75	0.005923885	0.043973579
Grem2			-1.20	0.08	0.005941644	0.044058852
Gjd2			-2.06	-0.94	0.005966332	0.04414898
LOC119715271	*no match*		1.65	-1.46	0.005982207	0.044219995
Kctd16			1.86	1.68	0.006065332	0.044717146
Cntn1			-1.21	1.61	0.006130119	0.04502031
LOC101802909	*no match*		3.05	-1.80	0.006239573	0.045548884
Jakmip3			-1.62	0.16	0.006265804	0.045645768
Sytl5			-2.28	-0.31	0.006270731	0.045658053
LOC106015023	*no match*		2.29	-1.10	0.006326615	0.045937902
LOC101791362	*no match*		-2.34	-1.28	0.006386219	0.04623276
Agbl1			-1.40	-0.33	0.006392321	0.04623276

Supplemental Table 10. Differentially expressed genes in duck mandibular primordia following *Gas1* morpholino knockdown

gene name	LOC match	confidence	logFC	logCPM	p-value	FDR (0.05)
LOC101798361	*H2b-V*	*high*	1.54	-0.54	0.006617162	0.047469043
Srgn			1.89	-0.26	0.006658498	0.047694584
LOC113845712	*no match*		1.02	0.99	0.006713389	0.048012658
LOC113843308	*no match*		1.67	1.06	0.00675295	0.048236358
LOC119717547	*no match*		-1.52	0.33	0.006766889	0.048275757
LOC101795263	*no match*		-2.15	-1.45	0.006849601	0.04873941
Ecel1			1.27	0.33	0.006883266	0.048904856
Fstl5			-1.27	3.16	0.006916037	0.049088186
Mfsd2B			-1.95	1.58	0.00693207	0.049127735
LOC101802378	*no match*		-1.59	-0.07	0.006937901	0.049144334
LOC119713450	*no match*		-1.32	-0.81	0.00697087	0.049254057
Cdh26			2.29	-1.56	0.006999361	0.049356352

Supplemental Table 11. Differentially expressed genes in duck mandibular primordia following *Gas1* over-expression

gene name	LOC match	confidence	logFC	logCPM	p-value	FDR (0.05)
Serpinh1			-1.44	6.50	4.22E-26	5.98E-22
Col17A1			1.59	5.11	1.19E-23	8.42E-20
Cdh1			-1.73	5.77	9.58E-22	3.91E-18
Gpat2			-1.51	6.64	1.10E-21	3.91E-18
Jarid2			-1.88	4.73	1.02E-20	2.87E-17
Adamts17			-1.49	7.19	1.33E-20	2.87E-17
Vit			-1.41	7.10	1.42E-20	2.87E-17
Ptprf			-1.67	5.77	2.88E-20	5.10E-17
Nptx2			-1.29	7.48	6.41E-19	1.01E-15
Ccn2			-1.41	6.41	1.34E-18	1.90E-15
Bhlhe41			-1.71	8.99	3.70E-18	4.77E-15
LOC101805185	*no match*		-1.31	5.35	2.88E-17	3.40E-14
Gbx2			-1.68	6.56	6.08E-17	6.63E-14
Kdm7A			-1.49	7.49	8.40E-17	8.47E-14
LOC101805317	*Ccm1*	*high*	-1.44	5.38	9.57E-17	8.47E-14
Epha1			-1.32	6.32	9.29E-17	8.47E-14
Cdh3			-1.18	6.69	1.83E-16	1.52E-13
Chdh			-1.30	5.44	2.53E-16	1.99E-13
LOC101804508	*Akr1b10*	*high*	-1.20	8.64	2.79E-16	2.03E-13
Fat2			-1.12	8.39	2.87E-16	2.03E-13
Lamb4			-1.21	6.38	4.23E-16	2.85E-13
Antkmt			-1.43	8.53	6.30E-16	4.05E-13
Slitrk6			-2.82	2.56	2.12E-15	1.31E-12
St14			-1.52	6.78	2.83E-15	1.65E-12
Card9			-1.27	6.35	2.92E-15	1.65E-12
LOC119713220	*Myh1b*	*high*	-1.08	7.47	3.79E-15	2.07E-12
Dtl			-1.85	3.75	4.38E-15	2.30E-12
Lgr6			-1.27	5.90	5.31E-15	2.69E-12
Shh			-1.18	5.55	8.11E-15	3.96E-12
Tnnt2			-1.24	8.76	1.37E-14	6.49E-12
LOC101805264	*no match*		-1.37	6.94	1.54E-14	7.04E-12
LOC101797182	*no match*		-1.47	5.12	2.60E-14	1.15E-11
LOC101795354	*no match*		-1.04	7.52	3.79E-14	1.63E-11
Myl10			-1.95	3.18	3.96E-14	1.65E-11
Alx1			-1.38	5.44	5.47E-14	2.21E-11
Lmx1A			-1.33	6.04	7.81E-14	3.07E-11
Dpp7			-1.25	5.73	8.95E-14	3.43E-11
LOC119713600	*no match*		-1.06	8.78	1.93E-13	7.21E-11
Mettl24			-1.15	8.15	2.02E-13	7.32E-11
LOC101803228	*no match*		-1.19	8.24	2.18E-13	7.55E-11
Fgf7			-1.05	7.70	2.15E-13	7.55E-11
Actc1			-1.26	7.16	2.88E-13	9.71E-11

Supplemental Table 11. Differentially expressed genes in duck mandibular primordia following *Gas1* over-expression

gene name	LOC match	confidence	logFC	logCPM	p-value	FDR (0.05)
Purg			-1.63	3.49	3.61297E-13	1.1807E-10
LOC110354662	*no match*		-1.19	6.24	3.66755E-13	1.1807E-10
Mapt			-1.07	7.21	4.04403E-13	1.27297E-10
Gucy1A2			-1.60	6.91	5.24638E-13	1.61554E-10
Dlx4			1.07	8.66	5.87712E-13	1.77126E-10
Prps2			-1.30	9.96	7.23663E-13	2.13556E-10
Abca5			-1.07	5.95	9.47206E-13	2.7382E-10
P4Ha2			-1.13	6.38	1.00404E-12	2.84446E-10
Kit			-1.00	8.79	1.04253E-12	2.89558E-10
Tmem196			-1.11	7.28	1.287E-12	3.50583E-10
LOC101794490	*no match*		-1.56	5.24	1.46233E-12	3.8359E-10
Ccnt1			-1.71	4.22	1.55729E-12	4.01074E-10
Aldob			1.06	5.57	2.0194E-12	4.93187E-10
Pthlh			-1.74	5.10	2.2228E-12	5.24767E-10
Cbx7			-1.06	5.63	2.1884E-12	5.24767E-10
Pla2G4F			-1.40	4.71	3.39689E-12	7.86369E-10
LOC101791691	*no match*		-1.07	7.23	3.44193E-12	7.86369E-10
Pdzrn4			1.04	6.59	3.69477E-12	8.30736E-10
Vsig8			-1.12	6.74	3.91395E-12	8.66266E-10
Tmem179B			-1.42	4.37	4.12625E-12	8.99206E-10
Kiaa1755			-1.35	6.64	4.20296E-12	9.02044E-10
Foxa1			-1.05	9.28	4.45895E-12	9.42703E-10
Dcn			-1.30	10.14	6.57477E-12	1.31171E-09
Atp6V1B1			-1.19	8.33	8.17624E-12	1.58653E-09
Klhdc8B			-1.37	5.47	1.09383E-11	1.98987E-09
Sgsm1			-1.18	9.10	1.10978E-11	1.98987E-09
Blvrb			-1.10	7.50	1.09547E-11	1.98987E-09
LOC106020320	*no match*		-1.03	7.14	1.12742E-11	1.99625E-09
Epcam			-1.21	5.91	1.17738E-11	2.05897E-09
Jun			-1.20	7.37	1.35111E-11	2.33395E-09
LOC106019797	*no match*		-1.15	6.83	1.43025E-11	2.4409E-09
Gal3St1			-1.12	7.39	1.54242E-11	2.601E-09
LOC101803782	*no match*		-1.06	6.29	1.6357E-11	2.72584E-09
Grm8			1.23	6.02	1.76795E-11	2.91198E-09
Steap3			-1.19	6.66	1.95479E-11	3.1827E-09
LOC101795757	*no match*		-1.04	8.41	2.03468E-11	3.27513E-09
Sox6			-1.18	6.82	2.25145E-11	3.58335E-09
Dnali1			-1.10	6.78	2.8228E-11	4.39396E-09
Hspa2			-1.05	6.72	3.18479E-11	4.80281E-09
Ypel2			-1.02	7.55	3.18718E-11	4.80281E-09
LOC101794001	*no match*		1.06	5.83	3.3016E-11	4.92285E-09
Rasd1			-1.13	6.04	3.36455E-11	4.96447E-09

Supplemental Table 11. Differentially expressed genes in duck mandibular primordia following *Gas1* over-expression

gene name	LOC match	confidence	logFC	logCPM	p-value	FDR (0.05)
Ackr1			-1.00	7.31	3.58975E-11	5.24214E-09
Meox1			-1.16	5.95	3.9094E-11	5.65068E-09
Slc35G1			-1.21	4.78	4.18191E-11	5.98351E-09
LOC101804267	*Cyp2w1*	*moderate*	-1.66	5.24	4.44137E-11	6.2912E-09
Lama3			-1.07	5.79	4.80559E-11	6.67364E-09
Tspo2			-1.25	4.85	5.16173E-11	7.03038E-09
LOC119718660	*no match*		-1.46	5.37	5.82308E-11	7.81233E-09
Ntn4			-1.22	7.21	5.84615E-11	7.81233E-09
Ank1			-1.07	5.59	6.08665E-11	8.0577E-09
LOC101797113	*Perp*	*moderate*	-1.25	8.05	6.55841E-11	8.60184E-09
Trpa1			-1.35	5.63	8.75248E-11	1.12708E-08
LOC113841596	*no match*		-1.06	8.94	9.4761E-11	1.19847E-08
LOC101792412	*Hbad*	*high*	-1.03	6.04	1.00672E-10	1.26196E-08
Il8			-1.29	6.16	1.07169E-10	1.30867E-08
LOC101803633	*no match*		-1.09	7.24	1.32598E-10	1.59174E-08
Ripk4			-1.03	5.38	1.38469E-10	1.64825E-08
LOC101797666	*no match*		-1.08	5.63	1.57074E-10	1.85413E-08
Fbxl22			1.07	5.72	1.6382E-10	1.90206E-08
LOC101802933	*Ca3*	*high*	-1.54	4.07	1.72471E-10	1.98622E-08
Kctd21			-1.07	8.53	1.88039E-10	2.13086E-08
LOC101804634	*no match*		-1.05	7.41	2.00229E-10	2.25099E-08
Nmur1			1.14	7.27	2.13017E-10	2.37589E-08
Pax7			-1.09	4.41	2.16644E-10	2.39747E-08
LOC101795437	*no match*		-1.12	6.06	2.53482E-10	2.76198E-08
LOC101793029	*no match*		-1.08	6.24	3.27949E-10	3.51924E-08
LOC113842243	*no match*		-1.30	4.35	3.48851E-10	3.7154E-08
LOC101800520	*Hbad*	*high*	-1.15	7.03	3.61259E-10	3.81883E-08
Rasgrp1			-1.07	7.83	4.53836E-10	4.6584E-08
Tubb1			-1.26	8.14	4.7802E-10	4.83654E-08
Ackr3			-1.20	4.34	5.31254E-10	5.29944E-08
LOC101796643	*no match*		-1.07	6.27	5.91314E-10	5.85732E-08
LOC119712989	*no match*		1.02	5.23	6.93636E-10	6.77611E-08
Efcab5			-1.14	5.04	8.03103E-10	7.73875E-08
Dop1A			1.07	4.84	8.14182E-10	7.74019E-08
Itgb8			-1.04	7.37	9.09869E-10	8.42372E-08
Mgat4D			1.19	7.23	9.07021E-10	8.42372E-08
LOC101798111	*Hbe*	*high*	-1.04	6.46	9.71028E-10	8.87394E-08
Wnt10A			-1.22	4.37	1.04798E-09	9.3953E-08
LOC101798290	*Hbe*	*high*	-1.15	4.97	1.22274E-09	1.08251E-07
LOC119713756	*no match*		-1.11	5.44	1.24388E-09	1.09439E-07
Aldh1A2			-1.07	7.42	1.5453E-09	1.33471E-07
Ntn1			-1.24	8.76	1.56533E-09	1.34381E-07

Supplemental Table 11. Differentially expressed genes in duck mandibular primordia following *Gas1* over-expression

gene name	LOC match	confidence	logFC	logCPM	p-value	FDR (0.05)
LOC101792780	*no match*		-1.50	3.70	1.62935E-09	1.3738E-07
LOC101802015	*Lgalsl-A*	*moderate*	-1.09	7.38	1.62616E-09	1.3738E-07
Tnnc1			-1.13	7.89	1.88736E-09	1.57261E-07
B3Gnt9			-1.06	7.04	1.98242E-09	1.64217E-07
LOC101800713	*no match*		-1.04	5.64	2.05384E-09	1.69143E-07
Znf131			-1.10	5.76	2.42474E-09	1.98535E-07
Pcdh10			-1.17	4.37	2.59876E-09	2.10351E-07
Kcng4			-1.15	4.81	2.92952E-09	2.33127E-07
Ptges			-1.24	4.28	3.01935E-09	2.38934E-07
Wnt9B			-1.16	5.16	3.71481E-09	2.82905E-07
Sesn2			-1.64	3.31	4.49153E-09	3.34856E-07
Dmrt2			-1.07	6.83	4.51848E-09	3.35101E-07
Gdpd2			-1.89	2.54	4.7442E-09	3.464E-07
Trim55			-1.28	5.76	5.05083E-09	3.61339E-07
LOC106015023	*no match*		-2.51	1.49	5.3197E-09	3.78661E-07
Gja3			1.08	5.63	6.06928E-09	4.21428E-07
Pde9A			-1.03	6.32	6.25412E-09	4.30774E-07
Gatm			-1.29	4.56	6.47383E-09	4.40874E-07
LOC101791534	*no match*		-1.10	5.91	6.6229E-09	4.4673E-07
Sele			1.06	5.14	8.08794E-09	5.30396E-07
LOC101794275	*no match*		-1.23	5.68	9.67192E-09	6.1713E-07
LOC119713219	*Myh1b*	*high*	-1.12	5.03	9.81263E-09	6.20517E-07
Rdh5			-1.19	4.47	1.40329E-08	8.53118E-07
LOC113841786	*no match*		-1.07	5.25	1.42847E-08	8.61036E-07
Flvcr2			-1.18	5.98	1.56415E-08	9.3093E-07
LOC101801043	*no match*		-1.14	5.36	1.80526E-08	1.05353E-06
Dok2			-1.04	7.02	1.85325E-08	1.07148E-06
LOC101790005	*no match*		-2.27	1.16	1.88494E-08	1.08538E-06
Slc39A14			1.17	4.36	1.92453E-08	1.09923E-06
LOC119713491	*no match*		-1.24	3.51	1.98372E-08	1.1195E-06
Gper1			-1.03	7.23	2.09421E-08	1.16789E-06
Tal1			-1.12	4.32	2.10439E-08	1.16897E-06
S100A16			-1.09	5.97	2.296E-08	1.26548E-06
Gabrb1			-1.05	4.66	2.3194E-08	1.26949E-06
Clgn			-1.04	5.23	2.52394E-08	1.36456E-06
Sptb			-1.24	3.70	2.67025E-08	1.42733E-06
Actn2			1.01	4.64	3.40756E-08	1.7552E-06
Wnt2B			-1.19	4.31	3.66536E-08	1.83772E-06
Ripor2			-1.37	7.07	3.76186E-08	1.85668E-06
LOC101797389	*no match*		-1.01	8.51	3.99171E-08	1.95649E-06
Emp1			8.55	2.12	4.23303E-08	2.06762E-06
Znf367			-1.31	4.88	4.94296E-08	2.35748E-06

Supplemental Table 11. Differentially expressed genes in duck mandibular primordia following *Gas1* over-expression

gene name	LOC match	confidence	logFC	logCPM	p-value	FDR (0.05)
Mfsd2B			1.28	4.39	5.40193E-08	2.53372E-06
Oprd1			-1.14	5.12	5.458E-08	2.54318E-06
LOC101789401	*no match*		-1.14	5.32	5.94718E-08	2.72742E-06
Wnt7A			-1.22	5.15	7.56226E-08	3.34748E-06
Wnt3			-1.20	4.58	7.73367E-08	3.41269E-06
Tmem216			-1.12	5.82	8.89922E-08	3.80838E-06
Aqp3			1.09	4.38	9.83863E-08	4.10717E-06
Slc26A9			1.30	6.46	9.85837E-08	4.10717E-06
Rictor			6.06	-1.23	1.07073E-07	4.38349E-06
Smc1B			-1.22	3.60	1.08286E-07	4.40768E-06
Ada			-1.29	3.11	1.15085E-07	4.63938E-06
Bdh2			-1.02	7.89	1.17902E-07	4.73111E-06
Pak6			1.36	5.06	1.19209E-07	4.77006E-06
Gfi1B			-1.25	3.67	1.31876E-07	5.18895E-06
Asb2			-1.01	4.82	1.38745E-07	5.42908E-06
LOC119717397	*no match*		-2.01	2.81	1.44823E-07	5.65129E-06
Hps6			-1.01	4.74	1.64171E-07	6.35379E-06
LOC101792365	*no match*		-1.01	6.14	1.67542E-07	6.449E-06
Trim63			-1.61	2.77	1.75525E-07	6.71977E-06
LOC101797528	*no match*		-1.37	3.17	1.76582E-07	6.74201E-06
Tmem141			-1.19	3.75	1.77827E-07	6.77127E-06
Hemgn			-1.41	3.66	2.13501E-07	7.93764E-06
LOC119713489	*no match*		-1.52	4.15	2.56877E-07	9.2823E-06
Vwc2			-1.04	4.49	2.61666E-07	9.43128E-06
LOC119713583	*no match*		1.07	5.06	2.82669E-07	1.00603E-05
Enc1			1.22	5.23	2.89894E-07	1.02916E-05
Txndc16			-1.15	4.89	2.91615E-07	1.03268E-05
Lsmem2			1.05	5.32	3.26743E-07	1.13998E-05
Dock8			-1.55	5.19	3.30144E-07	1.1434E-05
LOC119714248	*no match*		-1.46	3.90	3.99197E-07	1.3305E-05
Tbc1D8B			-1.06	4.36	4.63167E-07	1.50476E-05
Rab26			-1.00	7.11	4.76749E-07	1.54534E-05
LOC101791126	*no match*		-1.02	9.05	5.35931E-07	1.71752E-05
Slc30A10			-1.35	2.94	5.45945E-07	1.73393E-05
Mxra8			3.37	3.17	5.87526E-07	1.82908E-05
LOC101795816	*no match*		-1.06	5.59	6.33707E-07	1.94717E-05
LOC101790820	*no match*		-1.13	4.62	6.45049E-07	1.97773E-05
Klf17			1.85	1.15	7.2175E-07	2.16144E-05
Tnnt3			-2.97	1.83	7.729E-07	2.30927E-05
Hjv			-1.07	6.27	8.41718E-07	2.47364E-05
Sstr4			-1.47	3.43	8.5197E-07	2.48316E-05
Anhx			-1.13	4.50	8.57982E-07	2.49555E-05

Supplemental Table 11. Differentially expressed genes in duck mandibular primordia following *Gas1* over-expression

gene name	LOC match	confidence	logFC	logCPM	p-value	FDR (0.05)
LOC101790278	*no match*		-1.13	4.18	1.05969E-06	2.97827E-05
Fam167A			-1.12	4.29	1.07803E-06	3.02383E-05
Caps2			-1.02	5.79	1.16977E-06	3.22999E-05
LOC101797859	*no match*		2.06	1.32	1.17831E-06	3.24722E-05
LOC113844783	*no match*		1.69	1.76	1.21531E-06	3.33172E-05
Slc25A37			-1.78	2.40	1.22954E-06	3.35576E-05
LOC101803823	*no match*		-2.22	0.84	1.2678E-06	3.4469E-05
Tmprss15			-1.02	4.51	1.30829E-06	3.5434E-05
LOC101798499	*no match*		-1.13	5.28	1.31332E-06	3.54549E-05
LOC119714132	*no match*		-1.32	4.99	1.32871E-06	3.57816E-05
C28H17Orf113			-1.56	2.91	1.49862E-06	3.94572E-05
LOC101803187	*no match*		-1.21	3.37	1.5485E-06	4.06195E-05
C6H10Orf90			1.43	3.85	1.55832E-06	4.08014E-05
LOC113841948	*no match*		-1.04	4.35	1.58947E-06	4.14827E-05
Agpat2			-1.03	5.05	1.60126E-06	4.16947E-05
LOC119713001	*no match*		-1.55	2.91	1.61302E-06	4.19238E-05
Fate1			-1.21	4.96	1.66854E-06	4.30507E-05
LOC119713006	*no match*		-1.44	2.79	1.71176E-06	4.40055E-05
LOC119717910	*no match*		-1.53	2.58	1.80183E-06	4.59044E-05
Fam83F			-1.44	2.66	1.81578E-06	4.6177E-05
Gpr3			-1.87	1.68	1.8476E-06	4.67345E-05
Stard4			1.07	5.62	1.98213E-06	4.92577E-05
LOC101792171	*no match*		-1.05	3.67	2.02276E-06	4.99156E-05
Myl1			-1.04	4.44	2.24316E-06	5.45016E-05
Lhx9			2.24	-0.21	2.27911E-06	5.52802E-05
LOC119716104	*no match*		-1.09	3.42	2.39572E-06	5.76152E-05
Kcne4			-1.56	3.50	2.40137E-06	5.76532E-05
Tmod4			-1.01	4.05	2.55648E-06	6.02537E-05
LOC101803098	*no match*		2.14	1.42	2.71184E-06	6.34928E-05
Brpf3			-1.46	2.24	2.7889E-06	6.4975E-05
LOC101796186	*no match*		-1.47	3.96	2.84669E-06	6.5997E-05
Slc46A3			-1.09	4.63	3.27513E-06	7.48261E-05
LOC119714694	*no match*		-1.52	2.49	3.36889E-06	7.63526E-05
Aqp9			-1.17	4.75	3.4894E-06	7.80843E-05
Hcn2			1.13	5.89	3.66977E-06	8.13494E-05
Kcnip1			1.23	4.22	3.95043E-06	8.64881E-05
Urod			-1.21	3.00	4.06322E-06	8.85469E-05
Ascl4			1.34	3.10	4.78904E-06	0.000101704
Slc39A8			1.11	3.41	5.30585E-06	0.000109773
Mgat4A			2.39	0.52	5.30898E-06	0.000109773
Slc43A3			-1.86	3.52	5.59658E-06	0.00011423
Casq2			1.34	2.84	5.59531E-06	0.00011423

Supplemental Table 11. Differentially expressed genes in duck mandibular primordia following *Gas1* over-expression

gene name	LOC match	confidence	logFC	logCPM	p-value	FDR (0.05)
LOC113839608	*no match*		-1.01	3.37	5.82195E-06	0.000117811
Gh1			-1.08	4.53	6.15846E-06	0.000123352
Fzd5			-1.05	4.00	6.16543E-06	0.000123352
Pi15			-2.60	-0.34	6.43336E-06	0.00012817
Nell1			-1.26	3.49	7.4328E-06	0.000145021
Penk			-1.27	5.61	7.99085E-06	0.00015296
Slc22A18			-1.37	3.74	8.29641E-06	0.000157111
Adamtsl2			1.44	2.05	8.4695E-06	0.000158901
LOC101803845	*no match*		-1.27	6.22	8.50748E-06	0.00015916
Sox14			-1.09	3.68	9.09185E-06	0.000167909
Dkk2			-1.02	4.34	9.10554E-06	0.000167943
LOC101801622	*Il20*	*moderate*	-1.10	3.65	9.12765E-06	0.000168131
Irx1			-2.51	-0.59	1.32104E-05	0.00023045
Smpdl3B			-1.08	3.19	1.478E-05	0.000252375
LOC113840468	*no match*		-2.43	2.37	1.55967E-05	0.000263322
Col6A1			-1.54	2.22	1.66554E-05	0.00027887
LOC106016000	*Sbspon*	*moderate*	-1.04	3.67	1.78608E-05	0.000296945
Adap2			1.89	2.62	2.04163E-05	0.00033235
Sfn			-1.39	2.18	2.11994E-05	0.00034358
Sptlc3			1.68	2.27	2.12806E-05	0.000344502
Srrm4			1.34	2.53	2.18525E-05	0.000352892
Dhrs9			1.45	2.40	2.25296E-05	0.000361008
Foxq1			2.22	-0.21	2.4913E-05	0.000389924
Klhl31			3.13	-1.10	2.62444E-05	0.000406286
Cbln4			-1.07	6.24	2.67922E-05	0.000411617
Acsl6			-1.10	3.78	2.69856E-05	0.000414139
LOC113841521	*no match*		1.06	2.81	2.78369E-05	0.000424445
Prss35			1.07	4.72	2.82635E-05	0.000429563
Hapln4			1.15	4.13	2.90736E-05	0.000437694
LOC113840231	*no match*		-1.07	4.87	3.0008E-05	0.000447907
Vstm4			1.30	3.09	3.053E-05	0.00045474
Mkx			-1.07	3.45	3.09973E-05	0.000460731
Hdc			-1.25	2.40	3.24923E-05	0.000477937
LOC113842171	*no match*		-1.08	3.37	3.32656E-05	0.000485781
Ccnd3			3.24	-1.76	3.41845E-05	0.000497149
Rfesd			1.02	3.90	3.44853E-05	0.000500495
Myl2			1.04	4.20	3.62017E-05	0.000520343
LOC119713409	*no match*		1.12	3.19	3.69711E-05	0.00052952
Adprh			2.18	0.29	3.75221E-05	0.000536327
Adra1B			1.04	3.22	3.84563E-05	0.000546952
LOC119713165	*no match*		-1.99	2.27	3.94022E-05	0.000557574
LOC119713066	*no match*		-1.65	3.57	3.98245E-05	0.000561867

Supplemental Table 11. Differentially expressed genes in duck mandibular primordia following *Gas1* over-expression

gene name	LOC match	confidence	logFC	logCPM	p-value	FDR (0.05)
LOC113840511	*no match*		-1.22	3.76	4.00966E-05	0.000564581
Spns3			-1.04	4.10	4.15516E-05	0.000581599
Ercc8			-1.07	7.02	4.29822E-05	0.000599255
LOC101796284	*no match*		-2.45	1.79	4.47339E-05	0.000617581
LOC101795218	*no match*		-1.02	7.55	4.47763E-05	0.000617581
Cavin4			1.12	3.10	4.74371E-05	0.000649224
LOC101791103	*no match*		-1.03	4.57	4.80646E-05	0.000657176
LOC101791461	*no match*		1.05	3.31	5.00135E-05	0.000680539
LOC101801789	*no match*		1.13	3.96	5.48969E-05	0.000735681
Rasd2			1.13	5.42	5.53224E-05	0.000739048
Enpp7			-1.11	3.77	5.54815E-05	0.000740014
Cidec			-1.30	1.62	5.65552E-05	0.000751505
Smim5			1.48	2.98	5.73876E-05	0.000761138
LOC113840537	*no match*		1.10	2.56	5.98284E-05	0.000790549
Siglec1			2.48	-0.09	6.22497E-05	0.000817345
Metap1D			1.03	3.53	6.24397E-05	0.00081743
Cish			-1.43	2.36	6.31304E-05	0.000823428
LOC110352387	*no match*		-1.01	3.48	6.3745E-05	0.000830679
LOC101803439	*no match*		1.29	3.29	6.97012E-05	0.000893499
Fech			3.54	-2.07	7.76638E-05	0.000975741
Mlycd			1.81	3.77	8.18007E-05	0.001011971
Kel			1.07	5.04	8.28619E-05	0.001020643
Helb			-1.40	2.53	8.76064E-05	0.001075342
LOC106016036	*no match*		-1.03	3.45	9.81866E-05	0.001180656
Pdzk1Ip1			1.32	5.21	0.000100586	0.00120542
Fstl5			-1.46	2.06	0.000102815	0.001230045
Muc13			-1.37	1.60	0.000105629	0.001254177
LOC101804496	*no match*		1.36	3.54	0.00010759	0.001272127
LOC113841033	*no match*		-1.12	3.28	0.000107744	0.001272892
Crygs			-1.30	2.18	0.000110759	0.001299834
Tcim			1.09	4.55	0.000114395	0.001336968
Pde11A			2.72	-1.46	0.000115865	0.001349696
Drd4			-1.29	2.58	0.000116687	0.001358155
Blvra			1.37	1.76	0.000120153	0.001382587
Wnt2			-2.02	-0.39	0.000120594	0.001386536
LOC101794408	*no match*		-1.03	3.75	0.000126141	0.001437484
LOC119716995	*no match*		1.03	3.69	0.000132538	0.001492009
LOC119716010	*no match*		1.30	1.99	0.00014112	0.00156413
Pkd1L2			2.27	-1.12	0.000145328	0.001598274
Ssc4D			1.09	3.74	0.000146206	0.001604193
LOC101803713	*no match*		1.00	3.81	0.000154382	0.001679581
Edar			-1.86	0.68	0.000156661	0.00170177

Supplemental Table 11. Differentially expressed genes in duck mandibular primordia following *Gas1* over-expression

gene name	LOC match	confidence	logFC	logCPM	p-value	FDR (0.05)
Col21A1			1.66	1.23	0.000169196	0.001815654
LOC101794820	*no match*		1.02	2.66	0.000175586	0.001875698
LOC113840437	*no match*		1.84	0.57	0.000179245	0.001900456
LOC101798680	*no match*		1.16	2.32	0.000188665	0.001978122
Myot			-1.07	6.77	0.000190896	0.001994135
LOC101804927	*no match*		-1.18	2.09	0.000197658	0.002052661
Wdr93			-1.53	3.06	0.000201299	0.002082836
Apela			-1.35	3.09	0.000208081	0.002142051
Ppp1R42			1.17	2.01	0.000209791	0.002150127
Fam210B			1.03	2.86	0.000212075	0.002167416
Npy			2.19	-0.71	0.000217642	0.002211665
Csmd3			-1.18	2.60	0.000237752	0.002378355
LOC119713975	*Kcna2*	*high*	1.14	2.26	0.000251576	0.002502509
LOC119715450	*no match*		2.27	6.15	0.00025224	0.002506596
Rgcc			-1.37	2.43	0.000257167	0.002549172
LOC101800414	*no match*		-1.10	2.08	0.000276015	0.002707589
C2H7Orf57			-1.17	2.25	0.000279653	0.002735698
Ankrd2			1.17	1.70	0.000287572	0.002798961
Bmx			1.21	3.72	0.000288774	0.002807468
Slc38A3			1.56	1.83	0.000297801	0.002875493
LOC119718271	*no match*		2.61	-1.13	0.000309309	0.002954392
Myod1			1.27	3.81	0.000309763	0.002956731
LOC101794806	*Tppp2*	*high*	2.52	-1.43	0.000327661	0.003077744
Gpr50			1.68	1.69	0.000329313	0.003085129
LOC101802499	*no match*		-1.39	2.81	0.000331392	0.003100503
Kctd16			-1.44	2.60	0.000371534	0.003390966
LOC119714133	*no match*		2.71	-1.59	0.000373331	0.003405171
LOC101793739	*no match*		-1.16	3.71	0.00037632	0.003425818
LOC106017909	*no match*		-1.76	1.01	0.000379409	0.003449509
LOC119713016	*no match*		-1.04	2.70	0.000383	0.003475463
Slc9A3			1.31	3.18	0.00038533	0.003494368
Abcb11			2.58	-0.64	0.000387397	0.003506376
Vwa3B			-2.39	-1.14	0.000400766	0.003602157
Myo18B			1.04	2.77	0.0004039	0.003625628
LOC101799683	*no match*		1.34	1.10	0.000410368	0.003669736
Adamtsl5			1.38	1.44	0.000429335	0.003799523
Arhgef38			2.10	0.79	0.000440176	0.003878827
Ddx43			2.73	1.17	0.000440321	0.003878827
LOC113841747	*no match*		-3.84	-2.00	0.00046516	0.004057259
C7H2Orf66			1.77	0.31	0.000466754	0.004068658
LOC101801727	*Selenbp1*	*high*	1.26	1.96	0.000468788	0.004076357
Rd3			1.60	0.34	0.000470586	0.004089152

Supplemental Table 11. Differentially expressed genes in duck mandibular primordia following *Gas1* over-expression

gene name	LOC match	confidence	logFC	logCPM	p-value	FDR (0.05)
LOC119714638	*no match*		-1.10	7.06	0.000472017	0.004091873
Cdh26			2.27	3.84	0.000492774	0.004243246
Ghrh			3.31	-1.54	0.000514827	0.004402192
Cacnb4			2.39	-1.59	0.000526316	0.004483025
Ush2A			-1.21	2.34	0.000530211	0.004508064
Meiob			1.98	1.33	0.000532381	0.004521006
Kcnj16			-1.07	5.12	0.00053773	0.004558312
Smyd1			-1.61	0.37	0.000586327	0.004935962
Mtnr1A			-1.11	2.04	0.000590572	0.004964664
Gcnt4			1.16	1.90	0.000597031	0.004998194
Tnni1			-1.09	2.80	0.000645931	0.005310284
Mstn			-2.75	-1.85	0.000649951	0.005327871
Dpp6			3.20	-1.37	0.000673663	0.005487309
LOC101804150	*no match*		1.90	-0.36	0.000679433	0.005527952
Xk			1.17	2.40	0.000697269	0.005643896
LOC113843747	*no match*		-1.30	1.71	0.000710098	0.005724834
Taf8			-1.14	2.23	0.000726832	0.005826587
LOC110352235	*no match*		1.79	6.13	0.000726488	0.005826587
Lrriq1			2.14	-1.26	0.000727534	0.00582891
Pi16			1.23	1.51	0.000749227	0.005989163
Srd5A2			2.41	-1.41	0.00075798	0.006041966
LOC119716331	*no match*		-1.41	2.02	0.000793992	0.006250783
LOC101804257	*no match*		1.40	1.02	0.000795369	0.006252162
Plcxd1			1.10	2.91	0.000800734	0.006283874
LOC119713857	*no match*		1.07	3.90	0.000809677	0.006326024
Tnni2			1.22	2.16	0.000814577	0.006350293
Pdlim3			-1.26	2.35	0.000836612	0.006482829
Foxi1			1.66	-0.59	0.000858884	0.006630021
Asip			1.67	1.84	0.000910838	0.006974067
LOC101803972	*no match*		1.17	2.63	0.000919861	0.007031749
LOC119718661	*no match*		1.95	-0.50	0.000940674	0.007148968
Tnfrsf25			1.16	2.79	0.000964015	0.007298383
C2H9Orf152			-1.23	2.82	0.000984893	0.007416804
Smpx			1.05	3.26	0.001005584	0.00755655
LOC101798148	*no match*		1.77	-0.89	0.001041356	0.007775857
Tdo2			1.08	2.29	0.001055573	0.00784892
Pp2D1			1.33	1.43	0.001091404	0.008064544
Drd1			1.14	1.56	0.001105192	0.008134335
LOC113844492	*no match*		1.20	2.43	0.001105443	0.008134335
Nrg2			1.62	1.44	0.001108057	0.008145113
Cfap44			1.90	-0.89	0.001117272	0.008200079
Cabcoco1			-1.28	1.47	0.001148767	0.008379137

Supplemental Table 11. Differentially expressed genes in duck mandibular primordia following *Gas1* over-expression

gene name	LOC match	confidence	logFC	logCPM	p-value	FDR (0.05)
LOC106015775	*no match*		-2.21	-1.27	0.001161989	0.008440808
LOC119716581	*no match*		-1.07	2.72	0.001184922	0.008580994
Obsl1			2.61	-1.30	0.001189576	0.008605897
Htr2A			1.31	1.09	0.001209698	0.008715858
Slitrk3			-1.08	2.63	0.001284423	0.009147238
LOC119713562	*no match*		1.99	-0.23	0.00129161	0.009193795
Tmc5			-1.12	1.47	0.001316647	0.009301897
LOC119714503	*no match*		-1.05	1.43	0.001323644	0.009342008

Supplemental Table 12. Differentially expressed genes in quail mandibular primordia following *Gas1* morpholino knockdown

gene name	LOC match	confidence	logFC	logCPM	p-value	FDR (0.05)
Tjp2			-1.44	6.50	4.22E-26	5.98E-22
Gpx3			1.59	5.11	1.19E-23	8.42E-20
Grhl2			-1.73	5.77	9.58E-22	3.91E-18
Pawr			-1.51	6.64	1.10E-21	3.91E-18
LOC107312805	*Klf5*	*moderate*	-1.88	4.73	1.02E-20	2.87E-17
Krt8			-1.49	7.19	1.33E-20	2.87E-17
LOC107315782	*no match*		-1.41	7.10	1.42E-20	2.87E-17
Slc9A3R1			-1.67	5.77	2.88E-20	5.10E-17
Hk1			-1.29	7.48	6.41E-19	1.01E-15
Sp1			-1.41	6.41	1.34E-18	1.90E-15
Myh9			-1.71	8.99	3.70E-18	4.77E-15
Kiaa1522			-1.31	5.35	2.88E-17	3.40E-14
Tp63			-1.68	6.56	6.08E-17	6.63E-14
Supt16H			-1.49	7.49	8.40E-17	8.47E-14
Arid3C			-1.44	5.38	9.57E-17	8.47E-14
LOC107315820	*no match*		-1.32	6.32	9.29E-17	8.47E-14
Esrp2			-1.18	6.69	1.83E-16	1.52E-13
Klf5			-1.30	5.44	2.53E-16	1.99E-13
Acly			-1.20	8.64	2.79E-16	2.03E-13
Anxa2			-1.12	8.39	2.87E-16	2.03E-13
Dtx4			-1.21	6.38	4.23E-16	2.85E-13
Snrnp200			-1.43	8.53	6.30E-16	4.05E-13
Gap43			-2.82	2.56	2.12E-15	1.31E-12
Pola1			-1.52	6.78	2.83E-15	1.65E-12
Oxct1			-1.27	6.35	2.92E-15	1.65E-12
Tln1			-1.08	7.47	3.79E-15	2.07E-12
Fam83H			-1.85	3.75	4.38E-15	2.30E-12
LOC107307449	*no match*		-1.27	5.90	5.31E-15	2.69E-12
LOC107307669	*no match*		-1.18	5.55	8.11E-15	3.96E-12
Lmnb2			-1.24	8.76	1.37E-14	6.49E-12
LOC107307607	*no match*		-1.37	6.94	1.54E-14	7.04E-12
Foxe1			-1.47	5.12	2.60E-14	1.15E-11
Mib1			-1.04	7.52	3.79E-14	1.63E-11
Sox21			-1.95	3.18	3.96E-14	1.65E-11
Znf503			-1.38	5.44	5.47E-14	2.21E-11
Frmd1			-1.33	6.04	7.81E-14	3.07E-11
Stk17A			-1.25	5.73	8.95E-14	3.43E-11
Psmd2			-1.06	8.78	1.93E-13	7.21E-11
Cltc			-1.15	8.15	2.02E-13	7.32E-11
Cs			-1.19	8.24	2.18E-13	7.55E-11
Pfkl			-1.05	7.70	2.15E-13	7.55E-11
Mcm7			-1.26	7.16	2.88E-13	9.71E-11

Supplemental Table 12. Differentially expressed genes in quail mandibular primordia following *Gas1* morpholino knockdown

gene name	LOC match	confidence	logFC	logCPM	p-value	FDR (0.05)
Nkx2-3			-1.63	3.49	3.61297E-13	1.1807E-10
Ncoa1			-1.19	6.24	3.66755E-13	1.1807E-10
Tjp1			-1.07	7.21	4.04403E-13	1.27297E-10
Dsp			-1.60	6.91	5.24638E-13	1.61554E-10
LOC107312032	*Cox7a2*	*high*	1.07	8.66	5.87712E-13	1.77126E-10
Tubb			-1.30	9.96	7.23663E-13	2.13556E-10
Cbx6			-1.07	5.95	9.47206E-13	2.7382E-10
Pitx2			-1.13	6.38	1.00404E-12	2.84446E-10
LOC107307277	*no match*		-1.00	8.79	1.04253E-12	2.89558E-10
Ubash3B			-1.11	7.28	1.287E-12	3.50583E-10
Zfhx3			-1.56	5.24	1.46233E-12	3.8359E-10
Ngef			-1.71	4.22	1.55729E-12	4.01074E-10
Timm10			1.06	5.57	2.0194E-12	4.93187E-10
Znf385C			-1.74	5.10	2.2228E-12	5.24767E-10
Pak1			-1.06	5.63	2.1884E-12	5.24767E-10
LOC107307816	*no match*		-1.40	4.71	3.39689E-12	7.86369E-10
LOC107307631	*no match*		-1.07	7.23	3.44193E-12	7.86369E-10
Clmp			1.04	6.59	3.69477E-12	8.30736E-10
Kiaa1217			-1.12	6.74	3.91395E-12	8.66266E-10
Ar			-1.42	4.37	4.12625E-12	8.99206E-10
Arhgap35			-1.35	6.64	4.20296E-12	9.02044E-10
Caprin1			-1.05	9.28	4.45895E-12	9.42703E-10
Ncl			-1.30	10.14	6.57477E-12	1.31171E-09
Prrc2C			-1.19	8.33	8.17624E-12	1.58653E-09
Med11			-1.37	5.47	1.09383E-11	1.98987E-09
Kpnb1			-1.18	9.10	1.10978E-11	1.98987E-09
Nxn			-1.10	7.50	1.09547E-11	1.98987E-09
Mybbp1A			-1.03	7.14	1.12742E-11	1.99625E-09
LOC107307756	*no match*		-1.21	5.91	1.17738E-11	2.05897E-09
Arid3B			-1.20	7.37	1.35111E-11	2.33395E-09
LOC107307490	*no match*		-1.15	6.83	1.43025E-11	2.4409E-09
Ap2B1			-1.12	7.39	1.54242E-11	2.601E-09
Lrba			-1.06	6.29	1.6357E-11	2.72584E-09
Ednra			1.23	6.02	1.76795E-11	2.91198E-09
LOC107307629	*no match*		-1.19	6.66	1.95479E-11	3.1827E-09
LOC107307221	*Ilf3*	*moderate*	-1.04	8.41	2.03468E-11	3.27513E-09
Kmt2D			-1.18	6.82	2.25145E-11	3.58335E-09
Bcar1			-1.10	6.78	2.8228E-11	4.39396E-09
Acaca			-1.05	6.72	3.18479E-11	4.80281E-09
Mroh1			-1.02	7.55	3.18718E-11	4.80281E-09
Fkbp7			1.06	5.83	3.3016E-11	4.92285E-09
Arl4C			-1.13	6.04	3.36455E-11	4.96447E-09

Supplemental Table 12. Differentially expressed genes in quail mandibular primordia following *Gas1* morpholino knockdown

gene name	LOC match	confidence	logFC	logCPM	p-value	FDR (0.05)
Sf3B4			-1.00	7.31	3.58975E-11	5.24214E-09
Exoc4			-1.16	5.95	3.9094E-11	5.65068E-09
Trim29			-1.21	4.78	4.18191E-11	5.98351E-09
Clic6			-1.66	5.24	4.44137E-11	6.2912E-09
Pdlim1			-1.07	5.79	4.80559E-11	6.67364E-09
Ctnnd2			-1.25	4.85	5.16173E-11	7.03038E-09
Evpl			-1.46	5.37	5.82308E-11	7.81233E-09
LOC107307294	*Psmd8*	*high*	-1.22	7.21	5.84615E-11	7.81233E-09
Rbbp8			-1.07	5.59	6.08665E-11	8.0577E-09
Fasn			-1.25	8.05	6.55841E-11	8.60184E-09
Map7D2			-1.35	5.63	8.75248E-11	1.12708E-08
Myh10			-1.06	8.94	9.4761E-11	1.19847E-08
Pard3			-1.03	6.04	1.00672E-10	1.26196E-08
Capn2			-1.29	6.16	1.07169E-10	1.30867E-08
Hnrnpa0			-1.09	7.24	1.32598E-10	1.59174E-08
Otud7B			-1.03	5.38	1.38469E-10	1.64825E-08
Elp3			-1.08	5.63	1.57074E-10	1.85413E-08
Cnih4			1.07	5.72	1.6382E-10	1.90206E-08
Ints5			-1.54	4.07	1.72471E-10	1.98622E-08
Prpf8			-1.07	8.53	1.88039E-10	2.13086E-08
LOC107307550	*no match*		-1.05	7.41	2.00229E-10	2.25099E-08
Magt1			1.14	7.27	2.13017E-10	2.37589E-08
Ston2			-1.09	4.41	2.16644E-10	2.39747E-08
Dmd			-1.12	6.06	2.53482E-10	2.76198E-08
Cdc37			-1.08	6.24	3.27949E-10	3.51924E-08
LOC107307604	*no match*		-1.30	4.35	3.48851E-10	3.7154E-08
Creb3L2			-1.15	7.03	3.61259E-10	3.81883E-08
LOC107325235	*Krt19*	*high*	-1.07	7.83	4.53836E-10	4.6584E-08
Tubb3			-1.26	8.14	4.7802E-10	4.83654E-08
LOC107318208	*no match*		-1.20	4.34	5.31254E-10	5.29944E-08
Elob			-1.07	6.27	5.91314E-10	5.85732E-08
Nme3			1.02	5.23	6.93636E-10	6.77611E-08
Kif3B			-1.14	5.04	8.03103E-10	7.73875E-08
LOC107312420	*Gulo*	*high*	1.07	4.84	8.14182E-10	7.74019E-08
Pbx1			-1.04	7.37	9.09869E-10	8.42372E-08
Mmp2			1.19	7.23	9.07021E-10	8.42372E-08
Ppp3Ca			-1.04	6.46	9.71028E-10	8.87394E-08
Cap2			-1.22	4.37	1.04798E-09	9.3953E-08
Rhou			-1.15	4.97	1.22274E-09	1.08251E-07
Palm2Akap2			-1.11	5.44	1.24388E-09	1.09439E-07
Add1			-1.07	7.42	1.5453E-09	1.33471E-07
LOC107307149	*no match*		-1.24	8.76	1.56533E-09	1.34381E-07

Supplemental Table 12. Differentially expressed genes in quail mandibular primordia following *Gas1* morpholino knockdown

gene name	LOC match	confidence	logFC	logCPM	p-value	FDR (0.05)
Esrp1			-1.50	3.70	1.62935E-09	1.3738E-07
Larp1			-1.09	7.38	1.62616E-09	1.3738E-07
Vcl			-1.13	7.89	1.88736E-09	1.57261E-07
Gbf1			-1.06	7.04	1.98242E-09	1.64217E-07
Mad1L1			-1.04	5.64	2.05384E-09	1.69143E-07
Tet3			-1.10	5.76	2.42474E-09	1.98535E-07
Irs1			-1.17	4.37	2.59876E-09	2.10351E-07
LOC107307343	*no match*		-1.15	4.81	2.92952E-09	2.33127E-07
LOC107307861	*no match*		-1.24	4.28	3.01935E-09	2.38934E-07
Pkp2			-1.16	5.16	3.71481E-09	2.82905E-07
Sox2			-1.64	3.31	4.49153E-09	3.34856E-07
Ccdc50			-1.07	6.83	4.51848E-09	3.35101E-07
LOC107307683	*no match*		-1.89	2.54	4.7442E-09	3.464E-07
LOC107314966	*Meis2*	*high*	-1.28	5.76	5.05083E-09	3.61339E-07
C4H4Orf19			-2.51	1.49	5.3197E-09	3.78661E-07
Serpine2			1.08	5.63	6.06928E-09	4.21428E-07
LOC107307401	*no match*		-1.03	6.32	6.25412E-09	4.30774E-07
Ccdc85C			-1.29	4.56	6.47383E-09	4.40874E-07
Dab2			-1.10	5.91	6.6229E-09	4.4673E-07
Kera			1.06	5.14	8.08794E-09	5.30396E-07
LOC107318444	*Psmd8*	*low*	-1.23	5.68	9.67192E-09	6.1713E-07
Pard3B			-1.12	5.03	9.81263E-09	6.20517E-07
LOC107325740	*no match*		-1.19	4.47	1.40329E-08	8.53118E-07
Pygl			-1.07	5.25	1.42847E-08	8.61036E-07
Col17A1			-1.18	5.98	1.56415E-08	9.3093E-07
Patj			-1.14	5.36	1.80526E-08	1.05353E-06
Dock1			-1.04	7.02	1.85325E-08	1.07148E-06
Fam83G			-2.27	1.16	1.88494E-08	1.08538E-06
Plvap			1.17	4.36	1.92453E-08	1.09923E-06
Samd12			-1.24	3.51	1.98372E-08	1.1195E-06
Gsk3B			-1.03	7.23	2.09421E-08	1.16789E-06
Tlx1			-1.12	4.32	2.10439E-08	1.16897E-06
Mrtfa			-1.09	5.97	2.296E-08	1.26548E-06
Alpk3			-1.05	4.66	2.3194E-08	1.26949E-06
Ascc3			-1.04	5.23	2.52394E-08	1.36456E-06
Baiap2L1			-1.24	3.70	2.67025E-08	1.42733E-06
Kcne2			1.01	4.64	3.40756E-08	1.7552E-06
Tll2			-1.19	4.31	3.66536E-08	1.83772E-06
Scml2			-1.37	7.07	3.76186E-08	1.85668E-06
Eif3A			-1.01	8.51	3.99171E-08	1.95649E-06
Tmprss15			8.55	2.12	4.23303E-08	2.06762E-06
Ddah1			-1.31	4.88	4.94296E-08	2.35748E-06

Supplemental Table 12. Differentially expressed genes in quail mandibular primordia following *Gas1* morpholino knockdown

gene name	LOC match	confidence	logFC	logCPM	p-value	FDR (0.05)
Emcn			1.28	4.39	5.40193E-08	2.53372E-06
Phka2			-1.14	5.12	5.458E-08	2.54318E-06
LOC107315884	*Anxa8*	*high*	-1.14	5.32	5.94718E-08	2.72742E-06
Ndrg1			-1.22	5.15	7.56226E-08	3.34748E-06
LOC107306278	*Fbp1*	*high*	-1.20	4.58	7.73367E-08	3.41269E-06
Ddx10			-1.12	5.82	8.89922E-08	3.80838E-06
Anapc13			1.09	4.38	9.83863E-08	4.10717E-06
Dpcd			1.30	6.46	9.85837E-08	4.10717E-06
Marco			6.06	-1.23	1.07073E-07	4.38349E-06
LOC107325872	*Znf628*	*moderate*	-1.22	3.60	1.08286E-07	4.40768E-06
Arhgap8			-1.29	3.11	1.15085E-07	4.63938E-06
Ubr4			-1.02	7.89	1.17902E-07	4.73111E-06
LOC107310334	*no match*		1.36	5.06	1.19209E-07	4.77006E-06
Ripk4			-1.25	3.67	1.31876E-07	5.18895E-06
Txnip			-1.01	4.82	1.38745E-07	5.42908E-06
LOC107325817	*Krt75*	*high*	-2.01	2.81	1.44823E-07	5.65129E-06
LOC107307508	*no match*		-1.01	4.74	1.64171E-07	6.35379E-06
Arvcf			-1.01	6.14	1.67542E-07	6.449E-06
Lmx1B			-1.61	2.77	1.75525E-07	6.71977E-06
Irx1			-1.37	3.17	1.76582E-07	6.74201E-06
LOC107307882	*no match*		-1.19	3.75	1.77827E-07	6.77127E-06
Cavin1			-1.41	3.66	2.13501E-07	7.93764E-06
Ppl			-1.52	4.15	2.56877E-07	9.2823E-06
Crybg1			-1.04	4.49	2.61666E-07	9.43128E-06
Tmem26			1.07	5.06	2.82669E-07	1.00603E-05
Serpinf1			1.22	5.23	2.89894E-07	1.02916E-05
Wdr81			-1.15	4.89	2.91615E-07	1.03268E-05
Pi15			1.05	5.32	3.26743E-07	1.13998E-05
Mov10			-1.55	5.19	3.30144E-07	1.1434E-05
Plek2			-1.46	3.90	3.99197E-07	1.3305E-05
Cnksr1			-1.06	4.36	4.63167E-07	1.50476E-05
Tfap2B			-1.00	7.11	4.76749E-07	1.54534E-05
LOC107307645	*no match*		-1.02	9.05	5.35931E-07	1.71752E-05
Znf750			-1.35	2.94	5.45945E-07	1.73393E-05
LOC107321681	*no match*		3.37	3.17	5.87526E-07	1.82908E-05
Hspa2			-1.06	5.59	6.33707E-07	1.94717E-05
Gmip			-1.13	4.62	6.45049E-07	1.97773E-05
LOC107320215	*Havcr2*	*low*	1.85	1.15	7.2175E-07	2.16144E-05
Rab3B			-2.97	1.83	7.729E-07	2.30927E-05
Usp39			-1.07	6.27	8.41718E-07	2.47364E-05
Foxl2			-1.47	3.43	8.5197E-07	2.48316E-05
Fis1			-1.13	4.50	8.57982E-07	2.49555E-05

Supplemental Table 12. Differentially expressed genes in quail mandibular primordia following *Gas1* morpholino knockdown

gene name	LOC match	confidence	logFC	logCPM	p-value	FDR (0.05)
Trerf1			-1.13	4.18	1.05969E-06	2.97827E-05
Otx1			-1.12	4.29	1.07803E-06	3.02383E-05
Gtf2F1			-1.02	5.79	1.16977E-06	3.22999E-05
Ace			2.06	1.32	1.17831E-06	3.24722E-05
Slc9A9			1.69	1.76	1.21531E-06	3.33172E-05
Lingo1			-1.78	2.40	1.22954E-06	3.35576E-05
Foxi3			-2.22	0.84	1.2678E-06	3.4469E-05
Pla2G7			-1.02	4.51	1.30829E-06	3.5434E-05
Rhob			-1.13	5.28	1.31332E-06	3.54549E-05
Irx4			-1.32	4.99	1.32871E-06	3.57816E-05
LOC107306862	*Nalf2*	*moderate*	-1.56	2.91	1.49862E-06	3.94572E-05
Nacc1			-1.21	3.37	1.5485E-06	4.06195E-05
Lrrc17			1.43	3.85	1.55832E-06	4.08014E-05
LOC107307344	*no match*		-1.04	4.35	1.58947E-06	4.14827E-05
Tns4			-1.03	5.05	1.60126E-06	4.16947E-05
Fat2			-1.55	2.91	1.61302E-06	4.19238E-05
Krt18			-1.21	4.96	1.66854E-06	4.30507E-05
C26H6Orf132			-1.44	2.79	1.71176E-06	4.40055E-05
Wnt10A			-1.53	2.58	1.80183E-06	4.59044E-05
Oplah			-1.44	2.66	1.81578E-06	4.6177E-05
Shisa6			-1.87	1.68	1.8476E-06	4.67345E-05
Dnajc19			1.07	5.62	1.98213E-06	4.92577E-05
Lzts1			-1.05	3.67	2.02276E-06	4.99156E-05
Grhl1			-1.04	4.44	2.24316E-06	5.45016E-05
C1Qa			2.24	-0.21	2.27911E-06	5.52802E-05
LOC107308206	*H2b-v*	*high*	-1.09	3.42	2.39572E-06	5.76152E-05
Nwd2			-1.56	3.50	2.40137E-06	5.76532E-05
Lrrn4			-1.01	4.05	2.55648E-06	6.02537E-05
Aqp1			2.14	1.42	2.71184E-06	6.34928E-05
Eppk1			-1.46	2.24	2.7889E-06	6.4975E-05
LOC107314117	*Emx1*	*high*	-1.47	3.96	2.84669E-06	6.5997E-05
Cadps2			-1.09	4.63	3.27513E-06	7.48261E-05
Pkp1			-1.52	2.49	3.36889E-06	7.63526E-05
Map7			-1.17	4.75	3.4894E-06	7.80843E-05
Tf			1.13	5.89	3.66977E-06	8.13494E-05
Chodl			1.23	4.22	3.95043E-06	8.64881E-05
Ovol2			-1.21	3.00	4.06322E-06	8.85469E-05
Adgrg6			1.34	3.10	4.78904E-06	0.000101704
Adgrl4			1.11	3.41	5.30585E-06	0.000109773
Ly96			2.39	0.52	5.30898E-06	0.000109773
Capn6			-1.86	3.52	5.59658E-06	0.00011423
LOC107321660	*no match*		1.34	2.84	5.59531E-06	0.00011423

Supplemental Table 12. Differentially expressed genes in quail mandibular primordia following *Gas1* morpholino knockdown

gene name	LOC match	confidence	logFC	logCPM	p-value	FDR (0.05)
Wnt2B			-1.01	3.37	5.82195E-06	0.000117811
Rnf43			-1.08	4.53	6.15846E-06	0.000123352
LOC107307371	*no match*		-1.05	4.00	6.16543E-06	0.000123352
Wnt2			-2.60	-0.34	6.43336E-06	0.00012817
LOC107325286	*Krt15*	*high*	-1.26	3.49	7.4328E-06	0.000145021
Astn2			-1.27	5.61	7.99085E-06	0.00015296
Sh3Bgrl2			-1.37	3.74	8.29641E-06	0.000157111
Bpi			1.44	2.05	8.4695E-06	0.000158901
Vit			-1.27	6.22	8.50748E-06	0.00015916
LOC107307590	*no match*		-1.09	3.68	9.09185E-06	0.000167909
Maml3			-1.02	4.34	9.10554E-06	0.000167943
Acsbg2			-1.10	3.65	9.12765E-06	0.000168131
Hoxd1			-2.51	-0.59	1.32104E-05	0.00023045
Fbxl17			-1.08	3.19	1.478E-05	0.000252375
Apod			-2.43	2.37	1.55967E-05	0.000263322
LOC107307792	*no match*		-1.54	2.22	1.66554E-05	0.00027887
Kcnab1			-1.04	3.67	1.78608E-05	0.000296945
Sctr			1.89	2.62	2.04163E-05	0.00033235
LOC116652679	*no match*		-1.39	2.18	2.11994E-05	0.00034358
LOC107322042	*no match*		1.68	2.27	2.12806E-05	0.000344502
Scarf1			1.34	2.53	2.18525E-05	0.000352892
Flt1			1.45	2.40	2.25296E-05	0.000361008
LOC107309356	*Ccr2*	*moderate*	2.22	-0.21	2.4913E-05	0.000389924
Acsl5			3.13	-1.10	2.62444E-05	0.000406286
Ap3B1			-1.07	6.24	2.67922E-05	0.000411617
Hspb8			-1.10	3.78	2.69856E-05	0.000414139
Cd93			1.06	2.81	2.78369E-05	0.000424445
Itgb3			1.07	4.72	2.82635E-05	0.000429563
LOC107311894	*no match*		1.15	4.13	2.90736E-05	0.000437694
Eps8L2			-1.07	4.87	3.0008E-05	0.000447907
Tfpi			1.30	3.09	3.053E-05	0.00045474
Smyd1			-1.07	3.45	3.09973E-05	0.000460731
Mbp			-1.25	2.40	3.24923E-05	0.000477937
LOC107313674	*no match*		-1.08	3.37	3.32656E-05	0.000485781
LOC107308607	*no match*		3.24	-1.76	3.41845E-05	0.000497149
Cmc1			1.02	3.90	3.44853E-05	0.000500495
Tpst2			1.04	4.20	3.62017E-05	0.000520343
S1Pr1			1.12	3.19	3.69711E-05	0.00052952
LOC107324922	*no match*		2.18	0.29	3.75221E-05	0.000536327
Emid1			1.04	3.22	3.84563E-05	0.000546952
Pax2			-1.99	2.27	3.94022E-05	0.000557574
LOC107306830	*Dock2*	*moderate*	-1.65	3.57	3.98245E-05	0.000561867

Supplemental Table 12. Differentially expressed genes in quail mandibular primordia following *Gas1* morpholino knockdown

gene name	LOC match	confidence	logFC	logCPM	p-value	FDR (0.05)
LOC107307682	*no match*		-1.22	3.76	4.00966E-05	0.000564581
Usp2			-1.04	4.10	4.15516E-05	0.000581599
Nol6			-1.07	7.02	4.29822E-05	0.000599255
LOC107324007	*no match*		-2.45	1.79	4.47339E-05	0.000617581
Ptprf			-1.02	7.55	4.47763E-05	0.000617581
Hand1			1.12	3.10	4.74371E-05	0.000649224
Elmo3			-1.03	4.57	4.80646E-05	0.000657176
Rnf24			1.05	3.31	5.00135E-05	0.000680539
Vstm4			1.13	3.96	5.48969E-05	0.000735681
Nenf			1.13	5.42	5.53224E-05	0.000739048
Prkch			-1.11	3.77	5.54815E-05	0.000740014
Sowaha			-1.30	1.62	5.65552E-05	0.000751505
Gabrd			1.48	2.98	5.73876E-05	0.000761138
LOC107312463	*Enpp4*	*high*	1.10	2.56	5.98284E-05	0.000790549
C1Qb			2.48	-0.09	6.22497E-05	0.000817345
Emilin3			1.03	3.53	6.24397E-05	0.00081743
Hoxd3			-1.43	2.36	6.31304E-05	0.000823428
Ak4			-1.01	3.48	6.3745E-05	0.000830679
Slc31A2			1.29	3.29	6.97012E-05	0.000893499
LOC107309033	*Mrc1*	*moderate*	3.54	-2.07	7.76638E-05	0.000975741
Chid1			1.81	3.77	8.18007E-05	0.001011971
Col6A1			1.07	5.04	8.28619E-05	0.001020643
Sstr2			-1.40	2.53	8.76064E-05	0.001075342
Sytl3			-1.03	3.45	9.81866E-05	0.001180656
BLOC1S3			1.32	5.21	0.000100586	0.00120542
Foxq1			-1.46	2.06	0.000102815	0.001230045
Drc7			-1.37	1.60	0.000105629	0.001254177
Asip			1.36	3.54	0.00010759	0.001272127
Hic2			-1.12	3.28	0.000107744	0.001272892
Dnah9			-1.30	2.18	0.000110759	0.001299834
LOC107309559	*no match*		1.09	4.55	0.000114395	0.001336968
LOC107321618	*Entpd2*	*low*	2.72	-1.46	0.000115865	0.001349696
Rims2			-1.29	2.58	0.000116687	0.001358155
Gja5			1.37	1.76	0.000120153	0.001382587
Gata4			-2.02	-0.39	0.000120594	0.001386536
Tfap2E			-1.03	3.75	0.000126141	0.001437484
Dkk3			1.03	3.69	0.000132538	0.001492009
Tcim			1.30	1.99	0.00014112	0.00156413
LOC107309034	*Mrc1*	*moderate*	2.27	-1.12	0.000145328	0.001598274
Ephx1			1.09	3.74	0.000146206	0.001604193
Spag1			1.00	3.81	0.000154382	0.001679581
Tgm4			-1.86	0.68	0.000156661	0.00170177

Supplemental Table 12. Differentially expressed genes in quail mandibular primordia following *Gas1* morpholino knockdown

gene name	LOC match	confidence	logFC	logCPM	p-value	FDR (0.05)
LOC107320762	*Cyp3a40*	*moderate*	1.66	1.23	0.000169196	0.001815654
Scx			1.02	2.66	0.000175586	0.001875698
LOC107320213	*Havcr1*	*low*	1.84	0.57	0.000179245	0.001900456
Cfh			1.16	2.32	0.000188665	0.001978122
Focad			-1.07	6.77	0.000190896	0.001994135
Cracdl			-1.18	2.09	0.000197658	0.002052661
Tagln			-1.53	3.06	0.000201299	0.002082836
Ahnak2			-1.35	3.09	0.000208081	0.002142051
LOC107312057	*no match*		1.17	2.01	0.000209791	0.002150127
Kcnip4			1.03	2.86	0.000212075	0.002167416
Rasal3			2.19	-0.71	0.000217642	0.002211665
Macc1			-1.18	2.60	0.000237752	0.002378355
Gria4			1.14	2.26	0.000251576	0.002502509
Rsrp1			2.27	6.15	0.00025224	0.002506596
Dock8			-1.37	2.43	0.000257167	0.002549172
Otx2			-1.10	2.08	0.000276015	0.002707589
Usp13			-1.17	2.25	0.000279653	0.002735698
Angpt1			1.17	1.70	0.000287572	0.002798961
Tmem144			1.21	3.72	0.000288774	0.002807468
Fos			1.56	1.83	0.000297801	0.002875493
P2Ry8			2.61	-1.13	0.000309309	0.002954392
Lyrm2			1.27	3.81	0.000309763	0.002956731
Kcnh8			2.52	-1.43	0.000327661	0.003077744
Tnfaip6			1.68	1.69	0.000329313	0.003085129
Drd4			-1.39	2.81	0.000331392	0.003100503
Myh15			-1.44	2.60	0.000371534	0.003390966
LOC107314934	*Endod1*	*low*	2.71	-1.59	0.000373331	0.003405171
Nr5A2			-1.16	3.71	0.00037632	0.003425818
Efhc1			-1.76	1.01	0.000379409	0.003449509
Mlph			-1.04	2.70	0.000383	0.003475463
LOC107308084	*no match*		1.31	3.18	0.00038533	0.003494368
LOC107323573	*no match*		2.58	-0.64	0.000387397	0.003506376
Mctp1			-2.39	-1.14	0.000400766	0.003602157
LOC107325870	*no match*		1.04	2.77	0.0004039	0.003625628
Mmrn1			1.34	1.10	0.000410368	0.003669736
LOC107306001	*Arsd*	*high*	1.38	1.44	0.000429335	0.003799523
Laptm5			2.10	0.79	0.000440176	0.003878827
LOC107309030	*Mrc1*	*moderate*	2.73	1.17	0.000440321	0.003878827
LOC107306792	*no match*		-3.84	-2.00	0.00046516	0.004057259
Slc2A12			1.77	0.31	0.000466754	0.004068658
Cxcr4			1.26	1.96	0.000468788	0.004076357
Clcn2			1.60	0.34	0.000470586	0.004089152

Supplemental Table 12. Differentially expressed genes in quail mandibular primordia following *Gas1* morpholino knockdown

gene name	LOC match	confidence	logFC	logCPM	p-value	FDR (0.05)
Rnf20			-1.10	7.06	0.000472017	0.004091873
Slc36A4			2.27	3.84	0.000492774	0.004243246
LOC107317183	*no match*		3.31	-1.54	0.000514827	0.004402192
Nr5A1			2.39	-1.59	0.000526316	0.004483025
Foxe3			-1.21	2.34	0.000530211	0.004508064
Grid2			1.98	1.33	0.000532381	0.004521006
Fgf8			-1.07	5.12	0.00053773	0.004558312
LOC107315628	*Lipm*	*moderate*	-1.61	0.37	0.000586327	0.004935962
LOC107325236	*Krt13*	*moderate*	-1.11	2.04	0.000590572	0.004964664
LOC107323479	*Hes5*	*moderate*	1.16	1.90	0.000597031	0.004998194
Ptk2B			-1.09	2.80	0.000645931	0.005310284
LOC107325888	*no match*		-2.75	-1.85	0.000649951	0.005327871
Sla			3.20	-1.37	0.000673663	0.005487309
Tnfrsf25			1.90	-0.36	0.000679433	0.005527952
Plpp5			1.17	2.40	0.000697269	0.005643896
Iqcd			-1.30	1.71	0.000710098	0.005724834
Rtn1			-1.14	2.23	0.000726832	0.005826587
Slc4A1			1.79	6.13	0.000726488	0.005826587
LOC107324050	*Cldn8*	*moderate*	2.14	-1.26	0.000727534	0.00582891
LOC107314671	*no match*		1.23	1.51	0.000749227	0.005989163
LOC107305742	*Aqp7*	*moderate*	2.41	-1.41	0.00075798	0.006041966
Nkain2			-1.41	2.02	0.000793992	0.006250783
Rap1Gap2			1.40	1.02	0.000795369	0.006252162
Acvrl1			1.10	2.91	0.000800734	0.006283874
Ptgs1			1.07	3.90	0.000809677	0.006326024
Ecel1			1.22	2.16	0.000814577	0.006350293
LOC107306428	*Trabd2a*	*high*	-1.26	2.35	0.000836612	0.006482829
Asmt			1.66	-0.59	0.000858884	0.006630021
Susd1			1.67	1.84	0.000910838	0.006974067
Zbbx			1.17	2.63	0.000919861	0.007031749
LOC116653491	*no match*		1.95	-0.50	0.000940674	0.007148968
Csf1R			1.16	2.79	0.000964015	0.007298383
Pde8B			-1.23	2.82	0.000984893	0.007416804
Dnajb9			1.05	3.26	0.001005584	0.00755655
C18H17Orf58			1.77	-0.89	0.001041356	0.007775857
Trim35			1.08	2.29	0.001055573	0.00784892
Myo15B			1.33	1.43	0.001091404	0.008064544
Lurap1L			1.14	1.56	0.001105192	0.008134335
Lyn			1.20	2.43	0.001105443	0.008134335
Ifi30			1.62	1.44	0.001108057	0.008145113
LOC107325877	*no match*		1.90	-0.89	0.001117272	0.008200079
Wnt3A			-1.28	1.47	0.001148767	0.008379137

Supplemental Table 12. Differentially expressed genes in quail mandibular primordia following *Gas1* morpholino knockdown

gene name	LOC match	confidence	logFC	logCPM	p-value	FDR (0.05)
LOC107307752	*no match*		-2.21	-1.27	0.001161989	0.008440808
LOC107308414	*no match*		-1.07	2.72	0.001184922	0.008580994
LOC107321564	*no match*		2.61	-1.30	0.001189576	0.008605897
Ifitm10			1.31	1.09	0.001209698	0.008715858
Unc5A			-1.08	2.63	0.001284423	0.009147238
Oca2			1.99	-0.23	0.00129161	0.009193795
Foxa2			-1.12	1.47	0.001316647	0.009301897
LOC107310135	*no match*		-1.05	1.43	0.001323644	0.009342008
Gpr174			2.86	-2.23	0.001371483	0.009612596
LOC107305888	*no match*		-1.06	3.63	0.001395325	0.009750754
Map1Lc3C			1.24	2.36	0.001414444	0.009845505
Pld6			-1.43	0.15	0.001421291	0.009883452
Krt23			-1.10	1.57	0.001441184	0.009987462
Dock2			1.47	0.83	0.001544026	0.010520235
Prdm1			-1.40	1.18	0.001547324	0.010537428
Nmb			2.11	0.88	0.001551073	0.010552807
C1Ql1			1.17	1.57	0.001582011	0.010737511
LOC107316805	*Tgfbr2*	*moderate*	1.01	2.37	0.001603442	0.010836238
Aqp4			1.18	2.17	0.00162246	0.010954309
LOC107323583	*no match*		1.10	1.74	0.001683809	0.011282473
Ackr1			1.67	-0.40	0.001792493	0.011815104
Pou3F4			-1.68	1.16	0.001818374	0.011935709
Stom			1.04	3.65	0.001846885	0.012100427
Il15			1.84	0.04	0.00190382	0.012416027
Hs3St1			1.35	1.05	0.001936874	0.012589938
Ccdc110			2.16	-0.66	0.001940275	0.012601555
LOC107311319	*no match*		1.89	-0.92	0.001966092	0.012722563
LOC107306768	*no match*		-1.28	0.81	0.001986384	0.01283628
Tm4Sf19			3.21	-1.88	0.001988523	0.012844245
Antkmt			1.17	4.18	0.001993346	0.012863668
Map3K7Cl			1.67	-0.42	0.002016822	0.012977642
Fsip1			1.15	1.59	0.002058847	0.013177595
Fgfbp2			1.68	-1.01	0.002059668	0.013177595
Nkx2-5			-1.75	-0.16	0.002188611	0.013867747
Acacb			1.69	3.05	0.002290713	0.014294253
LOC107307616	*no match*		-1.72	-0.61	0.002473722	0.015261443
Kirrel3			-1.04	3.28	0.002500052	0.015370326
LOC107324444	*Slamf8*	*low*	1.75	-0.23	0.002564928	0.015707829
Golph3L			-1.75	1.40	0.002642309	0.016042992
Steap1			1.55	1.25	0.002651153	0.016080435
Nxph1			1.95	0.15	0.002686472	0.01626234
Clec3B			1.02	2.16	0.002702623	0.016329633

Supplemental Table 12. Differentially expressed genes in quail mandibular primordia following *Gas1* morpholino knockdown

gene name	LOC match	confidence	logFC	logCPM	p-value	FDR (0.05)
Proca1			2.21	-0.38	0.002710509	0.016361194
LOC107309133	*Vwde*	*moderate*	1.10	4.37	0.002748029	0.01655714
LOC107320189	*no match*		1.05	2.40	0.002803244	0.016796932
Fgf13			-1.04	2.94	0.002832253	0.016906389
LOC107310095	*Hrh4*	*moderate*	1.65	0.68	0.00286475	0.017023407
Lpxn			2.27	-1.32	0.002865076	0.017023407
Mei1			1.07	2.21	0.002932847	0.017382333
Prr15			-1.40	0.50	0.003043005	0.017870717
Ghrh			2.52	-1.18	0.003057688	0.017927213
Il12Rb1			-3.29	-1.20	0.003079031	0.018007626
LOC107306990	*no match*		-2.98	2.22	0.003190005	0.018496281
LOC107324445	*Cd84*	*low*	1.79	-0.56	0.003240585	0.018728228
LOC107313428	*no match*		1.41	1.42	0.003307942	0.01903982
Amer3			-1.41	-0.13	0.003324281	0.019102818
Tubb1			1.06	2.92	0.003379114	0.019323837
Fas			1.05	2.78	0.003397813	0.01939163
Gal3St1			1.36	0.46	0.003597081	0.020267563
Ccna1			1.72	-0.39	0.0036995	0.0207482
LOC107306832	*Insyn2b*	*low*	-1.17	1.87	0.003705545	0.02077129
Tnfrsf4			1.76	0.33	0.003764646	0.021060907
Bmper			1.50	1.15	0.003824272	0.021323716
Fndc1			-1.35	3.21	0.003880018	0.021553119
LOC107306925	*no match*		1.87	-1.36	0.003997982	0.022078527
Slitrk4			1.15	1.45	0.00400279	0.022088137
LOC107324518	*no match*		1.39	1.01	0.004002841	0.022088137
Sncg			1.08	1.15	0.004033243	0.022212633
Ctcfl			1.12	2.34	0.004212765	0.022995693
Tent5B			-1.01	3.58	0.004244929	0.023162333
Acta2			1.09	2.78	0.004264027	0.023248629
Chrna1			1.18	2.31	0.004286873	0.023355214
Dlk1			1.22	2.13	0.004398811	0.023845833
Il2Rg			1.66	2.16	0.004417547	0.023901783
Flt3			2.19	-0.53	0.004422014	0.023908114
Cdk5R2			1.80	-1.09	0.004472903	0.024136151
Trappc3L			1.89	-1.85	0.004540504	0.024399181
Foxi1			1.86	-1.16	0.004542966	0.024402496
LOC107312635	*no match*		1.06	1.73	0.004571177	0.0245097
LOC107307868	*no match*		-2.05	-1.23	0.004605598	0.024611894
Znf488			-2.04	-0.39	0.004631137	0.024717431
Capn9			2.84	-0.63	0.00472461	0.025102814
LOC107324539	*no match*		1.73	-0.39	0.004783702	0.025284008
Sox14			-1.21	1.20	0.00483926	0.025492046

Supplemental Table 12. Differentially expressed genes in quail mandibular primordia following *Gas1* morpholino knockdown

gene name	LOC match	confidence	logFC	logCPM	p-value	FDR (0.05)
Adam28			3.00	-1.39	0.004869558	0.02560404
LOC116652409	*no match*		2.89	-1.64	0.005004993	0.026199453
Fgf7			1.23	3.40	0.005358282	0.027500022
Plppr1			1.53	-0.07	0.005432324	0.027819549
Gabrp			1.06	1.73	0.005483819	0.028052833
Stoml3			1.32	0.76	0.005619207	0.028567516
Tfpi2			1.00	1.52	0.005638325	0.028615864
Htra3			1.39	0.43	0.005641491	0.028621674
LOC107321483	*Tmem132b*	*high*	-1.61	2.32	0.005739564	0.029025676
Ccdc107			1.08	2.78	0.006116016	0.030558505
LOC107311723	*no match*		1.48	-0.33	0.006285141	0.031227294
Fam155B			-1.16	0.93	0.006303727	0.031286717
LOC107314689	*no match*		1.46	0.21	0.006574151	0.032334321
Kcne3			1.61	-0.75	0.006658365	0.032646501
LOC116653180	*no match*		2.78	-1.45	0.006680757	0.032733631
Dnah10			1.01	4.01	0.006789823	0.033176215
Tmem51			1.19	0.14	0.00683269	0.033328195
LOC107309463	*Itpripl1*	*low*	1.68	-1.08	0.006975085	0.033913871
Deup1			-1.67	0.19	0.007057669	0.034260414
Hsdl2			1.09	5.86	0.007066205	0.034290099
LOC107307857	*no match*		-1.18	1.09	0.007084809	0.034356836
Matn4			1.07	2.65	0.007123281	0.034458823
LOC107321554	*no match*		1.58	-0.35	0.007131446	0.034476769
Dnah7			-1.10	2.27	0.007149605	0.034517436
LOC107315547	*Stimate*	*moderate*	1.13	1.38	0.007189791	0.034652393
Cpn2			2.66	-1.18	0.007195174	0.034666543
LOC107325881	*Btn3a3*	*low*	2.15	-0.85	0.007209004	0.034709567
LOC107315164	*no match*		-1.05	6.46	0.007257174	0.034858553
Gpm6A			1.89	-0.93	0.00729342	0.034973358
Mcmdc2			1.38	1.53	0.007318601	0.035075657
Rbpjl			1.33	0.61	0.007375014	0.03528101
Kcnmb2			1.21	0.69	0.007381123	0.035298317
Hmgcs2			2.02	-0.90	0.007480674	0.035678031
Susd3			1.38	1.88	0.007541103	0.035869621
Gsdma			1.99	-0.28	0.007751324	0.036635804
LOC107323198	*Bpifb4*	*moderate*	2.31	-1.05	0.00782891	0.036903994
Lrrc3B			-1.42	-0.38	0.007897272	0.037102773
Alpk1			-1.11	0.89	0.00790251	0.03711507
LOC107312885	*Tmem182*	*moderate*	2.18	-0.63	0.008006174	0.037465297
C5H11Orf96			1.59	-0.66	0.008106226	0.037821042
Insm1			-1.05	1.85	0.008133493	0.037910802
F10			1.33	1.05	0.008155258	0.037968547

Supplemental Table 12. Differentially expressed genes in quail mandibular primordia following *Gas1* morpholino knockdown

gene name	LOC match	confidence	logFC	logCPM	p-value	FDR (0.05)
B3Galt5			1.77	0.51	0.008345274	0.038668892
LOC107313678	*Cyp4v2*	*moderate*	1.32	0.89	0.008354175	0.03868483
LOC107319047	*no match*		1.74	-1.39	0.008412409	0.038882386
Pcsk4			-1.45	-0.70	0.008481695	0.039096389
LOC107316069	*Gabrp*	*moderate*	1.58	-0.26	0.008509986	0.039175807
Col9A3			1.07	4.56	0.008541824	0.039278179
LOC116654405	*no match*		-2.11	-0.95	0.008586237	0.039446006
Gjd2			2.09	-0.68	0.008588555	0.039446006
Fbxo47			1.70	-1.61	0.0088274	0.04029704
LOC107305752	*Aqp3*	*high*	1.47	2.20	0.008852622	0.040359636
LOC107325409	*no match*		2.49	0.22	0.008872901	0.040421887
LOC107324970	*no match*		-1.72	-1.91	0.008994074	0.040807515
LOC107305757	*no match*		1.95	0.27	0.009005707	0.040841788
LOC107306000	*Gzmk*	*moderate*	2.06	-0.33	0.009036444	0.040894961
Phf24			-2.78	-1.56	0.009426869	0.042283597
LOC107318455	*no match*		1.33	0.61	0.009473749	0.042426703
Fam124A			-1.48	-1.13	0.009626097	0.042946839
Adamtsl3			1.00	3.18	0.009626277	0.042946839
LOC107323638	*Nt5c2*	*high*	1.23	2.64	0.00970337	0.04318198
Cdh12			1.35	-0.80	0.009745243	0.043313892
Nobox			1.52	-0.23	0.009899292	0.043852205
Klhl6			1.29	1.09	0.009929088	0.043933029
Fbxo39			1.42	-0.74	0.010103901	0.044503036
LOC107325477	*no match*		1.83	-0.63	0.010297445	0.045257001
Otos			1.29	-0.41	0.010349106	0.045413595
LOC107306586	*no match*		-1.92	1.90	0.010409449	0.045607746
S100A1			1.12	2.44	0.010447077	0.045730175
Ccdc113			1.11	0.87	0.010473413	0.045827654
Ncam2			1.07	2.42	0.010515881	0.04596034
LOC107320518	*no match*		-1.41	-0.82	0.010731285	0.046657046
Gpr139			-1.43	-1.08	0.010749806	0.0466862
LOC107305966	*Arsd*	*high*	1.72	-1.74	0.010763485	0.046711019
Col21A1			1.05	1.42	0.010898632	0.047204582
Csmd3			1.25	0.19	0.010909053	0.047212569
Chrm2			1.96	-1.08	0.010919634	0.047243929
Amigo2			1.08	1.00	0.010996351	0.047430973
Wnt7A			-1.20	0.61	0.011007492	0.047435692
Pax1			-1.45	0.29	0.011165618	0.047956634
Pou3F1			-1.33	0.39	0.011242984	0.048128399

Supplemental Table 13. Differentially expressed genes in quail mandibular primordia following *Gas1* over-expression

gene name	LOC match	confidence	logFC	logCPM	p-value	FDR (0.05)
LOC107310823	*Glipr1*	*moderate*	-7.33	1.31	6.81E-05	1.98E-02
LOC107325888	*no match*		-4.68	-1.85	7.29E-07	5.85E-04
Rorb			-3.04	-1.44	7.41E-05	2.10E-02
Gabra4			-2.30	-1.41	2.68E-04	4.79E-02
Rab3B			-2.22	1.83	1.18E-04	2.88E-02
Pcp4L1			-2.16	1.22	2.87E-05	1.04E-02
LOC116652502	*no match*		-2.13	5.93	6.80E-08	7.41E-05
LOC107309809	*no match*		-1.90	6.83	5.70E-12	2.02E-08
Aoah			-1.80	0.90	1.86E-04	4.02E-02
Col17A1			-1.68	5.98	2.10E-15	9.93E-12
Vit			-1.58	6.22	4.28E-08	5.66E-05
Wnt3A			-1.42	1.47	3.07E-04	4.83E-02
Sostdc1			-1.33	3.95	4.55E-06	2.80E-03
Wnt9B			-1.31	3.84	1.67E-05	8.15E-03
Lrrn4			-1.30	4.05	1.62E-09	3.27E-06
Fat2			-1.30	2.91	4.79E-05	1.58E-02
Fzd10			-1.29	4.38	4.89E-07	4.33E-04
Perp			-1.25	3.80	2.10E-06	1.49E-03
Wnt2B			-1.15	3.37	2.33E-07	2.36E-04
LOC107319512	*no match*		-1.11	8.28	2.78E-05	1.04E-02
A2M			-1.11	5.27	3.65E-07	3.45E-04
Astn2			-1.08	5.61	1.30E-04	2.96E-02
Ptprf			-1.03	7.55	3.86E-05	1.37E-02
Cfh			1.14	2.32	2.17E-04	4.27E-02
Gabrd			1.36	2.98	2.06E-04	4.18E-02
LOC107306747	*no match*		1.40	4.10	1.23E-04	2.91E-02
Bpi			1.60	2.05	7.43E-07	5.85E-04
Masp1			1.99	0.91	1.69E-05	8.15E-03
Ifitm10			2.20	1.09	4.40E-08	5.66E-05
LOC107324539	*no match*		2.54	-0.39	2.59E-05	1.00E-02
LOC107314934	*Endod1*	*low*	2.72	-1.59	3.02E-04	4.80E-02
Gas1			2.92	4.61	3.37E-11	9.53E-08
LOC107324591	*no match*		3.73	1.35	2.71E-04	4.79E-02
Marco			4.44	-1.23	1.30E-04	2.96E-02
LOC107307448	*no match*		6.11	0.40	2.89E-04	4.79E-02

Supplemental Table 14. Gene Ontology (GO) Analysis by Species and Treatment Group

Duck control versus Gas1 morpholino

term	count	list total	fold enrichment	p-value	FDR	genes
GO:0015671 ~oxygen transport	7	354	24.75	0.0000	0.0001	LOC113839608 (no match), LOC113844783 (no match), LOC101800713 (no match), LOC101798290 (Hbe), LOC101792412 (Hbad), LOC101800520 (Hbad), LOC101798111 (Hbe)
GO:0042744 ~hydrogen peroxide catabolic process	7	354	19.45	0.0000	0.0004	LOC113839608 (no match), LOC113844783 (no match), LOC101800713 (no match), LOC101798290 (Hbe), LOC101792412 (Hbad), LOC101800520 (Hbad), LOC101798111 (Hbe)
GO:0007275 ~multicellular organism development	16	354	4.79	0.0000	0.0004	WNT10A, EYA2, WNT7B, WNT9B, LOC101793040 (no match), WNT16, LOC101791691 (no match), FSTL5, SHH, CDH1, PPDPFL, OTX2, CDH26, OTX1, MET, WNT3
GO:0060048 ~cardiac muscle contraction	6	354	16.67	0.0000	0.0048	TNNT2, MYL2, CASQ2, TNNI1, TNNI2, NKX2-5
GO:0090374 ~oligopeptide export from mitochondrion	4	354	38.90	0.0001	0.0141	LOC119718656 (no match), LOC119718657 (no match), LOC101797091 (no match), LOC101797680 (no match)
GO:0030154 ~cell differentiation	21	354	2.72	0.0001	0.0172	FOXA1, FOXE1, DLX4, EYA2, WNT7B, FOXI2, HNF4G, SOX14, LYPD6, SOX21, FOXQ1, SOX2, FSTL5, NHSL2, HNF4A, ID1, PPDPFL, AGRN, NKX2-5, NKX2-3, FOXA2
GO:0045165 ~cell fate commitment	8	354	7.07	0.0001	0.0178	SOX2, WNT10A, GAP43, WNT7B, WNT9B, PRDM1, WNT16, WNT3
GO:0006357 ~regulation of transcription by RNA polymerase II	41	354	1.85	0.0002	0.0274	FOXA1, CEBPA, ASCL4, FOXE1, EPAS1, FOXI2, HNF4G, PRDM1, ASCL2, FOXQ1, PDLIM1, GBX2, SIX3, STAT4, OTX2, HIVEP3, HOXA1, OTX1, NKX2-5, LOC101791703 (Klf8), NKX2-3, TP63, IRX1, DMRT2, BCL11A, BRPF3, LOC106015023 (no match), FOS, GRHL2, KLF17, LOC101796186 (no match), DMRTA2, GFI1B, MAFB, KLF5, TAL1, LOC101805050 (no match), LOC101800522 (Zkscan7), IRF6, FOXA2, TP73

Supplemental Table 14. Gene Ontology (GO) Analysis by Species and Treatment Group

GO:0006805 ~xenobiotic metabolic process	7	354	7.56	0.0003	0.0331	LOC101797666 (no match), LOC101804267 (Cyp2w1), HNF4A, ABCB11, LOC101804496 (no match), LOC101797494 (no match), LOC101790094 (no match)
GO:0007043 ~cell-cell junction assembly	7	354	6.98	0.0004	0.0467	LOC101791691 (no match), CDH1, PKP2, PKP1, PKP3, CDH26, LOC101793040 (no match)
GO:0060070 ~canonical Wnt signaling pathway	9	354	4.80	0.0005	0.0530	WNT10A, EDN1, FZD5, WNT7B, WNT9B, RSPO2, FZD10, WNT16, WNT3
GO:0048247 ~lymphocyte chemotaxis	5	354	10.24	0.0012	0.1088	LOC110351183 (no match), LOC101791385 (no match), IL8, LOC101791569 (no match), LOC101802909 (no match)
GO:0006564 ~L-serine biosynthetic process	3	354	38.90	0.0019	0.1600	PSAT1, PHGDH, PSPH
GO:0002548 ~monocyte chemotaxis	5	354	8.84	0.0022	0.1656	LOC110351183 (no match), LOC101791385 (no match), IL8, LOC101791569 (no match), LOC101802909 (no match)
GO:0009653 ~anatomical structure morphogenesis	8	354	4.26	0.0026	0.1877	FOXQ1, SOX2, FOXA1, FOXE1, FOXI2, SOX14, SOX21, FOXA2
GO:0071542 ~dopaminergic neuron differentiation	4	354	12.97	0.0031	0.2080	DMRTA2, RSPO2, OTX2, FOXA2
GO:0030216 ~keratinocyte differentiation	5	354	7.48	0.0041	0.2571	CDKN1A, MAFB, IRF6, WNT16, TP63

Supplemental Table 14. Gene Ontology (GO) Analysis by Species and Treatment Group

GO:0042771 ~intrinsic apoptotic signaling pathway in response to DNA damage by p53 class mediator	4	354	11.11	0.0049	0.2946	CDKN1A, TP63, TP73, PHLDA3
GO:0070098 ~chemokine-mediated signaling pathway	5	354	6.95	0.0053	0.3026	LOC110351183 (no match), LOC101791385 (no match), IL8, LOC101791569 (no match), LOC101802909 (no match)
GO:0019885 ~antigen processing and presentation of endogenous peptide antigen via MHC class I	3	354	23.34	0.0062	0.3349	LOC119718656 (no match), LOC119718657 (no match), LOC101797091 (no match)
GO:0043616 ~keratinocyte proliferation	4	354	9.15	0.0087	0.4456	CDKN1A, IRF6, WNT16, TP63
GO:0007548 ~sex differentiation	3	354	16.67	0.0126	0.6129	DMRTA2, DMRT2, HNF4A
GO:0030593 ~neutrophil chemotaxis	5	354	5.40	0.0131	0.6129	LOC110351183 (no match), LOC101791385 (no match), IL8, LOC101791569 (no match), LOC101802909 (no match)
GO:0030182 ~neuron differentiation	7	354	3.17	0.0230	0.9908	IRX1, WNT10A, SHH, WNT7B, WNT9B, WNT16, WNT3
GO:0035914 ~skeletal muscle cell differentiation	4	354	6.22	0.0253	0.9908	DMRTA2, SMYD1, HIVEP3, FOS

Supplemental Table 14. Gene Ontology (GO) Analysis by Species and Treatment Group

GO:0045987 ~positive regulation of smooth muscle contraction	3	354	11.67	0.0257	0.9908	MYOCD, EDN1, ADA
GO:1904888 ~cranial skeletal system development	3	354	11.67	0.0257	0.9908	FOXE1, IRF6, TP63
GO:0045780 ~positive regulation of bone resorption	3	354	10.61	0.0309	0.9908	TFRC, FSHB, SPP1
GO:0055091 ~phospholipid homeostasis	3	354	10.61	0.0309	0.9908	FABP3, HNF4A, ABCB11
GO:0043547 ~positive regulation of GTPase activity	6	354	3.38	0.0318	0.9908	LOC110351183 (no match), LOC101791385 (no match), DOCK8, LOC101805062 (Adap1), LOC101791569 (no match), LOC101802909 (no match)
GO:0006936 ~muscle contraction	4	354	5.56	0.0341	0.9908	LOC119713220 (Myh1b), TNNI1, LOC119713219 (Myh1b), TNNI2
GO:0042572 ~retinol metabolic process	3	354	9.72	0.0365	0.9908	ADH1C, LOC101804496 (no match), LOC101797494 (no match)
GO:0019369 ~arachidonate metabolic process	3	354	8.98	0.0424	0.9908	LOC101804496 (no match), LOC101797494 (no match), LOC101790094 (no match)
GO:0007156 ~homophilic cell adhesion via plasma membrane adhesion molecules	9	354	2.29	0.0435	0.9908	IGSF11, LOC101791691 (no match), MYOT, CDH1, PCDH10, FAT2, CDH26, LOC101793040 (no match), PTPRF
GO:0007267 ~cell-cell signaling	4	354	5.02	0.0442	0.9908	GJD2, SHH, LOC101797182 (no match), ADRA1B

Supplemental Table 14. Gene Ontology (GO) Analysis by Species and Treatment Group

GO:0001817 ~regulation of cytokine production	4	354	5.02	0.0442	0.9908	LOC101795354 (no match), LOC113841481 (no match), LITAF, LOC101793739 (no match)
GO:0016339 ~calcium-dependent cell-cell adhesion via plasma membrane cell adhesion molecules	4	354	4.86	0.0479	0.9908	LOC101791691 (no match), CDH1, CDH26, LOC101793040 (no match)
GO:0071347 ~cellular response to interleukin-1	4	354	4.86	0.0479	0.9908	LOC110351183 (no match), LOC101791385 (no match), LOC101791569 (no match), LOC101802909 (no match)
GO:0048496 ~maintenance of animal organ identity	2	354	38.90	0.0506	0.9908	PKP2, USH2A
GO:0009888 ~tissue development	4	354	4.58	0.0557	0.9908	SHH, WNT7B, LAMB4, NTN1
GO:0030878 ~thyroid gland development	3	354	7.29	0.0621	0.9908	EDN1, FOXE1, NKX2-5
GO:0034332 ~adherens junction organization	4	354	4.32	0.0640	0.9908	LOC101791691 (no match), CDH1, CDH26, LOC101793040 (no match)
GO:0006955 ~immune response	9	354	2.10	0.0659	0.9908	LOC101799867 (no match), LOC110351183 (no match), LOC101791385 (no match), IL8, LOC119715258 (no match), LOC101799683 (no match), LOC101791569 (no match), LOC119718708 (no match), LOC101802909 (no match)
GO:0071346 ~cellular response to type II interferon	4	354	4.21	0.0684	0.9908	LOC110351183 (no match), LOC101791385 (no match), LOC101791569 (no match), LOC101802909 (no match)

Supplemental Table 14. Gene Ontology (GO) Analysis by Species and Treatment Group

GO:0031424 ~keratinization	3	354	6.86	0.0692	0.9908	LOC101797203 (no match), LOC101799764 (no match), LOC101799146 (no match)
GO:0048468 ~cell development	3	354	6.86	0.0692	0.9908	IRX1, SHH, IRF6
GO:0030308 ~negative regulation of cell growth	4	354	4.09	0.0729	0.9908	MINAR1, CDKN1A, HNF4A, MYL2
GO:0044331 ~cell-cell adhesion mediated by cadherin	3	354	6.48	0.0766	0.9908	LOC101791691 (no match), CDH1, CDH26
GO:0030890 ~positive regulation of B cell proliferation	3	354	5.83	0.0920	0.9908	CDKN1A, TFRC, ADA
GO:2000271 ~positive regulation of fibroblast apoptotic process	2	354	19.45	0.0987	0.9908	STK17A, TP63
GO:0006116 ~NADH oxidation	2	354	19.45	0.0987	0.9908	ALDOB, LOC101798440 (Gpd1l)
GO:0008652 ~amino acid biosynthetic process	2	354	19.45	0.0987	0.9908	PHGDH, BCAT1
GO:0048245 ~eosinophil chemotaxis	2	354	19.45	0.0987	0.9908	LOC101791385 (no match), LOC101791569 (no match)

Duck control versus Gas1 over-expression

Term	Count	List Total	Fold Enrichment	PValue	FDR	Genes

Supplemental Table 14. Gene Ontology (GO) Analysis by Species and Treatment Group

GO:0015671 ~oxygen transport	7	325	26.96	0.0000	0.0001	LOC113839608 (no match), LOC113844783 (no match), LOC101800713 (no match), LOC101798290 (Hbe), LOC101792412 (Hbad), LOC101800520 (Hbad), LOC101798111 (Hbe)
GO:0007275 ~multicellular organism development	16	325	5.21	0.0000	0.0001	WNT10A, WNT2B, WNT9B, WNT7A, LOC101794490 (no match), DKK2, LOC106020320 (no match), LOC101791691 (no match), FSTL5, SHH, CDH3, CDH1, KIT, CDH26, WNT2, WNT3
GO:0042744 ~hydrogen peroxide catabolic process	7	325	21.18	0.0000	0.0001	LOC113839608 (no match), LOC113844783 (no match), LOC101800713 (no match), LOC101798290 (Hbe), LOC101792412 (Hbad), LOC101800520 (Hbad), LOC101798111 (Hbe)
GO:0030182 ~neuron differentiation	11	325	5.42	0.0000	0.0085	IRX1, WNT10A, SHH, WNT2B, LMX1A, ALDH1A2, WNT9B, WNT7A, WNT2, LHX9, WNT3
GO:0060048 ~cardiac muscle contraction	5	325	15.13	0.0002	0.0515	TNNT2, MYL2, CASQ2, TNNI1, TNNI2
GO:0006936 ~muscle contraction	6	325	9.08	0.0004	0.0756	LOC119713220 (Myh1b), TMOD4, TNNT3, TNNI1, LOC119713219 (Myh1b), TNNI2
GO:0045165 ~cell fate commitment	7	325	6.74	0.0005	0.0793	WNT10A, WNT2B, WNT9B, WNT7A, SOX6, WNT2, WNT3
GO:0016339 ~calcium-dependent cell-cell adhesion via plasma membrane cell adhesion molecules	6	325	7.94	0.0008	0.1076	LOC106020320 (no match), LOC101791691 (no match), CDH3, CDH1, LOC101794490 (no match), CDH26
GO:0034332 ~adherens junction organization	6	325	7.06	0.0014	0.1659	LOC106020320 (no match), LOC101791691 (no match), CDH3, CDH1, LOC101794490 (no match), CDH26
GO:0007043 ~cell-cell junction assembly	6	325	6.52	0.0021	0.2153	LOC106020320 (no match), LOC101791691 (no match), CDH3, CDH1, LOC101794490 (no match), CDH26

Supplemental Table 14. Gene Ontology (GO) Analysis by Species and Treatment Group

GO:0055085 ~transmembrane transport	14	325	2.56	0.0034	0.3195	LOC110352387 (no match), TRPA1, ABCA5, SLC43A3, SPNS3, LOC113840468 (no match), ABCB11, LOC119713165 (no match), SLC22A18, LOC119716104 (no match), LOC101791126 (no match), FLVCR2, SLC26A9, HCN2
GO:0046330 ~positive regulation of JNK cascade	6	325	5.41	0.0048	0.4102	EDAR, CARD9, WNT7A, LOC106016036 (no match), CCN2, RASGRP1
GO:0007416 ~synapse assembly	4	325	9.97	0.0069	0.4779	LOC106020320 (no match), CDH1, SLITRK6, WNT7A
GO:0060070 ~canonical Wnt signaling pathway	7	325	4.06	0.0074	0.4779	WNT10A, WNT2B, FZD5, WNT9B, WNT7A, WNT2, WNT3
GO:0009888 ~tissue development	5	325	6.23	0.0080	0.4779	SHH, LAMA3, LAMB4, WNT7A, NTN1
GO:0044331 ~cell-cell adhesion mediated by cadherin	4	325	9.42	0.0081	0.4779	LOC106020320 (no match), LOC101791691 (no match), CDH1, CDH26
GO:0030036 ~actin cytoskeleton organization	9	325	3.13	0.0082	0.4779	PDLIM3, FGF7, ACTN2, KIT, LOC101790278 (no match), RICTOR, ASB2, LOC101804927 (no match), SPTB
GO:0007155 ~cell adhesion	10	325	2.86	0.0083	0.4779	RIPOR2, LOC106019797 (no match), LAMA3, LOC101790278 (no match), MXRA8, ITGB8, CCN2, HAPLN4, SELE, PTPRF
GO:0007218 ~neuropeptide signaling pathway	6	325	4.62	0.0093	0.4833	OPRD1, GHRH, NPY, PENK, LOC101790005 (no match), SSTR4
GO:0007156 ~homophilic cell adhesion via plasma membrane adhesion molecules	10	325	2.77	0.0103	0.4833	LOC106020320 (no match), LOC101791691 (no match), CDH3, MYOT, CDH1, PCDH10, FAT2, LOC101794490 (no match), CDH26, PTPRF

Supplemental Table 14. Gene Ontology (GO) Analysis by Species and Treatment Group

GO:0032725 ~positive regulation of granulocyte macrophage colony-stimulating factor production	3	325	18.16	0.0107	0.4833	LOC119714503 (no match), CARD9, RASGRP1
GO:0043303 ~mast cell degranulation	3	325	18.16	0.0107	0.4833	LOC119714503 (no match), KIT, RASGRP1
GO:0008584 ~male gonad development	5	325	5.73	0.0108	0.4833	LOC101803098 (no match), WNT2B, SRD5A2, KIT, LHX9
GO:0050852 ~T cell receptor signaling pathway	6	325	4.10	0.0152	0.6511	LOC110354662 (no match), CACNB4, LOC101795354 (no match), LOC113841521 (no match), ADA, LOC101793739 (no match)
GO:0007189 ~adenylate cyclase-activating G protein-coupled receptor signaling pathway	7	325	3.41	0.0166	0.6862	LOC101803098 (no match), GPER1, GHRH, LOC101803845 (no match), DRD1, LGR6, PTHLH
GO:0003009 ~skeletal muscle contraction	3	325	14.12	0.0178	0.7063	TNNT3, TNNI1, TNNI2
GO:0055001 ~muscle cell development	3	325	10.59	0.0312	0.9952	CACNB4, ACTN2, LOC101804927 (no match)
GO:0000902 ~cell morphogenesis	6	325	3.39	0.0317	0.9952	LOC106020320 (no match), LOC101791691 (no match), CDH3, CDH1, LOC101794490 (no match), CDH26
GO:0051260 ~protein homooligomerization	6	325	3.30	0.0349	0.9952	RIPOR2, KCNG4, LOC119713975 (Kcna2), KCTD21, CARD9, KCTD16

Supplemental Table 14. Gene Ontology (GO) Analysis by Species and Treatment Group

GO:0001817 ~regulation of cytokine production	4	325	5.47	0.0357	0.9952	LOC110354662 (no match), LOC101795354 (no match), LOC113841521 (no match), LOC101793739 (no match)
GO:0042981 ~regulation of apoptotic process	6	325	3.26	0.0366	0.9952	LOC113840537 (no match), LOC113841747 (no match), CARD9, LOC113840437 (no match), LOC119714638 (no match), CIDEC
GO:0050853 ~B cell receptor signaling pathway	4	325	5.14	0.0419	0.9952	LOC119714503 (no match), LOC119714133 (no match), LOC119714132 (no match), BMX
GO:0010468 ~regulation of gene expression	7	325	2.75	0.0421	0.9952	NELL1, SHH, CAVIN4, RICTOR, JARID2, PTHLH, WNT3
GO:0050731 ~positive regulation of peptidyl-tyrosine phosphorylation	4	325	4.98	0.0451	0.9952	FGF7, LOC119714503 (no match), RICTOR, HTR2A
GO:2000818 ~negative regulation of myoblast proliferation	2	325	42.37	0.0465	0.9952	MSTN, MYOD1
GO:0006805 ~xenobiotic metabolic process	4	325	4.71	0.0521	0.9952	LOC101797666 (no match), LOC101804267 (Cyp2w1), ABCB11, LOC101804496 (no match)
GO:0045214 ~sarcomere organization	3	325	7.94	0.0533	0.9952	ACTN2, TNNT2, TNNT3
GO:0006882 ~intracellular zinc ion homeostasis	3	325	7.94	0.0533	0.9952	SLC39A8, SLC30A10, SLC39A14
GO:0048468 ~cell development	3	325	7.48	0.0595	0.9952	IRX1, SHH, MKX

Supplemental Table 14. Gene Ontology (GO) Analysis by Species and Treatment Group

GO:0016239 ~positive regulation of macroautophagy	3	325	7.48	0.0595	0.9952	LOC101794001 (no match), SESN2, DCN
GO:0010628 ~positive regulation of gene expression	9	325	2.14	0.0596	0.9952	EDAR, GH1, FGF7, ACTC1, IL8, GPER1, ALDH1A2, LOC101790278 (no match), WNT7A
GO:0042904 ~9-cis-retinoic acid biosynthetic process	2	325	28.25	0.0689	0.9952	DHRS9, ALDH1A2
GO:0032962 ~positive regulation of inositol trisphosphate biosynthetic process	2	325	28.25	0.0689	0.9952	LOC101803098 (no match), GPER1
GO:0006937 ~regulation of muscle contraction	2	325	28.25	0.0689	0.9952	TNNT2, TNNT3
GO:0015791 ~polyol transmembrane transport	2	325	28.25	0.0689	0.9952	AQP9, AQP3
GO:0048541 ~Peyer's patch development	2	325	28.25	0.0689	0.9952	CACNB4, ADA
GO:0032765 ~positive regulation of mast cell cytokine production	2	325	28.25	0.0689	0.9952	LOC119714503 (no match), KIT

Supplemental Table 14. Gene Ontology (GO) Analysis by Species and Treatment Group

GO:0033089 ~positive regulation of T cell differentiation in thymus	2	325	28.25	0.0689	0.9952	RASGRP1, ADA
GO:1905606 ~regulation of presynapse assembly	3	325	6.69	0.0726	0.9952	SLITRK3, SLITRK6, WNT7A
GO:0007517 ~muscle organ development	3	325	6.69	0.0726	0.9952	RIPOR2, MYOD1, MKX
GO:0048513 ~animal organ development	3	325	6.36	0.0794	0.9952	GH1, SHH, NRG2
GO:0015793 ~glycerol transmembrane transport	2	325	21.18	0.0909	0.9952	AQP9, AQP3

Quail control versus Gas1 morpholino

Term	Count	List Total	Fold Enrichment	PValue	FDR	Genes
GO:0007420 ~brain development	12	433	6.84	0.0000	0.0004	ZFHX3, RTN1, LOC107307344 (no match), LOC107314966 (Meis2), SCTR, CXCR4, LOC107314117 (Emx1), APOD, GRHL2, PBX1, CDK5R2, POU3F4
GO:0009653 ~anatomical structure morphogenesis	13	433	5.90	0.0000	0.0004	ACVRL1, FOXE3, FOXE1, FOXI3, FOXI1, SOX14, FOXL2, SOX21, SOX2, FOXQ1, LOC107316805 (Tgfbr2), PITX2, FOXA2
GO:0030182 ~neuron differentiation	11	433	4.77	0.0001	0.0172	IRX1, WNT10A, FGF8, RTN1, WNT2B, WNT3A, IRX4, LOC107314117 (Emx1), LMX1B, INSM1, WNT2

Supplemental Table 14. Gene Ontology (GO) Analysis by Species and Treatment Group

GO:0006357 ~regulation of transcription by RNA polymerase II	49	433	1.68	0.0004	0.0601	FOXE3, FOXE1, FOXI3, FOXI1, SCX, LOC107323479 (Hes5), PRDM1, FOXQ1, MED11, CREB3L2, PITX2, TP63, LOC107312805 (Klf5), FOXL2, FOS, PAX2, OVOL2, POU3F4, PAX1, NR5A1, HIC2, NR5A2, HAND1, NOBOX, LMX1B, RBPJL, LOC107325872 (Znf628), HOXD1, NACC1, OTX2, OTX1, NKX2-5, NKX2-3, IRX1, TFAP2B, ZFHX3, TFAP2E, IRX4, ARID3B, GRHL1, ARID3C, GRHL2, TRERF1, PBX1, KLF5, SP1, TLX1, HOXD3, FOXA2
GO:0030154 ~cell differentiation	23	433	2.27	0.0005	0.0608	LYN, ACVRL1, FOXE3, FOXE1, ANGPT1, FOXI3, FOXI1, PRRC2C, SOX14, FOXL2, LOC107305757 (no match), SOX21, SOX2, FOXQ1, FGF7, CAPRIN1, LOC107316805 (Tgfbr2), NCAM2, NKX2-5, FGF13, NKX2-3, FOXA2, ZNF750
GO:0045165 ~cell fate commitment	7	433	6.16	0.0008	0.0778	SOX2, WNT10A, WNT2B, WNT3A, GATA4, PRDM1, WNT2
GO:0045104 ~intermediate filament cytoskeleton organization	5	433	8.07	0.0029	0.2392	DSP, FAM83H, KRT18, PPL, EVPL
GO:0007043 ~cell-cell junction assembly	6	433	5.45	0.0044	0.3195	ARVCF, CTNND2, PKP2, CDH12, FAT2, PKP1
GO:0098609 ~cell-cell adhesion	9	433	3.04	0.0093	0.5875	KIRREL3, DSP, TJP1, ARVCF, CTNND2, PKP2, LPXN, PKP1, TJP2
GO:0007507 ~heart development	6	433	4.47	0.0103	0.5875	ACVRL1, PDLIM1, GJA5, HAND1, PKP2, LOC107316805 (Tgfbr2)
GO:0042060 ~wound healing	4	433	8.30	0.0110	0.5875	DSP, EPPK1, PPL, EVPL
GO:0007275 ~multicellular organism development	11	433	2.48	0.0134	0.6522	CSF1R, WNT10A, FLT1, WNT2B, WNT3A, FLT3, CDH12, OTX2, OTX1, WNT2, DKK3
GO:0042438 ~melanin biosynthetic process	3	433	14.53	0.0161	0.7253	OCA2, TUBB3, ASIP

Supplemental Table 14. Gene Ontology (GO) Analysis by Species and Treatment Group

GO:0042391 ~regulation of membrane potential	6	433	3.79	0.0201	0.8414	RIMS2, CHRNA1, GABRP, KCNH8, LOC107316069 (Gabrp), GABRD
GO:0045216 ~cell-cell junction organization	3	433	10.90	0.0287	0.9949	TJP1, LPXN, TJP2
GO:0045110 ~intermediate filament bundle assembly	3	433	9.69	0.0361	0.9949	PKP2, PKP1, EPPK1
GO:1902260 ~negative regulation of delayed rectifier potassium channel activity	3	433	8.72	0.0441	0.9949	KCNE2, KCNE3, KCNAB1
GO:0045109 ~intermediate filament organization	4	433	4.84	0.0477	0.9949	LOC107325817 (Krt75), LOC107325236 (Krt13), LOC107325235 (Krt19), KRT8
GO:0000226 ~microtubule cytoskeleton organization	7	433	2.61	0.0512	0.9949	TUBB3, PARD3, TUBB, MAP7D2, TUBB1, MAP7, PARD3B
GO:0045944 ~positive regulation of transcription by RNA polymerase II	13	433	1.83	0.0520	0.9949	NCOA1, KMT2D, LOC107307277 (no match), SOX14, MRTFA, GATA4, SOX21, SOX2, AR, TUBB3, TET3, LOC107314966 (Meis2), ZNF750
GO:0048856 ~anatomical structure development	5	433	3.46	0.0550	0.9949	TFAP2B, TFAP2E, LOC107309133 (Vwde), PAX2, PAX1
GO:0006644 ~phospholipid metabolic process	4	433	4.47	0.0583	0.9949	PLPP5, PLPPR1, LOC107320189 (no match), PROCA1

Supplemental Table 14. Gene Ontology (GO) Analysis by Species and Treatment Group

GO:0006413 ~translational initiation	4	433	4.47	0.0583	0.9949	LOC107307669 (no match), LOC107307861 (no match), LOC107307629 (no match), LOC107307490 (no match)
GO:0051660 ~establishment of centrosome localization	2	433	29.06	0.0675	0.9949	PARD3, PARD3B
GO:0045087 ~innate immune response	7	433	2.34	0.0784	0.9949	LYN, LOC107321681 (no match), TRIM35, LY96, BPI, LOC107324518 (no match), HK1
GO:0009888 ~tissue development	4	433	3.87	0.0824	0.9949	NR5A1, ACVRL1, NR5A2, LOC107316805 (Tgfbr2)
GO:0016477 ~cell migration	7	433	2.26	0.0889	0.9949	LOC107306830 (Dock2), FLT1, CD93, ITGB3, DOCK2, DOCK1, BCAR1
GO:0009887 ~animal organ morphogenesis	5	433	2.85	0.0971	0.9949	FGF7, LOC107314966 (Meis2), FGF13, PITX2, PBX1
GO:0010466 ~negative regulation of peptidase activity	2	433	19.37	0.0995	0.9949	TFPI2, TFPI
GO:1905605 ~positive regulation of blood-brain barrier permeability	2	433	19.37	0.0995	0.9949	TJP1, TJP2
GO:0015791 ~polyol transmembrane transport	2	433	19.37	0.0995	0.9949	LOC107305742 (Aqp7), LOC107305752 (Aqp3)

Quail control versus Gas1 over-expression

Term	Count	List Total	Fold Enrichment	PValue	FDR	Genes

Supplemental Table 14. Gene Ontology (GO) Analysis by Species and Treatment Group

GO:0060070 ~canonical Wnt signaling pathway	3	17	43.54	0.0019	0.0708	WNT2B, WNT9B, FZD10
GO:0007275 ~multicellular organism development	3	17	17.21	0.0114	0.1602	WNT2B, LOC107319512 (no match), WNT9B
GO:0044331 ~cell-cell adhesion mediated by cadherin	2	17	148.05	0.0126	0.1602	LOC107319512 (no match), FAT2
GO:0016339 ~calcium-dependent cell-cell adhesion via plasma membrane cell adhesion molecules	2	17	59.22	0.0313	0.2235	LOC107319512 (no match), FAT2
GO:0034332 ~adherens junction organization	2	17	56.94	0.0326	0.2235	LOC107319512 (no match), FAT2
GO:0007043 ~cell-cell junction assembly	2	17	46.26	0.0399	0.2235	LOC107319512 (no match), FAT2
GO:0045165 ~cell fate commitment	2	17	44.86	0.0412	0.2235	WNT2B, WNT9B
GO:0000902 ~cell morphogenesis	2	17	38.96	0.0473	0.2245	LOC107319512 (no match), FAT2
GO:0030182 ~neuron differentiation	2	17	22.10	0.0819	0.3459	WNT2B, WNT9B

Supplemental Table 15. RNA-seq expression levels (CPM) of SHH pathway members in duck and quail mandibular primordia following *Gas1* morpholino knockdown and *Gas1* over-expression

gene	duck control		duck *Gas1* morpholino			duck *Gas1* over-expression		
	mean	SEM	mean	SEM	p-value	mean	SEM	p-value
Shh	21.1029	3.9801	5.7335	0.2752	<0.0001	6.9786	0.7423	<0.0001
Ptch1	176.9618	50.4556	135.4383	5.0052	0.2272	226.3931	31.4542	0.2272
Smo	136.1796	1.7363	141.3980	5.3199	0.6575	165.4687	8.9774	0.0436
Cdon	75.3229	0.1566	70.2822	6.4406	0.4764	65.4938	1.9948	0.3000
Boc	74.2091	3.6189	43.9198	14.8735	0.0145	37.4272	1.7832	0.0030
Gas1 (CDS)	18.7460	2.7527	11.2559	1.9844	0.0452	23.1586	4.9233	0.3358
Gli1	52.0812	3.3375	49.0659	3.2372	0.5531	59.4427	1.3517	0.3776
Gli2	55.2114	3.7597	55.8889	6.2352	0.9181	70.2603	3.8483	0.0815
Gli3	46.8910	5.7944	54.9676	7.9524	0.2790	71.4581	5.5003	0.0084

gene	quail control		quail *Gas1* morpholino			quail *Gas1* over-expression		
	mean	SEM	mean	SEM	p-value	mean	SEM	p-value
Shh	13.9526	0.2233	8.9259	1.5897	0.0364	10.5852	1.6100	0.1455
Ptch1	73.2314	6.8385	65.9930	3.9754	0.7863	69.4561	19.5992	0.7863
Smo	147.5185	2.3822	143.6427	10.2619	0.7956	143.6470	9.9660	0.7956
Cdon	136.9136	8.1749	134.8734	14.4387	0.8962	123.4766	10.9731	0.7660
Boc	51.6126	3.3349	67.4035	18.0258	0.2907	54.1169	3.3175	0.7944
Gas1 (CDS)	7.8892	0.6206	5.6103	1.1702	0.2339	59.6418	25.3833	<0.0001
Gli1	52.3131	0.9631	37.6265	5.0788	0.0246	48.7470	4.0586	0.5893
Gli2	103.3615	2.3025	69.5630	12.0958	0.0268	87.2157	12.3694	0.2869
Gli3	112.7140	4.0641	80.3088	9.8130	0.0168	108.0318	11.4619	0.7398

Supplemental Table 16. RNA-seq expression levels (CPM) of cell cycle genes in duck and quail mandibular primordia following *Gas1* morpholino knockdown and *Gas1* over-expression

gene	duck control		duck *Gas1* morpholino			duck *Gas1* over-expression		
	mean	SEM	mean	SEM	p-value	mean	SEM	p-value
Cdk1	436.5471	18.9692	506.8854	41.2402	0.2334	371.7485	19.2570	0.2260
Ccndbp1	104.6132	3.2580	123.3767	13.6830	0.2334	85.4926	4.7099	0.2183
Cdk9	58.3561	2.4607	51.0187	0.5760	0.2334	50.2456	1.7027	0.2260
Cdkn3	15.1681	1.8658	13.5984	1.6407	0.5768	9.4550	1.5802	0.0699
Ccny	33.2642	2.7317	29.7696	1.5719	0.4381	33.7894	1.1169	0.9150
Ccni	170.4262	15.2881	133.7834	8.9533	0.0946	178.7828	8.0481	0.7783
Cdk5R1	10.0555	0.7937	7.9931	0.6835	0.3186	9.8770	1.3759	0.9150
Cdk19	29.7042	1.6275	23.2103	1.7270	0.1024	33.0757	0.9289	0.5493
Cdk18	70.1404	4.7093	55.5935	3.4840	0.0946	80.4213	3.9506	0.3491
Ccnj	45.2977	3.7823	39.6120	5.9982	0.4381	49.0556	3.4378	0.7321
Ccnb3	210.7668	7.2526	223.8447	24.2056	0.5768	298.5390	2.7396	0.0060
Ccnk	90.8762	3.6578	96.2928	6.3812	0.5768	135.3714	6.2676	0.0004
Ccnl2	180.6933	3.1426	200.6330	8.1370	0.3186	199.6524	10.1575	0.4245
Ccnc	86.0953	1.1561	106.8921	2.8038	0.0552	98.1211	1.9498	0.2260
Cdkn1A	6.6697	1.1580	14.6549	1.9111	0.0031	11.1366	1.5557	0.0699
Cdk2Ap1	35.6523	1.5115	39.4210	3.4048	0.4381	36.6940	1.4251	0.8904
Cdk5Rap1	70.3937	3.5853	84.6748	4.1647	0.1439	75.8478	3.9226	0.6311
Ccne2	37.9291	4.7975	46.0168	1.6258	0.2334	40.9343	1.5933	0.7321

gene	quail control		quail *Gas1* morpholino			quail *Gas1* over-expression		
	mean	SEM	mean	SEM	p-value	mean	SEM	p-value
Cdk1	333.4931	2.4419	428.9526	42.4776	0.0865	349.7836	25.0451	0.9804
Ccndbp1	74.6477	3.5643	81.2453	15.1702	0.6323	72.5348	9.6881	0.9804
Cdk9	41.5129	0.9063	32.6085	3.2324	0.1009	36.0671	1.7668	0.6939
Cdkn3	58.8932	0.7039	62.3949	5.3269	0.6323	53.3599	2.9135	0.9324
Ccny	13.4361	1.1725	11.4527	1.2270	0.4144	14.4714	0.4931	0.9804
Ccni	315.8166	7.2560	200.5962	5.3184	0.0004	294.3246	31.4817	0.9804
Cdk5R1	3.4441	0.1024	3.1671	0.2312	0.7106	3.5129	0.2655	0.9804
Cdk19	36.0932	0.7751	30.2173	2.8894	0.2537	36.6166	2.1172	0.9804
Cdk18	33.7071	0.7449	26.6777	0.3121	0.0865	41.8166	0.7432	0.3428
Ccnj	37.8024	1.6209	34.0807	1.4709	0.4553	40.4800	2.2662	0.9804
Ccnb3	219.0595	4.1352	229.4777	7.9195	0.6323	245.2325	5.8238	0.6939
Ccnk	67.8908	1.8523	56.4348	4.7643	0.1637	80.0911	1.1424	0.4850
Ccnl2	180.7933	10.9323	253.3765	18.1395	0.0167	233.1433	19.1711	0.3389
Ccnc	133.9373	2.2594	153.7847	14.5844	0.2760	157.8821	2.3928	0.4850
Cdkn1A	0.5151	0.0441	0.9141	0.2042	0.2276	0.5197	0.0663	0.9804
Cdk2Ap1	34.0938	1.4579	39.0222	4.1043	0.4144	34.9588	2.8383	0.9804
Cdk5Rap1	54.0612	2.2334	67.9886	4.5585	0.0865	53.9103	2.4690	0.9804
Ccne2	37.2685	1.8871	48.8811	2.0873	0.0865	35.6848	3.4287	0.9804

Supplemental Table 17. RNA-seq expression levels (CPM) of WNT pathway members in duck and quail mandibular primordia following *Gas1* morpholino knockdown and *Gas1* over-expression

gene	duck control		duck *Gas1* morpholino			duck *Gas1* over-expression		
	mean	SEM	mean	SEM	p-value	mean	SEM	p-value
Ctnnb1	1332.6319	50.6990	819.0927	27.5345	<0.0001	1185.8967	13.7908	0.1804
Wnt4	10.0405	0.3867	7.1160	0.7233	0.1097	9.6467	1.7965	0.8355
Wnt16	2.1840	0.1925	0.6447	0.0709	0.0007	1.2897	0.4140	0.1266
Wnt11	34.1328	2.3446	23.2453	0.2946	0.0031	20.4479	1.9648	0.0002
Wnt7A	2.3648	0.3346	1.1900	0.0162	0.0083	0.8999	0.1336	0.0004
Wnt2B	11.8855	2.0579	6.4166	0.3703	0.0026	5.7717	0.2519	0.0004
Fzd6	70.8266	2.6732	46.6689	2.1620	<0.0001	42.3488	1.1977	<0.0001
Wnt10A	10.9793	1.0006	3.8152	0.2288	<0.0001	5.1406	0.7091	0.0002
Fzd8	19.6911	0.6062	12.5758	1.4016	0.0026	13.5402	0.4595	0.0115
Wnt3	7.1623	0.3588	1.5547	0.6634	0.0001	1.9236	0.5372	0.0004
Wnt3A	8.7684	1.3254	4.8073	0.2359	0.0037	4.9835	0.6054	0.0069
Smad4	102.1730	5.1701	97.8376	2.8198	0.6168	118.8256	4.9239	0.1158
Sox5	30.1767	1.1612	34.3561	3.7018	0.2853	44.4636	0.3829	0.0015
Tcf7L2	39.3520	0.5986	43.7663	1.2075	0.2853	51.2146	1.6056	0.0069
Sox6	34.6558	2.2405	61.8345	11.8526	0.0008	71.6108	5.1047	0.0001
Dixdc1	89.5424	1.6952	117.6291	0.9526	0.0083	101.3607	10.1508	0.2333
Cby1	17.9269	0.5079	26.9477	0.2678	0.0007	19.3509	0.9762	0.5148
Dkk3	39.7419	1.0504	43.7276	2.7710	0.3580	30.6681	0.4815	0.0141

gene	quail control		quail *Gas1* morpholino			quail *Gas1* over-expression		
	mean	SEM	mean	SEM	p-value	mean	SEM	p-value
Ctnnb1	1040.2444	10.0635	686.9758	16.5341	0.0002	947.8292	76.7289	0.6316
Wnt4	58.7175	2.3787	32.0670	5.8955	0.0004	40.5904	4.4178	0.0434
Wnt16	1.2701	0.1716	2.2365	0.7359	0.1489	1.4348	0.1721	0.8753
Wnt11	5.8001	0.3850	10.5258	2.3335	0.0235	5.7348	0.9163	0.9627
Wnt7A	2.4069	0.2893	1.0627	0.2606	0.0264	0.9830	0.2198	0.0185
Wnt2B	15.8041	0.6052	7.8876	0.6351	0.0001	7.1436	0.3969	<0.0001
Fzd6	47.5284	0.1655	39.0917	2.3701	0.1083	32.1575	1.1547	0.0021
Wnt10A	9.3996	0.3457	3.2736	0.7490	<0.0001	5.1384	0.5975	0.0185
Fzd8	15.8466	1.5562	14.9048	3.6211	0.7843	10.3591	1.0728	0.0928
Wnt3	5.4122	0.1657	5.7866	1.0847	0.7843	2.5104	0.2626	0.0045
Wnt3A	4.5450	0.4277	1.8678	0.2481	0.0038	1.7061	0.4194	0.0021
Smad4	87.9536	1.2095	83.0711	6.7802	0.7055	91.2173	5.6528	0.8753
Sox5	34.8753	2.2077	30.3346	6.0359	0.5246	35.8224	3.0851	0.9627
Tcf7L2	64.4670	2.1459	47.0070	6.4610	0.0453	63.8490	8.0198	0.9627
Sox6	28.4863	1.7560	29.7187	5.1936	0.7843	31.2628	2.7053	0.8312
Dixdc1	122.1743	8.9138	150.3405	2.3623	0.0842	134.6641	10.6515	0.6316
Cby1	16.2459	0.6299	19.0954	1.0531	0.2917	17.2993	0.6627	0.8704
Dkk3	9.2652	0.5329	18.8679	3.4214	0.0005	10.5202	1.2547	0.8046

Supplemental Table 18. Transcription factor binding sites (TFBS) on the duck and quail Gas1 promoter

duck Gas1 promoter (2 kb)

TFBS	class	sequence	start	end	score	ID
NR2C2	Nuclear receptors with C4 zinc fingers	GGGTCG	18	23	0.98	MA1536.2
ZNF354C	C2H2 zinc finger factors	CTCCAC	88	93	0.99	MA0130.1
SP5	C2H2 zinc finger factors	CCTCCC	104	109	1.00	MA1965.2
ZNF263	C2H2 zinc finger factors	GGGAGGA	104	110	1.00	MA0528.3
IKZF2	C2H2 zinc finger factors	AGGAAG	122	127	1.00	MA2326.1
RBPJ	Rel homology region (RHR) factors	TGGGAA	170	175	1.00	MA1116.2
MAZ	C2H2 zinc finger factors	CCCCTCCT	212	219	0.98	MA1522.2
FOXN1	Fork head/winged helix factors	GGAAGC	270	275	1.00	MA1684.1
VEZF1	C2H2 zinc finger factors	CCCCCC	296	301	1.00	MA1578.2
VEZF1	C2H2 zinc finger factors	CCCCCC	297	302	1.00	MA1578.2
KLF1	C2H2 zinc finger factors	GGGCGGGG	327	334	1.00	MA0493.3
KLF15	C2H2 zinc finger factors	CCCCGCCC	327	334	1.00	MA1513.2
KLF2	C2H2 zinc finger factors	CCCCGCCC	327	334	0.98	MA1515.2
KLF7	C2H2 zinc finger factors	GGGCGGGG	327	334	1.00	MA1959.2
VEZF1	C2H2 zinc finger factors	CCCCCC	331	336	1.00	MA1578.2
HIC2	C2H2 zinc finger factors	GTGCCC	343	348	1.00	MA0738.2
FOXN1	Fork head/winged helix factors	GGACGC	406	411	1.00	MA1684.1
SP5	C2H2 zinc finger factors	CCTCCC	461	466	1.00	MA1965.2
ZNF384	C2H2 zinc finger factors	AAAAAAAA	499	506	1.00	MA1125.2
ZNF384	C2H2 zinc finger factors	AAAAAAAA	500	507	1.00	MA1125.2
ISL2	Homeo domain factors	CACTTA	516	521	1.00	MA0914.2
HIC2	C2H2 zinc finger factors	GTGCCC	519	524	1.00	MA0738.2
ZNF93	C2H2 zinc finger factors	GGCGGCAGCAGCGG	527	540	0.98	MA1721.2
MXI1	Basic helix-loop-helix factors (bHLH)	CACATG	586	591	1.00	MA1108.3
HIC2	C2H2 zinc finger factors	ATGCCA	589	594	0.98	MA0738.2
NR2C2	Nuclear receptors with C4 zinc fingers	GGGTCG	650	655	0.98	MA1536.2
SP5	C2H2 zinc finger factors	CCTCCC	707	712	1.00	MA1965.2
SP5	C2H2 zinc finger factors	CCTCCC	711	716	1.00	MA1965.2
PRDM1	C2H2 zinc finger factors	CTTTCTC	732	738	1.00	MA0508.4
FOXN1	Fork head/winged helix factors	AGAAGC	756	761	0.99	MA1684.1
OSR2	C2H2 zinc finger factors	ACAGAAGC	756	763	1.00	MA1646.2
MEIS1	Homeo domain factors	TGACA	764	768	1.00	MA0498.3
ZNF354C	C2H2 zinc finger factors	ATCCAC	802	807	1.00	MA0130.1
LIN54	CRC domain	TTTAAAT	827	833	1.00	MA0619.2
SOX15	High-mobility group (HMG) domain factors	CTTTTGT	834	840	0.98	MA1152.2
HIC2	C2H2 zinc finger factors	GTGCCC	840	845	1.00	MA0738.2
NR1H3	Nuclear receptors with C4 zinc fingers	AGGGCA	841	846	0.99	MA2337.1
RFX7	Fork head/winged helix factors	CGTTGCTG	855	862	0.98	MA1554.2
ARNT::HIF1A	Basic helix-loop-helix factors (bHLH)	ACGTG	860	864	1.00	MA0259.2

Supplemental Table 18 (continued). Transcription factor binding sites (TFBS) on the duck and quail Gas1 promoter

duck Gas1 promoter (2 kb)

TFBS	class	sequence	start	end	score	ID
HIF1A	Basic helix-loop-helix factors (bHLH)	ACGTGC	860	865	1.00	MA1106.2
EVX1	Homeo domain factors	TGATTA	868	873	0.98	MA0887.2
EVX2	Homeo domain factors	TGATTA	868	873	0.98	MA0888.2
LHX8	Homeo domain factors	TGATTA	868	873	0.98	MA0705.2
LHX8	Homeo domain factors	TAATCA	868	873	0.99	MA0705.2
MNX1	Homeo domain factors	TGATTA	868	873	1.00	MA0707.3
HOXA3	Homeo domain factors	CTCATTA	877	883	0.98	MA2119.1
GSX2	Homeo domain factors	CTCATTA	877	883	0.99	MA0893.3
NKX6-3	Homeo domain factors	CTCATTAT	877	884	0.99	MA1530.2
NOTO	Homeo domain factors	CTCATTA	877	883	0.99	MA0710.2
POU6F1	Homeo domain factors	TAATGAG	877	883	1.00	MA1549.2
HOXA1	Homeo domain factors	TAATGA	878	883	0.98	MA1495.2
HOXA2	Homeo domain factors	TCATTA	878	883	0.99	MA0900.3
EVX2	Homeo domain factors	TCATTA	878	883	0.98	MA0888.2
HOXB2	Homeo domain factors	TCATTA	878	883	0.99	MA0902.3
HOXB3	Homeo domain factors	TCATTA	878	883	0.99	MA0903.2
HOXB4	Homeo domain factors	TCATTA	878	883	1.00	MA1499.2
HOXB5	Homeo domain factors	TAATGA	878	883	0.98	MA0904.3
HOXC4	Homeo domain factors	TCATTA	878	883	1.00	MA1504.2
HOXD4	Homeo domain factors	TCATTA	878	883	1.00	MA1507.2
NKX6-2	Homeo domain factors	TCATTA	878	883	0.99	MA0675.2
PDX1	Homeo domain factors	TCATTA	878	883	0.99	MA0132.3
VAX2	Homeo domain factors	TCATTA	878	883	0.98	MA0723.3
NFAT5	Rel homology region (RHR) factors	ATGGAAAA	891	898	1.00	MA0606.3
NFATC1	Rel homology region (RHR) factors	TGGAAA	892	897	1.00	MA0624.3
NFATC3	Rel homology region (RHR) factors	TGGAAA	892	897	1.00	MA0625.3
ZNF384	C2H2 zinc finger factors	AAAAAAAA	909	916	1.00	MA1125.2
RFX7	Fork head/winged helix factors	CGTTGCTA	918	925	1.00	MA1554.2
FOXN1	Fork head/winged helix factors	AGAAGC	925	930	0.99	MA1684.1
VEZF1	C2H2 zinc finger factors	CCCCCC	943	948	1.00	MA1578.2
FEZF2	C2H2 zinc finger factors	CCCAGCCT	946	953	1.00	MA2341.1
PRDM1	C2H2 zinc finger factors	CTTTCTC	969	975	1.00	MA0508.4
ZNF354C	C2H2 zinc finger factors	CTCCAC	981	986	0.99	MA0130.1
RBPJ	Rel homology region (RHR) factors	TGGGAA	1013	1018	1.00	MA1116.2
ZNF384	C2H2 zinc finger factors	AAAAAAAA	1058	1065	1.00	MA1125.2
ZNF384	C2H2 zinc finger factors	AAAAAAAA	1059	1066	1.00	MA1125.2
ZNF384	C2H2 zinc finger factors	AAAAAAAA	1072	1079	1.00	MA1125.2
ZNF384	C2H2 zinc finger factors	AAAAAAAA	1073	1080	1.00	MA1125.2
ZNF384	C2H2 zinc finger factors	AAAAAAAA	1074	1081	1.00	MA1125.2

Supplemental Table 18 (continued). Transcription factor binding sites (TFBS) on the duck and quail Gas1 promoter

duck Gas1 promoter (2 kb)

TFBS	class	sequence	start	end	score	ID
ZNF384	C2H2 zinc finger factors	AAAAAAAA	1075	1082	1.00	MA1125.2
ZNF384	C2H2 zinc finger factors	AAAAAAAA	1076	1083	1.00	MA1125.2
HOXA9	Homeo domain factors	ATCGTAA	1100	1106	0.99	MA0594.3
SP5	C2H2 zinc finger factors	CCTCCC	1115	1120	1.00	MA1965.2
VEZF1	C2H2 zinc finger factors	CCCCCC	1131	1136	1.00	MA1578.2
NR1H3	Nuclear receptors with C4 zinc fingers	AGGGCA	1141	1146	0.99	MA2337.1
LIN54	CRC domain	TTTGAAT	1153	1159	1.00	MA0619.2
NR2E3	Nuclear receptors with C4 zinc fingers	AAGCTT	1158	1163	1.00	MA0164.2
NR2E3	Nuclear receptors with C4 zinc fingers	AAGCTT	1158	1163	1.00	MA0164.2
RHOXF1	Homeo domain factors	TAAGCC	1173	1178	0.99	MA0719.2
MEIS3	Homeo domain factors	GTGACAG	1185	1191	0.98	MA0775.2
MEIS1	Homeo domain factors	TGACA	1186	1190	1.00	MA0498.3
VEZF1	C2H2 zinc finger factors	CCCCCC	1192	1197	1.00	MA1578.2
MAZ	C2H2 zinc finger factors	CCCCTCCT	1204	1211	0.98	MA1522.2
ZNF263	C2H2 zinc finger factors	GGGAGGA	1208	1214	1.00	MA0528.3
SP5	C2H2 zinc finger factors	CCTCCC	1209	1214	1.00	MA1965.2
KLF1	C2H2 zinc finger factors	GGGCGGGG	1353	1360	1.00	MA0493.3
KLF15	C2H2 zinc finger factors	CCCCGCCC	1353	1360	1.00	MA1513.2
KLF2	C2H2 zinc finger factors	CCCCGCCC	1353	1360	0.98	MA1515.2
KLF7	C2H2 zinc finger factors	GGGCGGGG	1353	1360	1.00	MA1959.2
NR2C2	Nuclear receptors with C4 zinc fingers	GGGTCG	1369	1374	0.98	MA1536.2
ZNF384	C2H2 zinc finger factors	AAAAAAAA	1401	1408	1.00	MA1125.2
ZNF384	C2H2 zinc finger factors	AAAAAAAA	1402	1409	1.00	MA1125.2
ZNF384	C2H2 zinc finger factors	AAAAAAAA	1403	1410	1.00	MA1125.2
ZNF384	C2H2 zinc finger factors	AAAAAAAA	1404	1411	1.00	MA1125.2
ZNF384	C2H2 zinc finger factors	AAAAAAAA	1405	1412	1.00	MA1125.2
ZNF384	C2H2 zinc finger factors	AAAAAAAA	1406	1413	1.00	MA1125.2
ZNF384	C2H2 zinc finger factors	AAAAAAAA	1407	1414	1.00	MA1125.2
ZNF384	C2H2 zinc finger factors	AAAAAAAA	1408	1415	1.00	MA1125.2
ZNF384	C2H2 zinc finger factors	AAAAAAAA	1409	1416	1.00	MA1125.2
ZNF384	C2H2 zinc finger factors	AAAAAAAA	1410	1417	1.00	MA1125.2
ZNF384	C2H2 zinc finger factors	AAAAAAAA	1411	1418	1.00	MA1125.2
ZNF384	C2H2 zinc finger factors	AAAAAAAA	1412	1419	1.00	MA1125.2
DMRT3	DM-type intertwined zinc finger factors	TGTATCA	1470	1476	1.00	MA0610.2
DMRTA2	DM-type intertwined zinc finger factors	GATACA	1471	1476	0.99	MA1478.2
CLOCK	Basic helix-loop-helix factors (bHLH)	ACACGTG	1474	1480	1.00	MA0819.3
ARNT	Basic helix-loop-helix factors (bHLH)	CACGTG	1475	1480	1.00	MA0004.1
ARNT	Basic helix-loop-helix factors (bHLH)	CACGTG	1475	1480	1.00	MA0004.1
ARNT::HIF1A	Basic helix-loop-helix factors (bHLH)	ACGTG	1475	1479	1.00	MA0259.2

Supplemental Table 18 (continued). Transcription factor binding sites (TFBS) on the duck and quail Gas1 promoter

duck Gas1 promoter (2 kb)

TFBS	class	sequence	start	end	score	ID
MAX	Basic helix-loop-helix factors (bHLH)	CACGTG	1475	1480	1.00	MA0058.4
MAX	Basic helix-loop-helix factors (bHLH)	CACGTG	1475	1480	1.00	MA0058.4
MLXIP	Basic helix-loop-helix factors (bHLH)	CACGTG	1475	1480	1.00	MA0622.2
MLXIP	Basic helix-loop-helix factors (bHLH)	CACGTG	1475	1480	1.00	MA0622.2
MNT	Basic helix-loop-helix factors (bHLH)	CACGTG	1475	1480	1.00	MA0825.2
MNT	Basic helix-loop-helix factors (bHLH)	CACGTG	1475	1480	1.00	MA0825.2
ARNT::HIF1A	Basic helix-loop-helix factors (bHLH)	ACGTG	1476	1480	1.00	MA0259.2
NR1H3	Nuclear receptors with C4 zinc fingers	AGGGCA	1481	1486	0.99	MA2337.1
SOX10	High-mobility group (HMG) domain factors	ACAAAG	1516	1521	1.00	MA0442.3
SOX11	High-mobility group (HMG) domain factors	GAACAAAG	1516	1523	1.00	MA0869.3
SP5	C2H2 zinc finger factors	CCTCCC	1661	1666	1.00	MA1965.2
AHR::ARNT	Basic helix-loop-helix factors (bHLH)	GCGTG	1672	1676	1.00	MA0006.2
HIF1A	Basic helix-loop-helix factors (bHLH)	ACGTGC	1694	1699	1.00	MA1106.2
ARNT::HIF1A	Basic helix-loop-helix factors (bHLH)	ACGTG	1695	1699	1.00	MA0259.2
AHR::ARNT	Basic helix-loop-helix factors (bHLH)	GCGTG	1730	1734	1.00	MA0006.2
ZNF354C	C2H2 zinc finger factors	ATCCAC	1778	1783	1.00	MA0130.1
ZSCAN21	C2H2 zinc finger factors	AAGCACT	1792	1798	1.00	MA2336.1
ZNF384	C2H2 zinc finger factors	AAAAAAAA	1818	1825	1.00	MA1125.2
ZNF384	C2H2 zinc finger factors	AAAAAAAA	1819	1826	1.00	MA1125.2
LBX1	Homeo domain factors	TAACTAG	1847	1853	0.98	MA0618.2
ZIC1::ZIC2	C2H2 zinc finger factors	CAGCAGG	1890	1896	1.00	MA1628.2
ZIC3	C2H2 zinc finger factors	CAGCAGG	1890	1896	1.00	MA0697.3
FOXN1	Fork head/winged helix factors	TGACGC	1895	1900	0.99	MA1684.1

quail *Gas1* promoter (2 kb)

TFBS	class	sequence	start	end	score	ID
AHR::ARNT	Basic helix-loop-helix factors (bHLH)	GCGTG	2	6	1.00	MA0006.2
TFAP2E	Basic helix-span-helix factors (bHSH)	GCCCGCGGC	24	32	0.98	MA1569.2
IKZF2	C2H2 zinc finger factors	AGGAAG	68	73	1.00	MA2326.1
RBPJ	Rel homology region (RHR) factors	TGGGAA	92	97	1.00	MA1116.2
VEZF1	C2H2 zinc finger factors	CCCCCC	167	172	1.00	MA1578.2
TFAP2A	Basic helix-span-helix factors (bHSH)	CGCCCCGGGGC	209	219	0.99	MA0810.2
SMAD2	SMAD/NF-1 DNA-binding domain factors	CCAGAC	253	258	1.00	MA1964.2
AHR::ARNT	Basic helix-loop-helix factors (bHLH)	GCGTG	282	286	1.00	MA0006.2
ZNF354C	C2H2 zinc finger factors	CTCCAC	284	289	0.99	MA0130.1
FOXN1	Fork head/winged helix factors	GGACGC	304	309	1.00	MA1684.1
NR2C1	Nuclear receptors with C4 zinc fingers	GGGTCA	374	379	1.00	MA1535.2
NR2C2	Nuclear receptors with C4 zinc fingers	GGGTCA	374	379	1.00	MA1536.2
ZNF384	C2H2 zinc finger factors	AAAAAAAA	423	430	1.00	MA1125.2

Supplemental Table 18 (continued). Transcription factor binding sites (TFBS) on the duck and quail Gas1 promoter

quail Gas1 promoter (2 kb)

TFBS	class	sequence	start	end	score	ID
CEBPD	Basic leucine zipper factors (bZIP)	TTGCACAA	429	436	1.00	MA0836.3
BARHL2	Homeo domain factors	TAAATG	439	444	0.99	MA0635.2
HIC2	C2H2 zinc finger factors	ATGCCC	442	447	1.00	MA0738.2
ZNF549	C2H2 zinc finger factors	TGCTGCCC	451	458	1.00	MA1728.2
MXI1	Basic helix-loop-helix factors (bHLH)	CACATG	503	508	1.00	MA1108.3
HIC2	C2H2 zinc finger factors	ATGCCA	506	511	0.98	MA0738.2
NR2C2	Nuclear receptors with C4 zinc fingers	GGGTCG	562	567	0.98	MA1536.2
ZNF549	C2H2 zinc finger factors	TGCTGCCC	574	581	1.00	MA1728.2
IKZF2	C2H2 zinc finger factors	AGGAAG	632	637	1.00	MA2326.1
PRDM1	C2H2 zinc finger factors	CTTTCTC	654	660	1.00	MA0508.4
MEIS1	Homeo domain factors	TGACA	686	690	1.00	MA0498.3
ZNF354C	C2H2 zinc finger factors	ATCCAC	724	729	1.00	MA0130.1
LIN54	CRC domain	TTTAAAT	749	755	1.00	MA0619.2
SOX15	High-mobility group (HMG) domain factors	CTTTTGT	756	762	0.98	MA1152.2
STAT3	STAT domain factors	TGCTTGGAA	767	775	0.98	MA0144.3
ARNT::HIF1A	Basic helix-loop-helix factors (bHLH)	ACGTG	782	786	1.00	MA0259.2
HIF1A	Basic helix-loop-helix factors (bHLH)	ACGTGC	782	787	1.00	MA1106.2
EVX1	Homeo domain factors	TGATTA	790	795	0.98	MA0887.2
EVX2	Homeo domain factors	TGATTA	790	795	0.98	MA0888.2
LHX8	Homeo domain factors	TGATTA	790	795	0.98	MA0705.2
LHX8	Homeo domain factors	TAATCA	790	795	0.99	MA0705.2
MNX1	Homeo domain factors	TGATTA	790	795	1.00	MA0707.3
HOXA3	Homeo domain factors	CTCATTA	799	805	0.98	MA2119.1
GSX2	Homeo domain factors	CTCATTA	799	805	0.99	MA0893.3
NKX6-3	Homeo domain factors	CTCATTAT	799	806	0.99	MA1530.2
NOTO	Homeo domain factors	CTCATTA	799	805	0.99	MA0710.2
POU6F1	Homeo domain factors	TAATGAG	799	805	1.00	MA1549.2
HOXA1	Homeo domain factors	TAATGA	800	805	0.98	MA1495.2
HOXA2	Homeo domain factors	TCATTA	800	805	0.99	MA0900.3
EVX2	Homeo domain factors	TCATTA	800	805	0.98	MA0888.2
HOXB2	Homeo domain factors	TCATTA	800	805	0.99	MA0902.3
HOXB3	Homeo domain factors	TCATTA	800	805	0.99	MA0903.2
HOXB4	Homeo domain factors	TCATTA	800	805	1.00	MA1499.2
HOXB5	Homeo domain factors	TAATGA	800	805	0.98	MA0904.3
HOXC4	Homeo domain factors	TCATTA	800	805	1.00	MA1504.2
HOXD4	Homeo domain factors	TCATTA	800	805	1.00	MA1507.2
NKX6-2	Homeo domain factors	TCATTA	800	805	0.99	MA0675.2
PDX1	Homeo domain factors	TCATTA	800	805	0.99	MA0132.3
VAX2	Homeo domain factors	TCATTA	800	805	0.98	MA0723.3

Supplemental Table 18 (continued). Transcription factor binding sites (TFBS) on the duck and quail Gas1 promoter

quail Gas1 promoter (2 kb)

TFBS	class	sequence	start	end	score	ID
NFAT5	Rel homology region (RHR) factors	ATGGAAAA	813	820	1.00	MA0606.3
NFATC1	Rel homology region (RHR) factors	TGGAAA	814	819	1.00	MA0624.3
NFATC3	Rel homology region (RHR) factors	TGGAAA	814	819	1.00	MA0625.3
ZNF384	C2H2 zinc finger factors	AAAAAAAA	831	838	1.00	MA1125.2
ZNF384	C2H2 zinc finger factors	AAAAAAAA	832	839	1.00	MA1125.2
PRDM1	C2H2 zinc finger factors	CTTTCTC	891	897	1.00	MA0508.4
ZNF354C	C2H2 zinc finger factors	CTCCAC	903	908	0.99	MA0130.1
NFATC1	Rel homology region (RHR) factors	TGGAAA	935	940	1.00	MA0624.3
NFATC3	Rel homology region (RHR) factors	TGGAAA	935	940	1.00	MA0625.3
NFYB	Heteromeric CCAAT-binding factors	CCATTGGCC	954	962	0.99	MA0502.3
FEZF2	C2H2 zinc finger factors	CCCAGCCT	961	968	1.00	MA2341.1
ZNF384	C2H2 zinc finger factors	AAAAAAAA	980	987	1.00	MA1125.2
ZNF384	C2H2 zinc finger factors	AAAAAAAA	981	988	1.00	MA1125.2
ZNF384	C2H2 zinc finger factors	AAAAAAAA	993	1000	1.00	MA1125.2
ZNF384	C2H2 zinc finger factors	AAAAAAAA	994	1001	1.00	MA1125.2
ZNF384	C2H2 zinc finger factors	AAAAAAAA	995	1002	1.00	MA1125.2
ZNF384	C2H2 zinc finger factors	AAAAAAAA	996	1003	1.00	MA1125.2
ZNF384	C2H2 zinc finger factors	AAAAAAAA	997	1004	1.00	MA1125.2
ZNF384	C2H2 zinc finger factors	AAAAAAAA	998	1005	1.00	MA1125.2
ZNF384	C2H2 zinc finger factors	AAAAAAAA	999	1006	1.00	MA1125.2
ZNF384	C2H2 zinc finger factors	AAAAAAAA	1000	1007	1.00	MA1125.2
ZNF384	C2H2 zinc finger factors	AAAAAAAA	1001	1008	1.00	MA1125.2
ZNF384	C2H2 zinc finger factors	AAAAAAAA	1002	1009	1.00	MA1125.2
ZNF384	C2H2 zinc finger factors	AAAAAAAA	1003	1010	1.00	MA1125.2
ZNF384	C2H2 zinc finger factors	AAAAAAAA	1004	1011	1.00	MA1125.2
ZNF384	C2H2 zinc finger factors	AAAAAAAA	1005	1012	1.00	MA1125.2
ZNF384	C2H2 zinc finger factors	AAAAAAAA	1006	1013	1.00	MA1125.2
ZNF384	C2H2 zinc finger factors	AAAAAAAA	1007	1014	1.00	MA1125.2
ZNF384	C2H2 zinc finger factors	AAAAAAAA	1008	1015	1.00	MA1125.2
ZNF384	C2H2 zinc finger factors	AAAAAAAA	1009	1016	1.00	MA1125.2
ZNF384	C2H2 zinc finger factors	AAAAAAAA	1010	1017	1.00	MA1125.2
ZNF384	C2H2 zinc finger factors	AAAAAAAA	1011	1018	1.00	MA1125.2
ZNF384	C2H2 zinc finger factors	AAAAAAAA	1012	1019	1.00	MA1125.2
ZNF384	C2H2 zinc finger factors	AAAAAAAA	1013	1020	1.00	MA1125.2
ZNF384	C2H2 zinc finger factors	AAAAAAAA	1014	1021	1.00	MA1125.2
ZNF384	C2H2 zinc finger factors	AAAAAAAA	1015	1022	1.00	MA1125.2
ZNF384	C2H2 zinc finger factors	AAAAAAAA	1016	1023	1.00	MA1125.2
ZNF384	C2H2 zinc finger factors	AAAAAAAA	1017	1024	1.00	MA1125.2
ZNF384	C2H2 zinc finger factors	AAAAAAAA	1018	1025	1.00	MA1125.2

Supplemental Table 18 (continued). Transcription factor binding sites (TFBS) on the duck and quail Gas1 promoter

quail Gas1 promoter (2 kb)

TFBS	class	sequence	start	end	score	ID
ZNF384	C2H2 zinc finger factors	AAAAAAAA	1019	1026	1.00	MA1125.2
ZNF384	C2H2 zinc finger factors	AAAAAAAA	1020	1027	1.00	MA1125.2
KLF5	C2H2 zinc finger factors	TCCCCTCCCT	1027	1036	0.98	MA0599.1
MAZ	C2H2 zinc finger factors	CCCCTCCC	1028	1035	1.00	MA1522.2
SP5	C2H2 zinc finger factors	CCTCCC	1030	1035	1.00	MA1965.2
HOXA9	Homeo domain factors	ATCGTAA	1044	1050	0.99	MA0594.3
FOXN1	Fork head/winged helix factors	GGAAGC	1064	1069	1.00	MA1684.1
VEZF1	C2H2 zinc finger factors	CCCCCC	1075	1080	1.00	MA1578.2
NR1H3	Nuclear receptors with C4 zinc fingers	AGGGCA	1085	1090	0.99	MA2337.1
SOX10	High-mobility group (HMG) domain factors	ACAAAG	1099	1104	1.00	MA0442.3
NR2E3	Nuclear receptors with C4 zinc fingers	AAGCTT	1102	1107	1.00	MA0164.2
NR2E3	Nuclear receptors with C4 zinc fingers	AAGCTT	1102	1107	1.00	MA0164.2
RHOXF1	Homeo domain factors	TAAGCC	1117	1122	0.99	MA0719.2
MEIS3	Homeo domain factors	ATGACAG	1129	1135	0.98	MA0775.2
MEIS1	Homeo domain factors	TGACA	1130	1134	1.00	MA0498.3
VEZF1	C2H2 zinc finger factors	CCCCCC	1136	1141	1.00	MA1578.2
VEZF1	C2H2 zinc finger factors	CCCCCC	1137	1142	1.00	MA1578.2
MAZ	C2H2 zinc finger factors	CCCCTCCT	1149	1156	0.98	MA1522.2
ZNF263	C2H2 zinc finger factors	GGGAGGA	1153	1159	1.00	MA0528.3
SP5	C2H2 zinc finger factors	CCTCCC	1154	1159	1.00	MA1965.2
HIF1A	Basic helix-loop-helix factors (bHLH)	ACGTGC	1198	1203	1.00	MA1106.2
ARNT::HIF1A	Basic helix-loop-helix factors (bHLH)	ACGTG	1199	1203	1.00	MA0259.2
ARNT	Basic helix-loop-helix factors (bHLH)	CACGTG	1239	1244	1.00	MA0004.1
ARNT	Basic helix-loop-helix factors (bHLH)	CACGTG	1239	1244	1.00	MA0004.1
ARNT::HIF1A	Basic helix-loop-helix factors (bHLH)	ACGTG	1239	1243	1.00	MA0259.2
MAX	Basic helix-loop-helix factors (bHLH)	CACGTG	1239	1244	1.00	MA0058.4
MAX	Basic helix-loop-helix factors (bHLH)	CACGTG	1239	1244	1.00	MA0058.4
MLXIP	Basic helix-loop-helix factors (bHLH)	CACGTG	1239	1244	1.00	MA0622.2
MLXIP	Basic helix-loop-helix factors (bHLH)	CACGTG	1239	1244	1.00	MA0622.2
MNT	Basic helix-loop-helix factors (bHLH)	CACGTG	1239	1244	1.00	MA0825.2
MNT	Basic helix-loop-helix factors (bHLH)	CACGTG	1239	1244	1.00	MA0825.2
ARNT::HIF1A	Basic helix-loop-helix factors (bHLH)	ACGTG	1240	1244	1.00	MA0259.2
ZNF354C	C2H2 zinc finger factors	CTCCAC	1242	1247	0.99	MA0130.1
SOX10	High-mobility group (HMG) domain factors	ACAAAG	1280	1285	1.00	MA0442.3
ARNT::HIF1A	Basic helix-loop-helix factors (bHLH)	ACGTG	1301	1305	1.00	MA0259.2
HIF1A	Basic helix-loop-helix factors (bHLH)	ACGTGC	1301	1306	1.00	MA1106.2
FOXN1	Fork head/winged helix factors	GGACGC	1348	1353	1.00	MA1684.1
NKX2-3	Homeo domain factors	CCACTTAA	1363	1370	1.00	MA0672.2
NKX2-8	Homeo domain factors	CCACTTAA	1363	1370	0.99	MA0673.2

Supplemental Table 18 (continued). Transcription factor binding sites (TFBS) on the duck and quail Gas1 promoter

quail Gas1 promoter (2 kb)

TFBS	class	sequence	start	end	score	ID
NKX3-1	Homeo domain factors	CCACTTA	1363	1369	1.00	MA0124.3
ISL2	Homeo domain factors	CACTTA	1364	1369	1.00	MA0914.2
AHR::ARNT	Basic helix-loop-helix factors (bHLH)	GCGTG	1389	1393	1.00	MA0006.2
NKX2-5	Homeo domain factors	CACTCAA	1393	1399	1.00	MA0063.3
AHR::ARNT	Basic helix-loop-helix factors (bHLH)	GCGTG	1426	1430	1.00	MA0006.2
GMEB1	SAND domain factors	GACGTA	1431	1436	0.98	MA0615.2
GMEB1	SAND domain factors	TACGTC	1431	1436	0.98	MA0615.2
BCL11A	C2H2 zinc finger factors	CTGACCA	1442	1448	1.00	MA2324.1
ETV7	Tryptophan cluster factors	GCGGAAGTG	1449	1457	1.00	MA1708.2
ETV6	Tryptophan cluster factors	GCGGAAGTG	1449	1457	1.00	MA0645.2
RHOXF1	Homeo domain factors	TGATCC	1464	1469	1.00	MA0719.2
TCF7	High-mobility group (HMG) domain factors	CTTTGAT	1478	1484	1.00	MA0769.3
NR1H3	Nuclear receptors with C4 zinc fingers	AGGGCA	1499	1504	0.99	MA2337.1
SATB1	Homeo domain factors	CTAATAA	1505	1511	1.00	MA1963.2
IKZF2	C2H2 zinc finger factors	AGGAAG	1545	1550	1.00	MA2326.1
FIGLA	Basic helix-loop-helix factors (bHLH)	CACCTG	1578	1583	1.00	MA0820.2
SNAI1	C2H2 zinc finger factors	ACAGGTG	1578	1584	0.99	MA1558.2
ZEB1	Homeo domain factors	CACCTG	1578	1583	1.00	MA0103.4
ARID3B	ARID	TTTTAAT	1599	1605	0.98	MA0601.2
ARID3A	ARID	ATTAAA	1600	1605	1.00	MA0151.1
NOTO	Homeo domain factors	CAAATTA	1602	1608	0.98	MA0710.2
FIGLA	Basic helix-loop-helix factors (bHLH)	CACCTG	1643	1648	1.00	MA0820.2
ZEB1	Homeo domain factors	CACCTG	1643	1648	1.00	MA0103.4
BARHL1	Homeo domain factors	CGTTTA	1683	1688	1.00	MA0877.4
BARHL2	Homeo domain factors	TAAACG	1683	1688	1.00	MA0635.2
MEIS2	Homeo domain factors	TTGACAGG	1763	1770	1.00	MA0774.1
MEIS3	Homeo domain factors	TTGACAG	1764	1770	1.00	MA0775.2
MEIS1	Homeo domain factors	TGACA	1765	1769	1.00	MA0498.3
NFATC4	Rel homology region (RHR) factors	ATGGAAAAA	1782	1790	1.00	MA1525.3
NFAT5	Rel homology region (RHR) factors	ATGGAAAA	1783	1790	1.00	MA0606.3
NFATC1	Rel homology region (RHR) factors	TGGAAA	1784	1789	1.00	MA0624.3
NFATC3	Rel homology region (RHR) factors	TGGAAA	1784	1789	1.00	MA0625.3
ATOH1	Basic helix-loop-helix factors (bHLH)	CAGATGG	1807	1813	1.00	MA1467.3
NEUROD1	Basic helix-loop-helix factors (bHLH)	ACAGATGG	1807	1814	1.00	MA1109.2
NEUROD2	Basic helix-loop-helix factors (bHLH)	ACAGATGG	1807	1814	1.00	MA0668.3
NEUROG2	Basic helix-loop-helix factors (bHLH)	CAGATGG	1807	1813	1.00	MA1642.2
HAND2	Basic helix-loop-helix factors (bHLH)	CAGATG	1808	1813	1.00	MA1638.2
MEIS3	Homeo domain factors	GTGACAG	1811	1817	0.98	MA0775.2
MEIS1	Homeo domain factors	TGACA	1812	1816	1.00	MA0498.3

Supplemental Table 18 (continued). Transcription factor binding sites (TFBS) on the duck and quail Gas1 promoter

quail Gas1 promoter (2 kb)

TFBS	class	sequence	start	end	score	ID
BARHL2	Homeo domain factors	TAAATG	1830	1835	0.99	MA0635.2
STAT4	STAT domain factors	TTCTGGGAAA	1838	1847	0.99	MA0518.2
RBPJ	Rel homology region (RHR) factors	TGGGAA	1839	1844	1.00	MA1116.2
STAT1	STAT domain factors	TTCTGGGAA	1839	1847	1.00	MA0137.4
STAT3	STAT domain factors	TTCTGGGAA	1839	1847	1.00	MA0144.3
STAT5A::STA	STAT domain factors	TTCCCAGAA	1839	1847	1.00	MA0519.2
STAT5B	STAT domain factors	TTCCCAGAA	1839	1847	1.00	MA1625.2
AHR::ARNT	Basic helix-loop-helix factors (bHLH)	GCGTG	1906	1910	1.00	MA0006.2
AHR::ARNT	Basic helix-loop-helix factors (bHLH)	GCGTG	1954	1958	1.00	MA0006.2
HES1	Basic helix-loop-helix factors (bHLH)	GGCGCGTG	1954	1961	1.00	MA1099.3
SOX10	High-mobility group (HMG) domain factors	ACAAAG	1967	1972	1.00	MA0442.3
TEAD3	TEA domain factors	GCATTCCT	1992	1999	0.99	MA0808.1
IKZF2	C2H2 zinc finger factors	AGGAAG	1998	2003	1.00	MA2326.1

Supplemental Table 19. Mandibular primordia incubation times in trypsin-pancreatin solution

	incubation times [min]	
stage	duck	quail
HH18	20	15
HH21	25	18
HH24	30	23
HH27	40	30

Supplemental Table 20. qRT-PCR primer sequences

		forward primer	*reverse primer*
r18s	duck quail	5'- GCG TGT GCC TAC CCT ACG CC -3'	5' - ACG CAA GCT TAT GGC CCG CA -3'
Shh	duck quail	5'- TGG CAG AGA AGA CCC TAG -3'	5'- TTG CAG CGC TGA GTC ATC -3'
Boc	duck quail	5'- CAT GCA GCA GTC ACA CGA G -3'	5'- AGT GGA GTC ATC TGG GAG -3'
Cdo	duck quail	5'- GCC ATC AGT GAC ACT CAG -3'	5'- GGC TGC AGG TGA TTT ATC -3'
Gas1	duck quail	5'- CCG CTA CAT GGC CTA CTG -3'	5'- CTT GAC CGA CTC GCA GAT -3'
Ptch	duck quail	5'- GAA CTC ATC ACA GAA GCA G -3'	5'- GAT CCA CTG CAA AGG AGG -3'
Smo	duck quail	5'- GAG AAG ATC AAC CTC TTT GC -3'	5'- CTT GCT CTT CTT GAT CCT C -3'
Gli1	duck quail	5'- TAG TGT TGA CCT GCA GAC -3' 5'- TAG CGT TGA CCT GCA GAC -3'	5'- GTG TGG CTG AAC AGA TGC -3' 5'- GTG TGG CTG AAC AGT TGC -3'
Gli2	duck quail	5'- GAC AGT TAA GGA TTC CTG C -3'	5'- GAC AGA CAG CTC CAT TAT TC -3'
Gli3	duck quail	5'- CTC TAC CAT TTC CAC AGC -3'	5'- GGT ACC ATT TCC TAT GAG AG -3'

Supplemental Table 21. *Gas1* primer sequences for in situ hybridization probes

		forward primer	*reverse primer*
Gas1	duck quail	5'- TAC AAC CAG TAC GCC GAG G -3'	5'- TCG GCT CCT CCT CGT AGT CC -3'
Gas1-T7	duck quail	5'- TAA TAC GAC TCA CTA TAG GG TAC AAC CAG TAC GCC GAG G -3'	5'- TAA TAC GAC TCA CTA TAG GG TCG GCT CCT CCT CGT AGT CC -3'

Supplemental Table 22. Primer sequences for cloning and sequencing *Gas1*

Sequencing full length Gas1	
duck forward	5'-GCCTCTCCCCCGCGAC-3'
duck reverse	5'-GGAAGGAGGCACGGGGC-3'
quail forward	5'-TGGATTGATGCGAGGAGACC-3'
quail reverse	5'-CACACGGGGACAGACACAC-3'

Cloning Gas1 into pPIDNB	
duck forward	5'ACCCTCGTAAAGCCGCCACCATGCTGGCCCGGCACG-3'
duck reverse	5'-GCCGCTTCACTTGTACTGCACTAGAGGCCGGCCAGCAG-3'
quail forward	5'-ACCCTCGTAAAGCCGCCACCATGCCGGCCCGCCCG-3'
quail reverse	5'-GCCGCTTCACTTGTACTGCACTAGAGCGGCGGTAGCAGC-3'

Sequencing Gas1 promoter	
duck forward	5'-AAAAGGTGGGCAAGGCGTCA-3'
quail forward	5'-GCAAACCCTGGTAGCTGGCA-3'
duck/quail reverse	5'-GCCTCGGCGTACTGGTTGTA-3'

Supplemental Table 23. *Vivo-Morpholino oligo* sequences

duck *Gas1*

5'- GCCGCCGTGCCGGCCAGCATC -3'

quail *Gas1*

5'- AGAAGGAGCTGCCGCCTCTGGGAAA -3'

GFP

5'- ACAGCTCCTCGCCCTTGCTCACCAT -3'